EXTENDED PHASE SPACE THERMODYNAMICS

OF REGULAR BARDEEN BLACK HOLE

Thesis

submitted in partial fulfillment of the requirements for the degree of

DOCTOR OF PHILOSOPHY

by

RAJANI K V

DEPARTMENT OF PHYSICS

NATIONAL INSTITUTE OF TECHNOLOGY KARNATAKA (NITK),

SURATHKAL, MANGALORE - 575 025

JANUARY, 2023

DECLARATION

By the Ph.D Research Scholar

I hereby *declare* that the Research Thesis entitled **"EXTENDED PHASE SPACE THERMODYNAMICS OF REGULAR BARDEEN BLACK HOLE"**, which is being submitted to the *National Institute of Technology Karnataka, Surathkal* in partial fulfillment of the requirements for the award of the Degree of *Doctor of Philosophy* in *Physics* is a *bonafide report of the research work carried out by me*. The material contained in this thesis has not been submitted to any University or Institution for the award of any degree.

Rajani K V
Register No.: 148028 PH14F07
Department of Physics
National Institute of Technology Karnataka
Surathkal.

Place: NITK - Surathkal

Date: 17 January, 2023

CERTIFICATE

This is to *certify* that the Research Thesis entitled **"EXTENDED PHASE SPACE THERMODYNAMICS OF REGULAR BARDEEN BLACK HOLE"**, submitted by **Rajani K V** (Register Number: 148028 PH14F07) as the record of the research work carried out by her, is *accepted* as the *Research Thesis submission* in partial fulfillment of the requirements for the award of degree of *Doctor of Philosophy*.

Dr. Deepak Vaid
Research Guide
Assistant Professor
Department of Physics
NITK Surathkal - 575025

Chairman - DRPC /9-1-2023
(Signature with Date and Seal)

This Thesis is dedicated to my teachers.

ACKNOWLEDGEMENT

Raji Haridas, Mr. Aneesh, Mr. Haridas, and my dearest nephews Abhinav, Harshith Krishna, and Aswanth, who are my greatest strength and weakness. I owe my love and gratitude to them for their unconditional love, trust in me, and whole-hearted support during every stage of my life and Ph.D. candidature. The immense encouragement and inspiration I received from my family for their pursuit were splendid.

Finally, I remember with gratefulness all the people and well-wishers for the help, support, and blessings for my research work which I may have unknowingly not mentioned. Many thanks to all who have made this happen.

Rajani K V

ABSTRACT

The existence of black holes were predicted by Einstein's general relativity, a remarkable theory that agrees with most observations at the solar system scale and beyond. However, in general relativity, black holes have singularities at their centers, as Hawking and Penrose's famous theorems claimed. Regular black hole models, for example, have been offered as a way to get around the central singularity. Regular black holes have a de Sitter core at their center, which generates outward radial pressure to prevent gravitational collapse and the formation of singularities. The exact nature of astrophysical black holes, however, is unknown. As a result, it is critical to deduce deformations to the classical Schwarzschild metric using regular black hole models as motivation and to confirm astrophysical observations in a more generic and relevant framework.

This thesis investigates the thermodynamic phase transition of regular Bardeen AdS black holes with and without quintessence surrounded by it. The cosmological constant Λ is given the status of thermodynamic variable pressure because of the inconsistency between the Smarr relation and the first law of black hole thermodynamics in AdS spacetime. The first law of black hole thermodynamics has been modified to include a pressure-volume term. Black hole phase behavior is found to be analogous to everyday physical phenomena in this extended phase space. The thermodynamics of the black hole is analyzed in extended phase space. A first-order phase transition analogous to the van der Waals system is evident from this study, which is affirmed by the specific heat divergence at the critical points. A conventional heat engine is constructed by considering the black hole as a working substance. The efficiency is obtained via a thermodynamic cycle in the $P - v$ plane, which receives and ejects heat. The heat engine efficiency in regular Bardeen AdS black holes is improved by adding a quintessence field. The analytical expression for heat engine efficiency is derived in terms of the quintessence dark energy parameter. The study of Joule Thomson (JT) expansion in the regular Bardeen AdS black holes in the quintessence background is based on the analysis of inversion temperature and isenthalpic curves. The derivation of the JT coefficient μ is used to plot the inversion and isenthalpic curves. The effect of

quintessence parameters a and ω_q on the JT coefficient and inversion temperature, especially with the case of $\omega_q = -1, -2/3$ and $-1/3$ shows that quintessence dark energy affects the inversion point (T_i, P_i).

Contents

List of Figures

List of Tables

Chapter 1

Introduction

This chapter provides a brief introduction to thermodynamics and its applications to black holes with a detailed literature survey. In addition to that, the objectives of the present research work and the thesis structure are also detailed in this section.

Gravity is one of the mysterious forces of nature. Our universe is surrounded by weak, strong, electromagnetic, and gravitational forces. Out of these four fundamental natural interactions, gravity is the weakest. We can study all interactions using the existing experimental and theoretical data knowledge. However, it has been a challenge to understand the gravitational force completely. Albert Einstein proposed the Special theory of relativity at the starting of the twentieth century, which considers spacetime as a fundamental entity instead of considering space and time to be independent of each other as in the Newtonian case. Special relativity describes an inertial observer; however, the presence of gravity is not introduced. We can get an idea about gravity by shifting to the general theory of relativity. Albert Einstein 1916 proposed the general theory of relativity (GR). One of the fundamental concepts in GR is the principle of equivalence, which explains that one cannot differentiate between the motion of a freely falling body in a uniform gravitational field and the motion of the same body in a uniformly accelerated frame in small enough regions of spacetime. Mathematically, it also tells us about the coupling of gravity with the energy-momentum tensor of the matter

field. A metric tensor, which contains information about spacetime, is used to describe the spacetime curvature. In GR, Einstein's equation relates the spacetime curvature in the presence of matter fields.

In GR information about the background geometry is encoded in the metric. A metric tensor $g_{\mu\nu}$ measures the distance between two points in spacetime, which give information about geometry. Einstein's field equations connect the dynamics of the metric tensor and the energy-momentum tensor of matter,

$$R_{\mu\nu} - \frac{1}{2}Rg_{\mu\nu} = \frac{8\pi G}{c^4}T_{\mu\nu}, \tag{1.1}$$

where $T_{\mu\nu}$ is the energy-momentum tensor of some matter field, $R_{\mu\nu}$ is the Ricci tensor, and R is the Ricci scalar, constructed from the metric tensor.

The existence of a black hole is considered one of the most remarkable predictions of GR. Einstein's equation will give different kinds of black hole solutions constructed from specific actions through the least action principle (Carroll 2019). Black holes are extremely dense objects confined within a bounded region of spacetime whose boundary is given by a null surface known as the event horizon. This surface divides the exterior region from the interior one because there do not exist any timelike or null geodesics which can take us from the point in the interior to the point in the exterior (Carroll 2019). It is a one-way surface because once an observer crosses the event horizon, she will never be able to communicate any information to the outside world. Significant efforts have been made to comprehend and understand what happens if any given amount of matter with mass M, which is squeezed into a region of spacetime of radius less than or equal to,

$$R_s = \frac{2GM}{c^2}, \tag{1.2}$$

where G is Newton's gravitational constant, and c is the speed of light. According to classical general relativity, no material particle or even light can escape to infinity from the inside of a black hole's event horizon, and there is a singularity inside it where density becomes infinitely large, rendering classical physics useless.

Karl Schwarzschild obtained the first static spherically symmetric vacuum solution ($T_{\mu\nu} = 0$) using Einstein's field equations (1.1) in 1916 (Schwarzschild 1916). In (t, r, θ, ϕ) coordinates, the Schwarzschild spacetime reads

$$ds^2 = -\left(1 - \frac{2M}{r}\right) dt^2 + \left(1 - \frac{2M}{r}\right)^{-1} dr^2 + r^2 d\Omega_2^2, \tag{1.3}$$

where M is the black hole's mass and $d\Omega_2^2 = d\theta^2 + \sin^2\theta d\phi^2$ is the metric of a unit 2-sphere. According to Birkhoff's theorem, Schwarzschild spacetime is the only spherically symmetric vacuum solution outside a spherical matter distribution (Itin 2008). The Schwarzschild spacetime is static because all metric components are independent of the time coordinate t, and the line element ds^2 is invariant by the transformation $t \to -t$, resulting in a timelike Killing vector ξ_t^μ (Itin 2008). Outside the black hole, this vector is timelike, but it is null at the event horizon and spacelike inside the event horizon. As a result, the Schwarzschild black hole's event horizon is calculated as (Poisson 2004)

$$g_{\mu\nu} \xi_t^\mu \xi_t^\nu = 1 - \frac{2M}{r_+} = 0, \tag{1.4}$$

resulting in $r_+ = 2M$.

The Killing horizon refers to a null surface where the Killing vector is also null. The Killing horizon is the same as the event horizon in a stationary, asymptotically flat spacetime. Singularities occur at $r = 2M$ and $r = 0$ in the Schwarzschild spacetime. It turns out that $r = 2M$ is a coordinate singularity that arises due to incorrect coordinate selection; it may be avoided by suitable coordinate transformations (Weyl 1917, Einstein and Rosen 1935, Synge 1950, Finkelstein 1958, Fronsdal 1959, Kruskal 1960). However, no coordinate change can remove the singularity at r = 0, suggesting the presence of a true singularity where all curvature invariants will blow out, which is referred to as curvature or the physical singularity.

According to the cosmic censorship hypothesis (Penrose 1969), black holes contain singularities always hidden by the event horizon. As a result, the formation of an event horizon and the presence of a singularity are two general characteristics of black hole spacetime. Regular black holes do not have a singularity at their center. Even though

obtaining a singularity-free solution is the domain of quantum gravity theory, a phenomenological model may be constructed in classical gravity. Bardeen was the first to derive such a regular solution (Bardeen 1968). Many researchers later found that regular black holes can be an exact solution to gravity when coupled with a non-linear electromagnetic source (Ayon-Beato and Garcia 1998, Ayon-Beato and Garcıa 1999, Hayward 2006). This research aims to explore the thermodynamic behavior of regular black holes.

This chapter is organized as follows. Section (1.1) presents a brief study of the evidence for black holes. Then we discuss the thermodynamic phase transition (1.2) and its application to black holes in (1.2.1), (1.2.2), and (1.2.3). Followed by this, we introduce Bardeen black holes (1.2.4). The objectives of this research (1.3) and the thesis organization (1.4) are included at the end of this chapter.

1.1   Evidence for Black Holes

Black holes cannot be seen directly but their presence can be estimated by analyzing the motion of nearby objects. The presence of a black hole can be detected in three ways: (i) mass estimates from objects circling or spiraling into the black hole, (ii) gravitational lensing, and (iii) emitted radiation from a companion star. Classically black holes do not produce radiation, and Hawking radiation is too weak to be observed directly. The Uhuru satellite was launched into space in 1970, and it soon found X-ray sources significantly stronger than our solar system . Webster and Murdin (Webster and Murdin 1972) discovered Cygnus X-1, an apparent binary partner in the Cygnus constellation consisting of a visible blue giant and a strong X-ray source .

The mass of a black hole can be determined by observing its effect on visible objects surrounding in its neighbourhood and measuring their movement. A brown, spiraling disc, for example, rotates inside the core of galaxy NGC 4261. It is nearly the size of the solar system, yet it weighs $1.2 \times 10^9 M_\odot$. A rotating disc with such a large mass could indicate the presence of a rotating black hole at its center.

As predicted by Einstein's general theory of relativity, light bends when it passes through an apparent gravitational field. Eddington (Eddington 1920) was the first person to observe the change in the apparent location of a star before and after a solar

eclipse. The light from the star was bent due to the sun's gravitational pull, as predicted by Einstein in 1917. Using GR, Einstein derived gravitational lensing deflection, ie, 1.75 seconds of arc. Eddington measured a value close to that of the GR prediction using data taken during a solar eclipse in 1920.
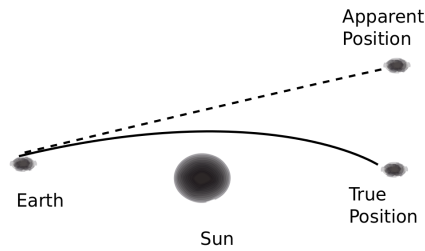
Figure 1.1: Gravitational Lensing

The night sky is populated by many binary systems, where one companion could be a neutron star or red giant and the other is a black hole. When matter from the star falls into its companion black hole, it is heated to a few million degrees Kelvin and then accelerated. It emits intense X-rays, which may be detected with X-ray telescopes.

Recently, scientists have speculated that intermediate-mass black holes exist (Abbott et al. 2019, Ebisuzaki et al. 2001) with mases between $10^2 M_\odot$ to $10^5 M_\odot$, which is larger than stellar black holes but smaller than supermassive black holes with masses of $10^5 M_\odot$ to $10^9 M_\odot$. These intermediate-mass constitute the missing link between stellar-mass and supermassive black holes. The presence of intermediate-mass black holes has been confirmed by numerous studies (Mezcua 2017). Ultra-luminous X-ray sources have been suggested as potential candidates for intermediate-mass black holes (Farrell et al. 2009). In the nuclei of dwarf galaxies and/or globular clusters, relatively large intermediate-mass black holes may exist (Reines et al. 2013, Miller et al. 2015). However, none of the intermediate-mass black hole hypotheses are considered definite (Ebisawa et al. 2003, Strader et al. 2012). High velocity Compact Clouds (HVCC) are a population of compact molecular clouds with extensive velocity widths that may sig-

nify the presence of intermediate-mass black holes (Oka et al. 1999a,b). The existence
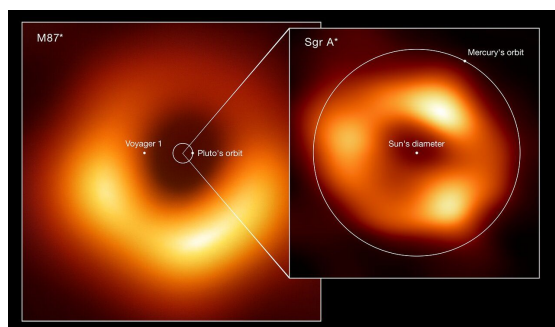
Figure 1.2: Sagittarius A^*

of black holes has recently been verified by observing their shadow templates. The Event Horizon Telescope revealed the existence of the event horizon of a supermassive black hole Messier 87^* ($M87^*$) in collaboration with the European BlackHoleCam group (Davoudiasl and Denton 2019) and also revealed Sagittarius A^* in our galaxy (see figure 1.2 [1]).

1.2   Black Hole Thermodynamics and Phase Transitions

One of the tremendous achievements of theoretical physics is the discovery of the correspondence between ordinary thermodynamic laws and the laws of black hole physics. This deep connection plays a vital role in guiding us towards a the theory of quantum gravity. The seminal work of Hawking and Bekenstein was the origin of the thermodynamics of black holes. They proposed a correspondence (Bekenstein 1972b,a, Hawking 1975) between the area of the black hole and its entropy, and between surface gravity at the horizon and temperature. Bardeen, Carter, and Hawking (Bardeen et al. 1973) showed that a black hole behaved as an object which follows the usual laws of thermodynamics. The original form of the first law of black hole thermodynamics is written by interpreting the mass of the black hole as internal energy. For an electrically charged rotating black hole, we have,

$$dM = TdS + \Omega dJ + \Phi dQ, \tag{1.5}$$

---

[1]https://cosmosmagazine.com/space/sagittarius-a-black-hole-image-nasa/

where temperature T and entropy S are related to surface gravity κ and area of event horizon A respectively. Ω and J are the angular velocities and the momentum associated with rotation; Q and Φ are the electric charge and potential. After the discovery of these thermodynamic laws, many researchers thought this was just a mathematical analogy because it was understood that black holes cannot radiate according to classical theory. This analogy began to be taken seriously only after the study of quantum particle-antiparticle production and annihilation near the black hole horizon by Hawking in 1975 (Hawking 1975) led to his famous discovery that black holes radiate like a black body at a temperature proportional to the surface gravity of the black hole horizon,

$$k_B T = \frac{\hbar \kappa}{2\pi c}, \tag{1.6}$$

where κ is the surface gravity [2], k_B is Boltzmann's constant , c is the light speed , and $\hbar$ is Planck's constant.

To understand the thermodynamics of black holes, first, people considered asymptotically flat cases (Hut 1977, Davies 1977). However, black holes in asymptotically flat space don't have a description in terms of a thermodynamic ensemble because it is an open system which does not have an equilibrium state. In the early nineties, people tried to construct gravitational theories within a bounded and finite spatial region of spacetime. Instead of asymptotically flat cases, one can consider an asymptotically curved spacetime. One way to do so is by introducing the cosmological constant Λ in the spacetime.

The cosmological constant is negative in the Anti-de Sitter (AdS) spacetime. Asymptotically AdS spacetime is like a confining box (see figure(1.3)). Hawking and Page (Hawking and Page 1983) first studied the thermodynamic behavior of black holes in an asymptotically AdS space. Their investigation found a phase transition between a spacetime containing only thermal radiation and one containing an AdS black hole. Phase transition of the AdS black hole in five dimensions has given more hints for the concept of AdS/CFT correspondence. The thermodynamic properties of various AdS black holes are investigated in the following literatures (Peca and Lemos 1999, Cai

---

[2]surface gravity = acceleration due to gravity
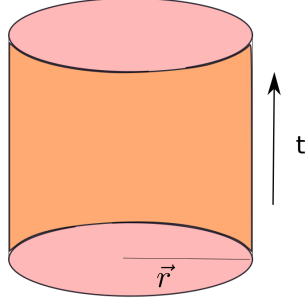
Figure 1.3: Penrose diagram of anti-de Sitter Space

2002, Myung et al. 2008b, Cvetič et al. 2002, Myung 2008, Birmingham 1999, Caldarelli et al. 2000, Chamblin et al. 1999a,b, Banerjee et al. 2011a,b, Gubser and Mitra 2001, Dey et al. 2007, Konoplya and Zhidenko 2008).

The cosmological constant is positive in an asymptotically de Sitter space. In addition to the event horizon, a cosmological horizon exists that also emits particles in this spacetime. Thermal equilibrium is possible only when the temperatures of both horizons are equal. The detailed study of the stability of charged de Sitter black hole is done by Carlip and Vaidya (Carlip and Vaidya 2003).

As shown by E. Witten, Hawking-Page phase transitions in the bulk of an AdS spacetime corresponds to the confinement-deconfinement phase transition of quark-gluon plasma in a gauge theory living on the boundary of that AdS spacetime (Witten 1998). The phase transition in the bulk spacetime is used to study specific field theories on its boundary by gauge gravity duality.

The pressure and volume term were absent in the first law (1.5) in literatures; remedied for that, the negative cosmological constant was identified as the pressure term with the volume of the spacetime being the corresponding conjugate variable (Kastor et al. 2009, Dolan 2011c,b,a, Teitelboim 1985, Brown and Teitelboim 1988) [4],

$$P = -\frac{\Lambda}{8\pi}.$$

(1.7)

---

[4]Refer chapter 2 for more details

8

$$dM = TdS + VdP + \Omega dJ + \Phi dQ. \tag{1.8}$$

The first law's extension with the pressure and volume term (1.8) leads to exciting developments in black hole thermodynamics. It was noticed that the black hole mass is more like the enthalpy H than internal energy U. With this identification, the phase diagram of AdS black hole was seen to be exactly same as that of the van der Waals liquid-gas transition (Chamblin et al. 1999b, Kubizňák and Mann 2012). There has been rapid progress in probing van der Waals fluid-like behavior in various black holes. An important feature of the black hole phase transition is that the four critical exponents are the same as in the van der Waals transition and therefore these two systems belong to the same universality class. It has led to a new avenue in theoretical high energy physics called black hole chemistry. Several studies have been carried out in different AdS black holes in the extended phase space, and the similarity as mentioned above to vdW system is observed (Gunasekaran et al. 2012, Belhaj et al. 2012, Altamirano et al. 2013, Zhao et al. 2013, Hendi and Vahidinia 2013, Chen et al. 2013b). These first-order phase transitions obey Maxwell's equal-area law and Clausius-Clapeyron equations (Spallucci and Smailagic 2013, Belhaj et al. 2015, Zhang et al. 2014, Zhao et al. 2015, Li et al. 2017).

1.2.1   Black Hole Heat Engine

A recent development in black hole thermodynamics is the holographic heat engine. The holographic heat engines are traditional heat engines but termed so by Clifford V. Johnson because conformal field theories can describe their operation on the boundary (Johnson 2014, Chakraborty and Johnson 2018). A sufficient amount of mechanical work can be drawn from heat energy in AdS black holes through this engine. In the first holographic heat engine constructed by Johnson for charged AdS black hole, he calculated the conversion efficiency of heat into work. The idea of holographic heat engine is realised in various other contexts, static dyonic and dynamic black hole (Jafarzade and Sadeghi 2017), polytropic black hole (Setare and Adami 2015), Born-Infield black holes (Johnson 2016b), $f(R)$ black holes (Zhang and Liu 2016), Gauss-Bonnet black holes (Johnson 2016c), higher dimensional theories (Belhaj et al. 2015,

Wei and Liu 2019), massive black hole (Mo and Li 2018, Hendi et al. 2018), in conformal gravity (Xu et al. 2017), in three dimensional charged BTZ black hole (Mo et al. 2017), in rotating black holes (Hennigar et al. 2017) and accelerating AdS black holes (Zhang et al. 2018).

1.2.2 Joule Thomson Expansion of Black Holes
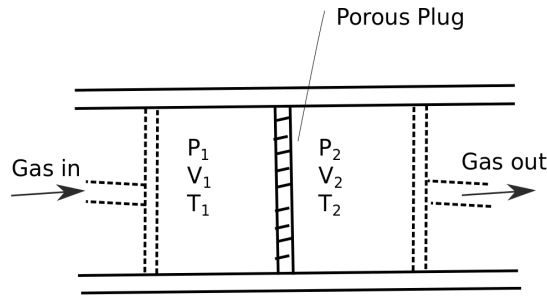
Figure 1.4: Joule Thomson Expansion

Okcu and Aydiner (Ökcü and Aydıner 2017) were the first to investigate the scope of black hole thermodynamics in the domain of Joule Thomson (JT) expansion. They investigated Joule Thomson expansion of charged AdS and Kerr AdS black hole and compared the result with the van-der Waals case. Joule-Thomson effect or throttling process happens in gas when it is allowed to move from the high-pressure region to the low-pressure region without any change in enthalpy (1.4). In the extended approach to thermodynamics, where black hole mass is understood as the enthalpy, the mass should remain constant during the process. This process is also called the isenthalpic process, leading to heating or cooling in the final phase. The JT coefficient μ, which is the gradient of temperature with pressure $(\mu = \frac{\partial T}{\partial P})$ determines the temperature change in the final phase. $\mu > 0$ implies a cooling and $\mu < 0$ heating. The point at which $\mu = 0$, denotes the position of inversion points (T_i, P_i). The inversion points distinguish the heating and cooling phases, and the inversion curve is the locus of inversion points for different isenthalpic curves.

Following the work of Okcu and Aydmer, there were many studies on JT expansion in various black holes such as in Kerr-AdS black hole (Ökcü and Aydıner 2018), higher
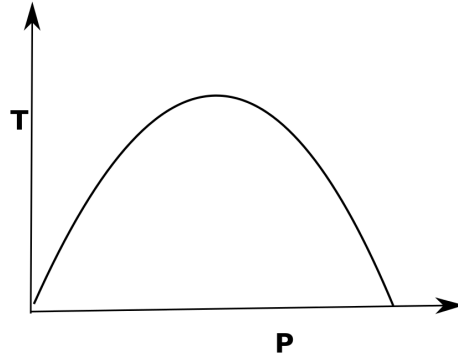
Figure 1.5: Schematic diagram of isenthalpic curve

dimensional AdS black hole (Ghaffarnejad et al. 2018), AdS black hole surrounded by quintessence (Mo et al. 2018), black holes in $f(R)$ gravity (Chabab et al. 2018), black holes in Lovelock gravity (Mo and Li 2020), Kerr-Newman AdS black holes (Zhao et al. 2018), charged Gauss-Bonnet black hole (Lan 2018), global monopole AdS black hole (Ahmed Rizwan et al. 2018). Recently, JT expansion is investigated in Einstein-Gauss-Bonnet AdS black hole with cloud of strings (Ghaffarnejad and Yaraie 2018), nonlinear electrodynamics AdS black hole (Kuang et al. 2018), AdS black holes with momentum relaxation (Cisterna et al. 2019), Einstein-Maxwell-Gauss-Bonnet AdS black holes (Haldar and Biswas 2018), regular Bardeen and Hayward AdS black hole (Li et al. 2020), non-linear charged AdS black hole in massive gravity (Hoang Nam 2019). Other noticeable studies are in charged accelerating AdS black hole of $f(R)$ gravity (Rostami et al. 2019), neutral AdS black holes in massive gravity (Lan 2019), Gauss-Bonnet massive black holes in the presence of external string cloud (Ranjbari et al. 2020), and hyperscaling violating black holes (Sadeghi and Toorandaz 2020).

1.2.3 Thermodynamic Geometry

The importance of differential geometry as a mathematical language with physical applications became clear after Albert Einstein's theory of gravity based on these tools

became a huge success. In the nineteenth century, Gibbs (Gibbs 1948) and Caratheodory (Carathéodory 1909) were the first to apply differential geometry to classical thermodynamics. Then Weinhold (Weinhold 1975) and later Ruppeiner (Ruppeiner 1979, 1983, 1995, 2008, Ruppeiner et al. 2012, Ruppeiner 2014) developed thermodynamic metric to investigate phase transitions and microscopic interactions in thermodynamic systems. Even though the discontinuity in the specific heat indicates the existence of a higher-order phase transition (Myung 2008, Caldarelli et al. 2000), it is not the best method to ultimately determine the nature of the phase transition. When we include statistical fluctuations, it is possible to define a metric which gives distance between two neighboring points in the state space. Doing so gives the state space, the structure of Riemannian manifold (Janyszek and Mrugała 1989, Ferrara et al. 1997, Cai and Cho 1999, Åman and Pidokrajt 2006, Sarkar et al. 2006, Shen et al. 2007, Åman et al. 2007, Myung et al. 2008a, Sahay et al. 2010, Niu et al. 2012, Weinhold 1975, Åman et al. 2003).

$$g_{ij}^R = -\partial_i \partial_j S(M, x^\alpha) \qquad (i, j = 1, 2), \qquad (1.9)$$

here, entropy S is a function of mass M and any other thermodynamic extensive variables x^α. The interaction between the states of the system is associated with Riemannian curvature, which can be derived from metric components given above (Ruppeiner 1979, 1995, 2007, 2008, Ruppeiner et al. 2012, Ruppeiner 2014, Weinhold 1975). In ordinary thermodynamics, scalar curvature becomes proportional to the correlation volume ξ^d of the thermodynamic system, where ξ is the correlation length and d is the spatial dimensionality of the system. In black hole thermodynamics, Ruppeiner (Ruppeiner 2008) interpreted the Ricci scalar R for black hole as the average number of correlated Plancks area on the event horizon . The divergence of Ricci scalar is associated with the divergence of specific heat (Ruppeiner 2008).

1.2.4 Bardeen Black Hole

The weak cosmic censorship hypothesis insists on the presence of singularity, hidden from the far observer by a membrane called the event horizon (Hawking and Penrose 1970, Hawking and Ellis 1973). All the spacetime solutions for Einstein's equa-

tions respect this conjecture. However, there are regular black hole spacetimes without singularity at the origin and possessing an event horizon. A repulsive de-Sitter core removes the singularity at the origin in regular black holes. For the first time, Bardeen, inspired by the works of Sakharov (Sakharov 1966b) and Gliner (Gliner 1966) came up with a regular black hole solution (Bardeen 1968). Following the idea of Bardeen, later, several regular solutions for Einstein's equations coupled to nonlinear electrodynamic sources were found (Hayward 2006, Ayon-Beato and Garcia 1998, Ayón-Beato and Garcıa 2000). The black hole thermodynamics in regular black holes are studied in detail (Man and Cheng 2014, 2013, Estrada and Aros 2019, Nam 2018, Ali and Ghosh 2018, Kumar et al. 2019).

The Bardeen black hole is found to be the solution to Einstein's gravity when it is coupled to a non-linear electrodynamics source with a negative cosmological constant Λ. We will look at an action,

$$\mathcal{S} = \frac{1}{16\pi} \int d^4x \sqrt{-\tilde{g}} (R - 2\Lambda - \mathcal{L}(\mathcal{F})), \tag{1.10}$$

in which R symbolises the Ricci scalar, and $\tilde{g}$ the determinant of the metric tensor $\tilde{g}_{\mu\nu}$. $\mathcal{L}(\mathcal{F})$ is the non-linear electrodynamics Lagrangian density, which is a function of field strength $\mathcal{F} = F_{\mu\nu}F^{\mu\nu}$ with $F_{\mu\nu} = \partial_\mu A_\nu - \partial_\nu A_\mu$. The Einstein and Maxwell equations of motion,

$$G_{\mu\nu} + \Lambda g_{\mu\nu} = T_{\mu\nu}, \quad \nabla_\mu \left(\frac{\partial \mathcal{L}(\mathcal{F})}{\partial \mathcal{F}} F^{\mu\nu} \right) = 0, \quad \nabla_\mu \left(*F^{\nu\mu} \right) = 0, \tag{1.11}$$

are obtained by varying the action (eqn.1.10). $T_{\mu\nu} = 2 \left(\frac{\partial \mathcal{L}(\mathcal{F})}{\partial \mathcal{F}} F_{\mu\lambda} F_\nu^\lambda - \frac{1}{4} g_{\mu\nu} \mathcal{L}(\mathcal{F}) \right)$ is the energy momentum tensor, while $G_{\mu\nu}$ is the Einstein tensor. In the case of Bardeen black holes, the Lagrangian density is,

$$\mathcal{L}(\mathcal{F}) = \frac{12}{\alpha} \left(\frac{\sqrt{\alpha\mathcal{F}}}{1 + \sqrt{\alpha\mathcal{F}}} \right)^{\frac{5}{2}}, \tag{1.12}$$

where α is a positive quantity with dimension [Length]^2. For Maxwell's field tensor,

13

we use

$$F_{\mu\nu} = 2\delta^{\theta}_{[\mu}\delta^{\phi}_{\nu]}Q(r)\sin\theta, \tag{1.13}$$

as an ansatz.

However, according to Maxwell's equations (eqn.1.11), $dF = \frac{dQ(r)}{dr}dr \wedge d\theta \wedge d\phi = 0$, where $Q(r)$ must be a constant Q_m. The non-vanishing components of Maxwell's field tensor for a spherically symmetric solution are F_{tr} and $F_{\theta\phi}$. We choose gauge potential and Maxwell's field tensor to be,

$$A_{\mu} = Q_m\cos\theta\,\delta^{\phi}_{\mu}, \quad F_{\theta\phi} = -F_{\phi\theta} = Q_m\sin\theta, \tag{1.14}$$

where Q_m is the magnetic monopole charge, because we want a magnetically charged regular solution.

$$F = \frac{2Q_m^2}{r^4}, \tag{1.15}$$

is the scalar function F derived from $F_{\theta\phi}$. Lagrangian density $\mathcal{L}(\mathcal{F})$ can be rewritten as a function of radial distance,

$$\mathcal{L}(r) = \frac{12}{\alpha}\left(\frac{2\alpha Q_m^2}{r^2 + 2\alpha Q_m^2}\right)^{\frac{5}{2}}. \tag{1.16}$$

With the metric function $f(r) = 1 - \frac{2m(r)}{r} - \frac{\Lambda r^2}{3}$, a static spherically symmetric solution for Einstein's equation can be written as

$$ds^2 = -f(r)dt^2 + \frac{dr^2}{f(r)} + r^2(d\theta^2 + \sin^2\theta d\phi^2). \tag{1.17}$$

The Einstein's equation is solved using the line element to fix the functional form of $m(r)$.

$$\frac{1}{r^2}\partial_r m(r) - \Lambda = \frac{1}{4}\mathcal{L}(r), \tag{1.18}$$

$$\frac{1}{r}\partial_r^2 m(r) - \Lambda = \left(\frac{1}{4}\mathcal{L}(r) - \frac{\partial\mathcal{L}}{\partial\mathcal{F}}F_{\theta\phi}F^{\theta\phi}\right), \tag{1.19}$$

are the G_{tt} and G_{rr} components of Einstein's equation.

We obtain the mass function $m(r)$ for a regular Bardeen AdS black hole as,

$$m(r) = \frac{\Lambda r^3}{6} + \frac{Mr^3}{(\beta^2 + r^2)^{\frac{3}{2}}}, \qquad (1.20)$$

where M is the black hole's mass and β is the charge parameter associated to total charge Q_m,

$$Q_m = \frac{\beta^2}{\sqrt{2\alpha}}, \qquad (1.21)$$

by integrating the aforementioned differential equations. As a result, the line element for Bardeen AdS black hole is written with the metric function,

$$f(r) = 1 - \frac{2Mr^2}{(\beta^2 + r^2)^{\frac{3}{2}}} - \frac{\Lambda r^2}{3}. \qquad (1.22)$$

In recent times, the black holes with quintessence have attracted wide attention. The quintessence is one of the most important candidates to explain the universe's accelerated expansion. The observational cosmological data supports the equation of state $p_q = \omega_q \rho_q$, where quintessence state parameter varies as $-1 < \omega_q < -1/3$. The energy density for quintessence has the form $\rho_q = -\frac{a}{2}\frac{3\omega_q}{r^{3(\omega_q+1)}}$, where a is normalization factor related to quintessence. The spherically symmetric black hole solution with quintessence was first obtained by Kiselev (Kiselev 2003). Since then, several attempts to investigate the thermodynamics of black holes with quintessence were carried out (Wei and Chu 2011, Li 2014, Thomas et al. 2012, Tharanath and Kuriakose 2013, Saleh et al. 2018).

1.3 Objectives of the Present Research Work

The Bardeen model is the most significant regular black hole model, generating much interest in regular black hole research to make strong-field gravity an exciting subject. We may now overcome pathologies in general relativity, such as the existence of spacetime singularity, using these models. As a result, studying the thermodynamics of these regular black holes is essential. This thesis's main objective is the study of "Extended Phase Space Thermodynamics of Regular Bardeen Black Hole". The work specifically focuses on:

- Study the phase transition of regular Bardeen AdS black holes by analyzing Hawking temperature, mass, entropy, and heat capacity in the extended phase space and investigate the influence of quintessence parameters in the phase transition.

- Study the heat engine constructed out of regular Bardeen AdS black holes and investigate the effect of quintessence on the engine's efficiency.

- Investigate the Joule Thomson expansion of regular Bardeen AdS black hole with quintessence through the inversion temperature and isenthalpic curves.

- Investigate the phase transition and thermodynamic geometry of regular Bardeen AdS black holes in higher dimensions.

1.4 Organization of the Thesis

The thesis is organized as follows:

Chapter 1 gives a brief introduction with history and evidence of the black holes. Next, we discuss the thermodynamic phase transition and its application to black holes and introduce Bardeen black holes. The objectives of this research and the thesis organization are included at the end of this chapter.

Chapter 2 gives a brief explanation of the laws of black hole thermodynamics. The involvement of pressure term in the first law using Smarr relation and the extended phase space thermodynamics of black holes are briefly discussed.

Chapter 3 shows the thermodynamics and phase transition of regular Bardeen AdS black holes and explains the influence of quintessence parameters on thermodynamics.

Chapter 4 shows that the efficiency of a heat engine is increased by adding a quintessence field, which is constructed of regular black holes. The heat engine's efficiency is calculated and compared to that of the conventional Carnot engine. The effect of magnetic charge and quintessence parameter on efficiency is investigated in depth.

chapter 5 explains the Joule-Thomson Expansion of Regular Bardeen AdS Black Hole Surrounded by Quintessence Field. Using the Joule-Thomson coefficient, the inversion and isenthalpic curves are discussed.

Chapter 6 shows the thermodynamics and also explains the thermodynamic geometry of regular Bardeen black holes in higher dimensions.

Chapter 7 summarizes the essential findings of the present research work by highlighting the thesis's remarkable results and conclusions.

Chapter 2

Fundamentals of Black Hole Thermodynamics

This chapter presents a brief introduction to the fundamentals and laws of black hole thermodynamics, followed by their extension to anti-de Sitter spacetime. The extended phase space thermodynamics is also briefly discussed.

2.1 Introduction

The relationship between thermodynamics, gravitation, and quantum theory has attracted researchers' attention over the last fifty years, owing to increasing evidence that such a relationship exists. The evidence for this is found in the subject of black hole thermodynamics, which describes the thermodynamic behavior of black holes. Due to the black hole's classical nature, which absorbs all types of matter but emits nothing, this relationship is counter-intuitive (Bardeen et al. 1973). As a result of no hair theorem, it should not have a entropy or temperature, and its only properties are mass, angular momentum, and, if possible, charge. Bekenstein introduced the idea that the area of a black hole corresponds to its entropy (Bekenstein 1972a), and Hawking found that the black hole's surface gravity corresponds to its temperature (Hawking

1975). These findings led to a new way of thinking about black holes as black bodies. The sub-discipline of black hole thermodynamics was born as a result.

Thermodynamics is a general and powerful approach in physics for understanding a system's physical properties and a wide range of phenomena. The vital part of thermodynamics is that it does not require knowledge of microscopic details to investigate macroscopic physics. However the thermodynamic state of a system is ultimately determine by the microscopic structure of the system. This characteristic is beneficial when working with systems such as black holes, where the microscopic details are not well understood. Black holes are thermodynamic systems and therefore like all thermodynamic systems, they have a rich class of phase transitions which can be used to investigate their properties under the heading of "black hole chemistry".

The phase transition and related phenomena in AdS spaces are an important aspect of black hole thermodynamics. Following the identification of the cosmological constant with the thermodynamic pressure (1.7) and the resulting modification of the first law (1.8) (Kastor et al. 2009, Dolan 2011b), researchers have been increasingly interested in AdS black hole thermodynamics. The phase diagram of AdS black holes was shown to be the same as that of a van der Waals like fluid and which could also exhibit with the possibility of reentrant phase transitions (RPT) (Kubizňák and Mann 2012, Gunasekaran et al. 2012, Kubizňák et al. 2017).

The goal of this chapter is to provide an overview of black hole chemistry. To begin, we will go through the fundamentals of black hole thermodynamics. For asymptotically flat and asymptotically AdS black holes, the Smarr relation is stated. We will describe the methods for obtaining the first law of black hole physics in AdS spacetime, motivated by the inclusion of the dynamical cosmological constant in black hole thermodynamics.

2.2   Laws of Black Hole Thermodynamics

According to Hawking's area theorem (Hawking 1972), the event horizon area of a black hole never decreases. Bekenstein observed the resemblance between area law and the second law of thermodynamics and he suggested (Bekenstein 1972a) that a black hole should have an entropy that is proportional to the event horizon area. Follow-

ing these proposals, Bardeen, Carter, and Hawking constructed the four laws of black hole thermodynamics (Bardeen et al. 1973) under the assumption that the event horizon of the black hole is a Killing horizon which is a null hypersurface generated by a corresponding Killing vector field. The four laws are as follows:

Zeroth law: The surface gravity κ is constant over the event horizon of a stationary black hole.

First Law: When a system, like a black hole, shifts from one stationary state to another, the first law states that the system's mass changes,

$$\delta M = \frac{\kappa}{8\pi G}\delta A + \Omega \delta J + \Phi \delta Q. \tag{2.1}$$

Second law: The event horizon area of the black hole never decreases, i.e., $\delta A \geq 0$.

Third law: It is impossible to reduce the surface gravity to zero in a finite number of steps.

These laws show the connection between black hole mechanics and ordinary thermodynamics, with the first law of ordinary thermodynamics given as,

$$\delta E = T\delta S - P\delta V + \sum_i \mu_i \delta N_i + \Phi \delta Q. \tag{2.2}$$

Comparing (2.1) and (2.2) we see that it is possible to identify surface gravity with temperature, and the event horizon area with black hole's entropy in this analogy.

Hawking implemented Parker's (Parker 1969) original formalism for calculating particle production in curved spacetimes in 1974. He found that when the quantum mechanical effects of scalar fields are taken into account, a black hole emits radiation at a certain temperature (1.6).

The comparison of the $T\delta S$ term in the first law of thermodynamics (2.2) with the $\kappa \delta A$ term for black holes (2.1), which was later verified by Gibbons using the Euclidean path integral approach (Gibbons and Hawking 1977), implies that entropy is

proportional to area.

$$S = \frac{Ac^3}{4\hbar G}.$$ (2.3)

The existence of $\hbar$ in this expression highlights black holes' quantum mechanical essence. The parameters in (2.1) are connected by the Smarr relation (Smarr 1973), which reads

$$M = 2(TS + \Omega J) + \Phi Q.$$ (2.4)

There has been much discussion about a fundamental relationship between black hole horizons and thermal ensembles because of the striking similarity between these black hole thermodynamic laws and classical thermodynamics. However, it is worth noting that the first law lacks the "work" term PdV that is common in classical thermodynamics. The notion of thermodynamic pressure and volume is not readily apparent in black hole spacetime.

2.3 Smarr Relations

The Smarr relation, or integral mass formula, was used to formulate the laws of black hole thermodynamics. Smarr (Smarr 1973) observed that the first law of black hole mechanics,

$$dM = \mathcal{T}dA + \Omega dJ + \Phi dQ,$$ (2.5)

applies to the Kerr black hole, where $\mathcal{T}$ is the effective surface tension. This expression can also be expressed in integral form as,

$$M = 2TS + 2\Omega J + \Phi Q.$$ (2.6)

In conventional thermodynamics, the Smarr formula is analogous to the Gibbs-Duhem relation. The black hole mass M is a homogeneous function of (A, J, Q) and therefore the integration of Eq. (2.5) to yield Eq. (2.6) is possible using Euler's homogeneous function theorem. This procedure is carried out in conventional thermodynamics by considering energy to be a homogenous function of extensive thermodynamic variables. It is also worth noting that the Smarr formula is not restricted to a particular black hole

solution or spacetime dimension. Myers and Perry showed that this relationship exists in higher dimensions as well (Myers and Perry 1986).

2.3.1 Smarr Formula for Asymptotically Flat Black Holes

Consider a stationary, axisymmetric black hole solution with a timelike Killing vector t^α and a rotational Killing vector ϕ^α, in the spacetime. On the black hole's event horizon, the combination of Killing vectors,

$$\xi^\alpha = t^\alpha + \Omega \phi^\alpha, \tag{2.7}$$

is a null vector, where Ω is the angular velocity of the horizon. Thus, the event horizon is a Killing horizon and ξ^α is tangent to the horizon's null generators. Let us denote κ as the surface gravity, which remains constant throughout the event horizon as a consequence of zeroth law. On the horizon, κ is therefore described by the relation,

$$\xi_\beta \xi^{\alpha;\beta} = \kappa \xi^\alpha. \tag{2.8}$$

Consider a spatial slice Σ with future-directed normal n^α that extends from the event
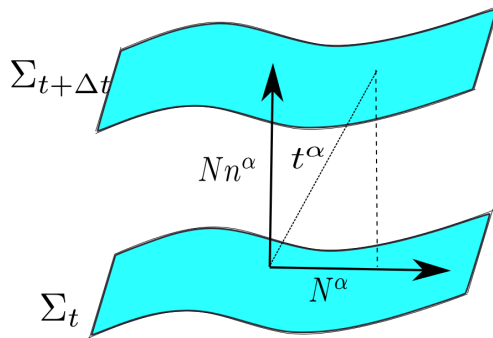
Figure 2.1: Foliation of spacetime. A spacetime $(\mathcal{M}, g_{\mu\nu})$ can be decomposed into two space like hypersurfaces Σ_t and $\Sigma_{t+\Delta t}$. A height function $t^\alpha = Nn^\alpha + N^\alpha$, where N is the lapse function, n^α is the unit timelike normal and N^α is the shift funcion.

horizon to infinity (2.1). We integrate

$$I = \int_\Sigma d\Sigma_\alpha \nabla_\beta \nabla^\beta \xi^\alpha, \tag{2.9}$$

on this hypersurface Σ. The aforementioned integration is assessed in two ways. We apply the relation $\nabla_\beta \nabla^\beta \xi^\alpha = -R^\alpha{}_\beta \xi^\beta$ in the first approach, which arises from the fact that ξ^α is a Killing vector. Assuming the vacuum Einstein equations apply,

$$\int_\Sigma d\Sigma_\alpha \nabla_\beta \nabla^\beta \xi^\alpha = -\int_\Sigma d\Sigma_\alpha R^\alpha{}_\beta \xi^\beta = 0. \tag{2.10}$$

Stokes' theorem is used in the second approach. Stokes' theorem for an antisymmetric tensor B is (Poisson 2004),

$$\int_\Sigma dA_\alpha \nabla_\beta B^{\alpha\beta} = \frac{1}{2} \oint_{\partial\Sigma} dS_{\alpha\beta} B^{\alpha\beta}. \tag{2.11}$$

Two $(D-2)$ dimensional surfaces, S_∞ and $\mathscr{H}$, are included in the integration over $\partial\Sigma$.
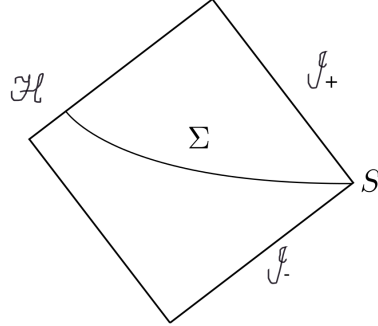
Figure 2.2: Spacelike hypersurface in black-hole spacetime. Spacelike hypersurface Σ extending from the event horizon $\mathscr{H}$ to spatial infinity S.

Where $dS_{\alpha\beta}$ is the two-dimensional surface element, S_∞ denotes the boundary of the spatial slice Σ at spatial infinity, and $\mathscr{H}$ denotes at the event horizon. Combining (2.10) and (2.11) we find,

$$0 = \oint_{\mathscr{H}} dS_{\alpha\beta} \nabla^\alpha \xi^\beta - \oint_{S_\infty} dS_{\alpha\beta} \nabla^\alpha \xi^\beta, \tag{2.12}$$

By taking advantage of the fact that we are assuming a vacuum solution, we may describe the integration at spatial infinity in terms of total mass and angular momentum. The Komar integrals, which in D dimensions read as (Poisson 2004)

$$M = -\frac{1}{16\pi G_N}\left(\frac{D-2}{D-3}\right)\oint_{S_\infty} dS_{\alpha\beta}\nabla^\alpha t^\beta, \tag{2.13}$$

$$J = \frac{1}{16\pi G_N}\oint_{S_\infty} dS_{\alpha\beta}\nabla^\alpha \Phi^\beta, \tag{2.14}$$

where G_N is the Newton's constant in D dimensions, yield the total mass and angular momentum of the spacetime. The integration at spatial infinity S_∞ is reduced to the following form using these Komar integrals:

$$\oint_{S_\infty} dS_{\alpha\beta}\nabla^\alpha \xi^\beta = 16\pi\left[\Omega_H J - \left(\frac{D-3}{D-2}\right)M\right]. \tag{2.15}$$

Now it's time to assess the horizon integral. We use the fact that $dS_{\alpha\beta} = 2\xi_{[\alpha}N_{\beta]}\sqrt{\sigma}d^{D-2}x$, where N^α is a normalised null vector on the event horizon with $\xi^\alpha N^\alpha = -1$ and σ is the determinant of the induced metric on the event horizon. With these inputs, we have

$$\oint_{\mathscr{H}} dS_{\alpha\beta}\nabla^\alpha \xi^\beta = 2\oint_{\mathscr{H}}\sqrt{\sigma}d^{D-2}x\xi_\alpha N_\beta\nabla^\alpha \xi^\beta \tag{2.16}$$

$$= 2\kappa\oint_{\mathscr{H}}\sqrt{\sigma}d^{D-2}xN_\beta\xi^\beta \tag{2.17}$$

$$= -2\kappa A. \tag{2.18}$$

We used the relation $\nabla^\alpha \xi^\beta = -\nabla^\beta \xi^\alpha$ to reduce the preceding equations since ξ^α is a Killing vector, which simplifies the contraction with the surface element. Then we used the previous relation, $\xi_\alpha\nabla^\alpha \xi^\beta = \kappa\xi^\beta$, to get the surface gravity term κ. Finally, the remaining integration is performed using the relation $N_\beta\xi^\beta = -1$, which yields the event horizon's area. We get,

$$(D-3)M = (D-2)\frac{\kappa A}{8\pi} + (D-2)\Omega_H J. \tag{2.19}$$

by combining the integrations we evaluated over S_∞ and $\mathscr{H}$. The Smarr formula, which we obtained using scaling arguments, can be identified by identifying the terms $T = \frac{\kappa}{2\pi}$

25

and $S = \frac{A}{4}$.

2.3.2 Smarr Formula for AdS Black Holes

Using the geometric method, we used the assumption of vacuum Einstein equations with a vanishing cosmological constant to construct the Smarr formula for an asymptotically flat black hole. In this section we derive the Smarr formula for a spacetime with a non-zero cosmological constant.

First we will illustrate how the difference originates, and then use the geometric method to offer the right Smarr formula. We will use the four-dimensional Schwarzschild-AdS black hole as an example, which has the metric

$$ds^2 = -f(r)dt^2 + \frac{dr^2}{f(r)} + r^2 d\Omega^2. \tag{2.20}$$

The metric function is

$$f(r) = 1 - \frac{m}{r} + \frac{r^2}{\ell^2}, \tag{2.21}$$

where ℓ is the AdS length, which is equal to $\Lambda = -\frac{3}{\ell^2}$ in terms of the cosmological constant. The temperature and entropy of the black hole are given by,

$$T = \frac{\kappa}{2\pi} = \frac{1}{4\pi r_h}\left[1 + \frac{3r_h^2}{\ell^2}\right], \qquad S = \frac{A}{4} = \pi r_h^2, \tag{2.22}$$

where r_h is the horizon radius.

The conserved quantity corresponding to the Killing vector[6] $t^\alpha = \delta_t^\alpha$ is expected to be the mass, but there is an issue with that assumption. To find the conserved charge, we note that, the non vanishing components of the entity $\nabla^\alpha t^\beta$ for Killing vector t^α are given by (Kastor et al. 2009),

$$\nabla^t t^r = -\nabla^r t^t = -\frac{m}{2r^2} - \frac{r}{\ell^2}, \tag{2.23}$$

---

[6]If X is a Killing vector field and $\gamma : (a,b) \to M$ is a geodesic in a Riemannian manifold (M,g). Let $Y = \dot{\gamma}$ then $\frac{d}{dt}Y_a X^a = 0$. the function $g(\dot{\gamma}, X)$ is conserved along the geodesic.

The usual definition of the Komar integral gives a diverging result,

$$M = -\frac{1}{8\pi} \oint_{S_\infty} dS_{\alpha\beta} \nabla^\alpha t^\beta = \frac{1}{4\pi} \lim_{R_0 \to \infty} \oint_{S_{R_0}} R_0^2 \left(\frac{m}{2R_0^2} + \frac{R_0}{\ell^2} \right) \sin\theta d\theta d\phi \to \infty. \quad (2.24)$$

Second term in the above equation goes as R_0^3 and diverges. The cosmological constant, which contributes an infinite quantity of energy, is responsible for the divergence. We can get around this problem by terminating the integral at a finite region R_0, subtracting the $m = 0$ contribution, and extending the finite cutoff to infinity. This gives,

$$M = \frac{m}{2}. \quad (2.25)$$

The mass, temperature, and entropy we acquired, however, do not satisfy the Smarr formula (2.19) with $\Omega_H = 0$, which is

$$M - 2TS = -\frac{r_h^3}{\ell^2} \neq 0. \quad (2.26)$$

This inconsistency in the Smarr formula in AdS spacetime necessitates a reconsideration of the cosmological constant term. We will use the geometric method to get the modified Smarr formula.

The introduction of a Killing potential, as done by (Kastor 2008) is the main component of the geometric approach in AdS spacetime, from which the extended Smarr formula can be derived (Kastor et al. 2009). For simplicity, we start with a static black hole solution. Because a Killing vector ξ^α satisfies the relation $\nabla_\alpha \xi^\alpha = 0$, we can represent the vector ξ^α as

$$\xi^\alpha = \nabla_\beta \omega^{\beta\alpha}, \quad (2.27)$$

using the Poincare lemma [7], where the anti symmetric tensor $\omega^{\alpha\beta} = \omega^{[\alpha\beta]}$ is the Killing potential. Using the Killing vector identity $\nabla_\alpha \nabla^\alpha \xi^\beta = R_{\beta\gamma} \xi^\gamma$ and the assumption of vacuum Einstein equations $R_{\alpha\beta} = \frac{2\Lambda}{(D-2)} g_{\alpha\beta}$, we can show that the Komar integral re-

---

[7]This is more common in the language of forms. As a result of Killing's equation, a Killing vector ξ^α satisfies $\nabla_\alpha \xi^\alpha = 0$. In 1-form $\xi = \xi_\alpha dx^\alpha$ this is $*d*\xi = 0$. Poincare's lemma implies that $*\xi$ may be represented locally as $*\xi = d*\omega$, where ω is a 2-form. This is equivalent to $\xi = *d*\omega$ or $\xi^\beta = \nabla_\alpha \omega^{\alpha\beta}$ in components.

lation (Kastor et al. 2009),

$$\int_{\partial\Sigma} dS_{\alpha\beta}\left(\nabla^\alpha\xi^\beta + \frac{2}{D-2}\Lambda\omega^{\alpha\beta}\right) = 0, \qquad (2.28)$$

where the integration is done on the boundary of a hypersurface Σ. The integration is the sum of two contributions, one from the sphere at infinity S_∞ and the other from a cross-section of the event horizon $\mathcal{H}$, as in the initial calculations. The asymptotic behavior of the AdS spacetime, which is investigated by Henneaux and Teitelboim (Henneaux and Teitelboim 1985), is required to evaluate the integral at infinity. Ref. ((Ashtekar and Magnon 1984, Ashtekar and Das 2000) also has a detailed discussion on this. For a static black hole, the asymptotic behaviour is given by

$$ds^2 = \left[-f_0 + \frac{c_t}{r^{D-3}}\right]dt^2 + \frac{1}{f_0}\left[\frac{1-(D-1)(D-2)c_r}{2\Lambda r^{D-1}}\right]dr^2 + \left[1 + \frac{2\Lambda}{(D-1)(D-2)}\frac{c_\theta}{r^{D-1}}\right]r^2 d\Omega_{D-2}^2, \qquad (2.29)$$

where

$$f_0 = 1 - \frac{2\Lambda}{(D-1)(D-2)}r^2. \qquad (2.30)$$

We can show that $c_t = c_r = m$ and $c_\theta = 0$ in the case of Einstein equations with negative Λ and localised stress energy source with no angular momentum. The Schwarzschild AdS black hole metric,

$$ds^2 = -f(r)dt^2 + \frac{1}{f(r)}dr^2 + r^2 d\Omega_{D-2}, \qquad (2.31)$$

is then reduced to the large r behaviour of the metric, with

$$f(r) = 1 - \frac{m}{r^{D-3}} - \frac{2\Lambda r^2}{(D-1)(D-2)}. \qquad (2.32)$$

For pure AdS spacetime, the Killing potential

$$\omega^{rt}_{r\to\infty} = -\omega^{tr}_{r\to\infty} = \frac{r}{D-1}, \qquad (2.33)$$

and

$$\nabla^r \xi^t = -\nabla^t \xi^r = \frac{(D-3)m}{2r^{D-2}} - \frac{2\Lambda r}{(D-1)(D-2)}, \tag{2.34}$$

are the non-zero components of the Killing potential now. The integration at infinity (2.14), as well as the term with Killing potential and the divergence term,

$$\int_{S_\infty} dS_{\alpha\beta} \left(\nabla^\alpha \xi^\beta + \frac{2}{D-2} \Lambda \omega^{\alpha\beta} \right) = -16\pi \frac{D-3}{D-2} M, \tag{2.35}$$

$$\int_{\mathscr{H}} dS_{\alpha\beta} \left[\nabla^\alpha \xi^\beta + \frac{2}{D-2} \Lambda \omega^{\alpha\beta} \right] = -2\kappa A + \frac{2\Lambda}{D-2} \left[\int_{\mathscr{H}} ds_{\alpha\beta} \omega^{\alpha\beta} \right], \tag{2.36}$$

where the first term is derived as in the case of asymptotically flat spacetime, is obtained by integrating on the cross section of the horizon. When all of the aforementioned results are added together, we get the extended Smarr formula,

$$(D-3)M = (D-2)TS - 2PV, \tag{2.37}$$

where the pressure and volume terms are,

$$P = -\frac{\Lambda}{8\pi G_N}, \tag{2.38}$$

and

$$V = -\frac{1}{2} \int_{\mathscr{H}} dS_{\alpha\beta} \omega^{\alpha\beta}, \tag{2.39}$$

respectively. The generalization of the earlier derivation to incorporate angular momentum is simple (Cvetič et al. 2011).

2.3.3 Thermodynamics of Black Holes in AdS Space

In AdS spacetime, we derive the first law of black hole mechanics using the Hamiltonian formalism (Mann 2015). It results from choosing an appropriate spacelike hypersurface Σ and considering the Killing vector ℓ^a to be the generator of a Killing horizon. Let's start with the relationship $g_{\alpha\beta} = -n_\alpha n_\beta + h_{\alpha\beta}$, where $n_\alpha n^\alpha = -1$ and $n^\alpha h_{\alpha\beta} = 0$.

$$H = -16\pi G_N T_{\alpha\beta} n^\alpha n^\beta, \qquad H_\alpha = -16\pi G_N T_{\sigma\beta} n^\sigma h_\alpha^\beta, \tag{2.40}$$

are the contractions of the Einstein tensor with a unit normal. We get $H = -2\Lambda$ and $H_\alpha = 0$ if the cosmological constant is the only source of stress energy. The total gravitational Hamiltonian is $\mathscr{H} = \sqrt{h}\,[N(H+\Lambda)+N^\alpha H_\alpha]$ if we consider the evolution of the system along the vector field $\xi^\alpha = Nn^\alpha + N^\alpha$, where $n_\alpha N^\alpha = 0$. The lapse function is $N = -\xi.n$, and the shift is N^α, which is tangential to Σ. The lapse function measures the proper time, while the shift function measures changes in spatial coordinates.

$$N\delta H + N^\alpha \delta H_\alpha = -D_\alpha B^\alpha = -2N\delta N, \tag{2.41}$$

is obtained by considering the perturbation $h_{\alpha\beta} \to h_{\alpha\beta} + s_{\alpha\beta}$, $\pi^{\alpha\beta} \to \pi^{\alpha\beta} + p^{\alpha\beta}$ ($\pi^{\alpha\beta}$ is the conjugate momentum), and $\Lambda \to \Lambda + \delta\Lambda$, and performing a simple computation, where

$$B^\alpha = N\left[D^\alpha s - D_\beta s^{\alpha\beta}\right] - sD^\alpha N + s^{\alpha\beta}D_\beta N + \frac{1}{\sqrt{h}}N^\beta\left[\pi^{\sigma\rho}s_{\sigma\rho}h^\alpha_\beta - 2\pi^{\alpha\sigma}s_{\beta\sigma} - 2p^\alpha_\beta\right]. \tag{2.42}$$

Since $N = -n_\alpha\xi^\alpha = -n_\alpha\nabla_\beta\omega^{\beta\alpha} = -D_\beta(n_\alpha\omega^{\beta\alpha})$, we have,

$$D_\alpha\left[B^\alpha + 2\omega^{\alpha\beta}n_{\alpha\beta}\delta\Lambda\right] = 0 \implies I := \oint_{\partial\Sigma} dA_\alpha\left[B^\alpha + 2\omega^{\alpha\beta}n_{\alpha\beta}\delta\Lambda\right] = 0. \tag{2.43}$$

The Killing Potential is the antisymmetric tensor $\omega^{\alpha\beta}$. Two bounds are included in the integration over $\partial\Sigma$: one at the black hole horizon and the other at infinity.

$$\oint_{S_\alpha} dA_\alpha B^\alpha = -16\pi G_N\delta N - \lim_{r\to\infty}\left(\frac{2r^{D-1}\Omega_{D-2}}{D-1}\right)\delta\Lambda, \tag{2.44}$$

and

$$\oint_{S_\alpha} dA_\alpha\left(2\omega^{\alpha\beta}n_\beta\delta\Lambda\right) = \lim_{r\to\infty}\left(\frac{2r^{D-1}\Omega_{D-2}}{D-1}\right)\delta\Lambda, \tag{2.45}$$

are obtained by evaluating the integral at infinity with appropriate inputs.

It's worth noting that the term due to the Killing potential wipes out the divergence caused by the change in Λ. At the horizon of a black hole, we get,

$$\oint_h dA_\alpha B^\alpha = 2\kappa\delta A, \tag{2.46}$$

where A is the horizon area and κ is the surface gravity. We rewrite the term with Killing potential as,

$$\oint_h dA_\alpha \left(2\omega^{\alpha\beta} n_\beta \delta\Lambda \right) = 2 \left(\oint_h dA_\alpha \omega^{\alpha\beta} n_\beta \right) \delta\Lambda. \tag{2.47}$$

The first law of black hole thermodynamics is,

$$\delta M = \frac{\kappa}{2\pi} \frac{\delta A}{4} + V\delta P = T\delta S + V\delta P, \tag{2.48}$$

which is obtained by combining the previous results. The pressure and volume terms are identified as ,

$$P = -\frac{\Lambda}{8\pi G_N} \quad \text{and} \quad V = -\oint_h dA_\alpha \omega^{\alpha\beta} n_\beta. \tag{2.49}$$

This agrees with the Smarr relation $M = 2(TS - PV)$ that we found in the previous section. We should consider the mass of the black hole as enthalpy rather than internal energy in extended thermodynamics because the enthalpy $H = E + PV$ satisfies $\delta H = T\delta S + V\delta P$.

2.4 Extended Phase Space and Wald's Formalism of the First Law

The extended version of the first law (Kastor et al. 2009, Dolan 2011c,b,a) was obtained when the cosmological constant (Λ) was taken as a variable in AdS spacetime, and the canonical definition of P and V was provided, where the pressure P was identified as $-\Lambda/8\pi$ and its conjugate quantity was interpreted as the thermodynamic volume (V). Later, it was discovered (Kubizňák and Mann 2012, Kubizňák et al. 2017, Bhattacharya et al. 2017, Majhi and Samanta 2017) that this identification is consistent throughout black hole thermodynamics and that the phase space diagram (i.e., the $P-V$ diagram), the $P-T$ diagram, the equations of state, and the behavior of the Gibbs free energy – all are very similar to the van der Waals fluid system in ordinary thermodynamics. Furthermore, the van der Waals criticality was discovered, which occurs when the two

independent conditions coincide, i.e. $(\partial P / \partial V)_{T,Y_i} = 0 = \partial^2 P / \partial V^2)_{T,Y_i}$. The technique for finding the thermodynamic first law in the extended phase space using Wald's approach is described below, with Λ as a variable.

The first law in extended phase space differs slightly from the first law in non-extended phase space. Here the black hole's mass M, is regarded as the system's enthalpy rather than its internal energy. Furthermore, as we will see, defining thermodynamic volume is not an easy task. The charge will not be included in the proof of the first law for the sake of simplicity. Due to the diffeomorphism invariance in the present instance, we must first properly identify the Noether current and potential to follow Wald's formalism. We will use the off-shell formulation to get the Noether current and potential at the operational level.

The action of an AdS black hole with a cosmological constant is denoted by

$$A = \int d^4 x \sqrt{-g} L = \frac{1}{16\pi} \int \sqrt{-g} (R - 2\Lambda). \qquad (2.50)$$

Take the variation of the total action to get the equation of motion and the boundary term. It yields

$$\delta(\sqrt{-g} L) = \frac{1}{16\pi} \left[\sqrt{-g} \left(G_{ab} + \Lambda g_{ab} \right) \delta g^{ab} + \sqrt{-g} \nabla_a \delta v^a - 2\sqrt{-g} \delta \Lambda \right], \qquad (2.51)$$

where $G_{ab} = R_{ab} - \frac{1}{2} R g_{ab}$ is the well-known Einstein tensor, and $\delta v^a = 2P^{ibad} \nabla_b \left(\delta g_{id} \right)$ with $P^{abcd} = \frac{\partial R}{\partial R_{abcd}} = \frac{1}{2} \left(g^{ac} g^{bd} - g^{ad} g^{bc} \right)$. We have taken into account the fact that Λ is also a variable. The operation δ is replaced by the Lie-derivative $\pounds_\xi$, with $\pounds_\xi g^{ab} = -\left(\nabla^a \xi^b + \nabla^b \xi^a \right)$, for the diffeomorphism symmetry $x^a \to x^a + \xi^a$.

$$\pounds_\xi \left(\sqrt{-g} L \right) = \frac{\sqrt{-g}}{16\pi} \left[-2\nabla_a \left(G^a_b \xi^b \right) + \nabla_a \pounds_\xi v^a - 2\nabla_a \left(\xi^a \Lambda \right) \right], \qquad (2.52)$$

can be obtained by applying the Bianchi identity $\nabla_a G^a_b = 0$, because Λ is a scalar, we have used $\Lambda g_{ab} \pounds_\xi g^{ab} - 2\pounds_\xi \Lambda = -2\Lambda \nabla_a \xi^a - 2\xi^a \nabla_a \Lambda = -2\nabla_a (\xi^a \Lambda)$. Also, for the diffeomorphism symmetry, the left hand side is given by $\pounds_\xi \left(\sqrt{-g} L \right) = \sqrt{-g} \nabla_a \left(\xi^a \right)$.

32

Therefore, finally one obtains

$$\sqrt{-g}\nabla_a\left[L\xi^a + \frac{1}{16\pi}\left(2G_b^a\xi^b + 2\Lambda\xi^a - \pounds_\xi v^a\right)\right] = 0, \qquad (2.53)$$

from which the explicit statement, $\pounds_\xi v^a = \nabla_b\nabla^a\xi^b + \Box\xi^a - 2\nabla_a\nabla_b\xi^b$ can be obtained. As a result,

$$J^a = L\xi^a + \frac{1}{16\pi}\left(2G_b^a\xi^b + 2\Lambda\xi^a - \pounds_\xi v^a\right), \qquad (2.54)$$

is the conserved Noether current for the diffeomorphism symmetry.

The following equation (2.54) provides $J^a = \nabla_b J^{ab} = \frac{1}{16\pi}\nabla_b\left[\nabla^a\xi^b - \nabla^b\xi^a\right]$, resulting in the anti-symmetric Noether potential as,

$$J^{ab} = \frac{1}{16\pi}\left[\nabla^a\xi^b - \nabla^b\xi^a\right], \qquad (2.55)$$

using the results $2G_b^a\xi^b + R\xi^a = 2R_j^a\xi^j = 2\left[\nabla_a\nabla^a\xi^b - \nabla^a\nabla_b\xi^b\right]$ and the previously indicated expression of $\pounds_\xi v^a$.

Although Λ affects the Noether current J^a, the Noether potential is unaffected. It is also worth noting that the expression of the Noether potential remains unchanged whether Λ is treated as a pure constant or not at all in theory. We will prove later that the black hole system's entropy and energy are proportional to the Noether potential. As a result, it may be stated that those quantities are not subject to any changes due to Λ. It is also worth noting that we never used Einstein's equations of motion to arrive at the expression mentioned above. As a result, it is an off-shell result.

On-shell, $G_b^a\xi^b = -\Lambda\xi^a$ is found from the equation of motion $G_{ab} + \Lambda g_{ab} = 0$, resulting in the on-shell Noether current (from 2.54) being,

$$J^a = L\xi^a - \frac{\pounds_\xi v^a}{16\pi}, \qquad (2.56)$$

implying

$$\delta\left(\sqrt{-g}J^a\right) = \delta\left(\sqrt{-g}L\right)\xi^a + \sqrt{-g}L\delta\xi^a - \frac{\delta\left(\sqrt{-g}\pounds_\xi v^a\right)}{16\pi}, \qquad (2.57)$$

33

where δ represents arbitrary field variation that has no effect on the vector ξ^a. So, $\delta\xi^a = 0$ but $\delta\xi_a \neq 0$, we get,

$$\delta\left(\sqrt{-g}J^a\right) = \frac{\xi^a}{16\pi}\left[\sqrt{-g}\left(G_{ij} + \Lambda g_{ij}\right)\delta g^{ij} + \sqrt{-g}\nabla_i\delta v^i - 2\sqrt{-g}\delta\Lambda\right] - \frac{\delta\left(\sqrt{-g}\pounds_\xi v^a\right)}{16\pi},$$
(2.58)

using (2.51). Let us calculate the aforementioned variation on-shell, which yields,

$$\delta\left(\sqrt{-g}J^a\right) = \frac{\sqrt{-g}\xi^a}{16\pi}\left[\nabla_i\delta v^i - 2\delta\Lambda\right] - \frac{\delta\left(\sqrt{-g}\pounds_\xi v^a\right)}{16\pi}.$$
(2.59)

With $A^{[a}B^{b]} = \frac{1}{2}\left(A^aB^b - A^bB^a\right)$, one can get $\pounds_\xi\left(\sqrt{-g}\delta v^a\right) = -2\sqrt{-g}\nabla_b\left(\xi^{[a}\delta v^{b]}\right) + \sqrt{-g}\xi^a\nabla_b\delta v^b$.

$$\delta\left(\sqrt{-g}J^a\right) = \frac{1}{16\pi}\left[\pounds_\xi\left(\sqrt{-g}\delta v^a\right) - \delta\left(\sqrt{-g}\pounds_\xi v^a\right) + 2\sqrt{-g}\nabla_b\left(\xi^{[a}\delta v^{b]}\right) - 2\sqrt{-g}\xi^a\delta\Lambda\right],$$
(2.60)

is obtained by applying this relation in (2.59).

Now, let's define

$$\omega^a = -\frac{1}{16\pi}\mathcal{L}_\xi\left(\sqrt{-g}\delta v^a\right) + \frac{1}{16\pi}\delta\left(\sqrt{-g}\pounds_\xi v^a\right).$$
(2.61)

The significance of ω^a will be explained later in our discussions. As a result of this convention, one obtains

$$\delta\left(\sqrt{-g}J^a\right) = -\omega^a + \frac{2\sqrt{-g}}{16\pi}\left[\nabla_b\left(\xi^{[a}\delta v^{b]}\right) - \xi^a\delta\Lambda\right]$$
(2.62)

implying,

$$\omega^a = -\delta\left(\sqrt{-g}J^a\right) + \frac{2\sqrt{-g}}{16\pi}\left[\nabla_b\left(\xi^{[a}\delta v^{b]}\right) - \xi^a\delta\Lambda\right].$$
(2.63)

Let us turn to classical mechanics for help in properly understanding everything. $\delta L(q,\dot{q}) = \left[\left(\frac{\partial L}{\partial q}\right) - d_t\left(\frac{\partial L}{\partial\dot{q}}\right)\right]\delta q + d_t\left[p\delta q\right]$ can be obtained using classical calculations, where the first term is the equation of motion, which disappears on-shell, and the last term is the temporal derivative of the boundary term, which we will designate as v. Let us take the

conventions,

$$v(\delta q) = p\delta q, \tag{2.64}$$

$$v(\dot{q}) = p\dot{q} \tag{2.65}$$

The variation of the Hamiltonian can be explained as follows using this convention:

$$\delta H(q,p) = \delta\left[p(d_t q)\right] - d_t\left[p(\delta q)\right] = \delta\left[v(\dot{q})\right] - d_t\left[v(\delta q)\right]. \tag{2.66}$$

Let us now attempt to comprehend the physical meaning of the term ω^a. However, first, in order to compare ω^a to the classical term, consider the one-to-one correspondence as follows.

In classical mechanics, the metric tensor g^{ab} corresponds to q. δQ corresponds to the arbitrary variation of the metric tensor δg^{ab}, and $\dot{q}$ corresponds to the Lie-derivative of the metric tensor $\pounds_\xi g^{ab}$. It is possible to write using this format.

$$\sqrt{-g}\pounds_\xi v^a \equiv v(\dot{q}) \tag{2.67}$$

$$\sqrt{-g}\delta v^a \equiv v(\delta q). \tag{2.68}$$

So, if one compares (2.61) and (2.66) using the above-mentioned convention (2.68), one finds that (aside from the normalisation factor $\frac{1}{16\pi}$) ω^a corresponds to $\delta\mathcal{H}$, where $\mathcal{H}$ is the Hamiltonian density. As a result, the total Hamiltonian's variation is represented as,

$$\delta H[\xi] = \delta\int_c d\Sigma_a \frac{\omega^a}{\sqrt{-g}} = -\int_c d\Sigma_a \nabla_b(J^{ab}) + \frac{2}{16\pi}\int_c d\Sigma_a\left[\nabla_b\left(\xi^{[a}\delta v^{b]}\right) - \xi^a\delta\Lambda\right], \tag{2.69}$$

the Cauchy surface is denoted by c. $J^a = \nabla_b J^{ab}$ in (2.63), where J^{ab} is the anti-symmetric Noether potential, is used to obtain the final step. With h as the determinant of 3-metric and n_a as the normal to the surface, $d\Sigma_a = n_a\sqrt{h}d^3y$ is the infinitesimal surface area of a three-dimensional hypersurface. Let us now substitute the pressure for

35

the cosmological constant Λ. (2.69) can be written as,

$$\delta H[\xi] = -\frac{1}{2}\delta\int_{\pounds}d\Sigma_{ab}J^{ab} + \frac{1}{2}\delta\int_{\partial c\infty}d\Sigma_{ab}J^{ab} - \frac{1}{16\pi}\int_{\partial c\infty}d\Sigma_{ab}\xi^{[a}\delta v^{b]} + \delta P\int_{c}d\Sigma_{a}\xi^{a},$$
(2.70)

after translating the volume integral to the surface integral, the new surface integrations will be performed on a bifurcation surface $\mathscr{H}$ and at the 2-dimensional boundary of c at asymptotic infinity (i.e., ∂c_{∞}). Taking ξ^{a} as a timelike Killing vector, one must have $\xi^{a} = 0$ on $\mathscr{H}$. As a result, the word containing $\xi^{[a}\delta v^{b]}$ makes no contribution. $\delta H[\xi] = 0$ in this case, while $H[\xi]$ might not be zero. Then, on the right-hand side, identify the first term as $-\frac{\kappa}{2\pi}\delta S$ from Wald's prescription, with κ as the surface gravity. As a whole, the second and third terms contribute as $\delta M - \Omega_{H}\delta J$ (see (Wald 1993) for rigorous discussion).

Let us now concentrate on the final term, $\int_{c}d\Sigma_{a}\xi^{a}$ of (2.70). The above integral can also be expressed as $\int_{\mathscr{H}}\sqrt{h}d^{3}yn_{a}\xi^{a} - \int_{\infty}\sqrt{h}d^{3}yn_{a}\xi^{a}$, with the first term calculated at the horizon and the second term evaluated at the asymptotic boundary. The first integral yields a finite result, whereas the second term yields a divergent result. The regularisation process must be used to eliminate the divergence. There are usually two prescriptions in the literature. One method includes a counter term in action whose contribution eliminates the divergence. The background subtraction method is another option. The background contribution eliminates the divergence in this situation, resulting in a finite volume. The additional term can be justified because one can always introduce a total derivative term along with the actual Lagrangian as long as the governing dynamics remain unchanged or because the Noether potential (J^{ab}) is not uniquely determined (one can include any arbitrary anti-symmetric tensor with it as long as the divergence of that arbitrary term vanishes). As a result, one can include a term in the Lagrangian or Noether potential to eliminate the noted divergence at infinity. As a result, the covariant definition of volume V is

$$V = -\int_{\mathscr{H}}\sqrt{h}d^{3}yn_{a}\xi^{a} + \int_{\infty}\sqrt{h}d^{3}y\left[n_{a}\xi^{a} - (n_{a}\xi^{a})BG\right],$$
(2.71)

we interpret the last component of (2.70) as $V\delta P$ since the term with $(n_{a}\xi^{a})_{BG}$ is con-

sidered the "background contribution" to eliminate the divergence. The thermodynamic volume is the name given to this volume in the literature. When one calculates (2.71) with the horizon radius r_h in the Reissner–Nordström AdS (RNAdS) black hole , one gets $V = 4\pi r_h^3/3$. The consmological constant that determines the pressure $P = -\Lambda/8\pi$. In (Kastor et al. 2009, Couch et al. 2017), similar prescriptions were implemented. As a result of (2.70), the required result,

$$\delta M = T\delta S + V\delta P + \Omega_H \delta J, \tag{2.72}$$

is obtained. $T = \frac{\kappa}{2\pi}$ is the temperature of a black hole, as can be deduced from this. As a result, the first law for the AdS black hole with varying cosmological constant is established in this study. For the sake of simplicity in the computations, we have not included any hair in this theory. As previously stated, the addition of hair provides a well-known contribution, and the final expression when all hairs are considered is,

$$dM = TdS + VdP + \Sigma_i X_i dY_i, \tag{2.73}$$

where $X = \{\Omega, \phi\}$ and $Y = \{J, Q\}$ with Ω, ϕ, J, and Q represent the angular velocity, electric potential, angular momentum, and electric charge (which contains all charges owing to symmetry and the hair in the system), respectively. When we compare the above equation (2.73) to the thermodynamic law $dH = TdS + VdP + \mu dN$ (where H is the enthalpy, μ is the chemical potential, and N is the number of particles in the thermodynamic system), we can see that the mass of the black hole is identified as the black hole system's enthalpy, rather than the internal energy. In non-extended phase space, on the other hand, the mass of the black hole is identified with the system's internal energy, as we saw earlier. Remember that in ordinary thermodynamics, the enthalpy is the amount of energy required to construct the system (i.e., the internal energy) and the amount required to establish the system's pressure and volume. As a result, the significance of black hole mass in the description of black hole thermodynamics in extended phase space is modified.

The fact that the Noether potential is independent of the cosmological constant has

earlier been studied in (Hollands et al. 2005). However, in that instance, Λ is treated as a proper constant; therefore, it is not included in the potential. However, in our case, we used the metric tensor and the variation of the cosmological constant to deduce the first law of the AdS black holes in the extended phase space. We have proved that, while the Noether current is affected by the cosmological constant, the potential is unaffected, even in the off-shell situation. In this regard, it is worth noting that the expressions of entropy and mass-energy in the extended phase space are identical to those in the non-extended phase space because the Noether-potential expression is the same in both circumstances.

2.5   Thermodynamics with Variable Λ

When looking at the first law (1.5), one cannot help but be intrigued by the pressure-volume expression $P\delta V$. The presence of such a term is unexpected. concept was misunderstood because there was no mention of pressure or volume correlated with a black hole. A new concept was suggested a few years ago. It was seen from the form of the corrected Smarr equation, the negative cosmological constant Λ may be identified with the thermodynamic pressure. Our Universe, cosmological constant is positive (Riess et al. 1998, Perlmutter et al. 1999). Positive Λ complicates the study of black hole thermodynamics for two reasons: First, in de Sitter space, there is no asymptotic regime that allows for the unambiguous determination of the ADM mass of a black hole embedded in a positive Λ space; second, $\Lambda > 0$ denotes negative pressure and, as a result, thermodynamic instability (Lukács and Martinás 1984). The first issue arises because a de Sitter black hole has two event horizons, a black hole horizon and a cosmological horizon, and the radial coordinate is time-like beyond the cosmological horizon for large enough values of r. The second issue is more easily understood because negative pressure systems are thermodynamically unstable. Although black holes are unstable even for $\Lambda = 0$ because their heat capacity (C_P) is negative, we may still discuss metastable circumstances in which a temperature can be determined for a period of time far shorter than the timescale of thermal instability. In metastable settings, negative pressures can be beneficial (Landau and Lifshitz 2013). In contrast, there is no cosmological horizon for negative Λ, and the pressure is positive everywhere the

thermodynamics is well defined.

The negative cosmological constant in a d dimensional space with AdS radius ℓ reads,

$$\Lambda = -\frac{(d-1)(d-2)}{2\ell^2} < 0. \tag{2.74}$$

Furthermore, (Kastor et al. 2009) proposed that the mass of a black hole embedded in anti-de Sitter space-time be interpreted as the enthalpy rather than the more conventional internal energy,

$$M = H(S,P) = U(S,V) + PV. \tag{2.75}$$

The *PV* term in this equation represents the contribution to the black hole's mass-energy due to the negative energy density of the vacuum, $\varepsilon = -P$, which is related to a negative cosmological constant. The total energy of a black hole with volume V is $U = M - PV$ because it includes energy $\varepsilon V = -PV$. This interpretation forces us to address the question of how to define the volume of a black hole. The black hole volume is the volume that is excluded from empty AdS when the black hole is introduced, according to (Kastor et al. 2009). We will call this the "geometric volume". Another definition of the black hole volume is the Legendre transform (2.75),

$$V := \frac{\partial H}{\partial P}, \tag{2.76}$$

which we will refer to as the "thermodynamic volume".

The concept of considering Λ as a dynamical variable was first proposed by Teitelboim and Brown (Teitelboim 1985, Brown and Teitelboim 1988). $P - V$ term was introduced into the first law of black hole mechanics by (Creighton and Mann 1995). Many aspects of which were discussed later in (Caldarelli et al. 2000, Padmanabhan 2002). The generalized first law of black hole mechanics becomes,

$$dM = TdS + VdP + \Omega dJ + \Phi dQ. \tag{2.77}$$

Pressure is related to the cosmological constant Λ and volume is its conjugate quantity (Kubizňák et al. 2017); it follows from the first law; this is true only when we consider

AdS black holes and satisfies the Smarr's relation (Kastor et al. 2009). The geometric volume of a spherically symmetric black hole turns out to be the spherical volume with radius as event horizon radius (Altamirano et al. 2014). For black holes which deviate from a spherically symmetric spacetime as in the case of a rotating AdS black hole which is axially symmetric, interpreting the pressure and volume of a black hole is not easy. Dolan (Dolan 2012) showed that thermodynamic volume for a non-rotating black hole is identical to the geometric volume, it hold for non-rotating black holes in all dimensions (Padmanabhan 2002, Tian and Wu 2011, Dolan 2011c). Volume and entropy cannot be considered independent thermodynamic variables since S determines V uniquely, and they can't be changed separately, making V redundant. However, this equality no longer holds for rotating Kerr-AdS black holes. V and S can and should be regarded as independent variables for a rotating black hole.

The main motivation for studying the phase transition of black holes is to reveal the phase structure of black holes and thermodynamic variables' behavior. The stability of the black holes can be analyzed by studying the order of phase transition and critical behavior. The conditions characterize the critical point,

$$\frac{\partial P}{\partial v} = 0 \quad , \qquad \frac{\partial^2 P}{\partial v^2} = 0, \tag{2.78}$$

where v is the specific volume. One of the essential physical quantities to study the stability in thermodynamics is heat capacity. It is customary to define heat capacity in two different ways for a given system, i.e., at constant volume and constant pressure.

$$C_V = T \left(\frac{\partial S}{\partial T} \right)_V, \quad C_P = T \left(\frac{\partial S}{\partial T} \right)_P. \tag{2.79}$$

The phase transition seen in charged black holes is similar to the Van der Waals system (Chamblin et al. 1999a, Kubizňák and Mann 2012). Consider the metric of a charged AdS black hole in four dimensions,

$$ds^2 = -f(r)dt^2 + \frac{1}{f(r)}dr^2 + r^2 d\Omega^2, \tag{2.80}$$

where,

$$f(r) = 1 - \frac{2M}{r} + \frac{Q^2}{r^2} + \frac{r^2}{\ell^2} \tag{2.81}$$

Black hole event horizon at $f(r_h) = 0$. The corresponding thermodynamic quantities are (Kubizňák and Mann 2012, Dolan 2011b),

Temperature,

$$T = \frac{1}{4\pi r_h} + \frac{3r_h}{4\pi\ell^2} - \frac{Q^2}{4\pi r_h^3}. \tag{2.82}$$

The equation of state becomes,

$$P = \frac{T}{2r_h} - \frac{1}{8\pi r_h^2} + \frac{Q^2}{8\pi r_h^4}. \tag{2.83}$$

Between the small black hole and the large black hole phases, the black hole undergoes a transition. The critical point is obtained from (2.78) leads to,

$$P_c = \frac{1}{96\pi Q^2}, \quad T_c = \frac{\sqrt{6}}{18\pi Q}, \quad v_c = 2\sqrt{6}Q, \tag{2.84}$$

Examining the critical values (2.84) reveals a surprising relationship $\frac{P_c v_c}{T_c} = \frac{3}{8}$, which is identical to the Van der Waals fluid and is a universal number anticipated for any RN-AdS black hole with arbitrary charge.

2.6 Conclusions and Discussions

One of the most exotic objects in physics is black holes, which behave like thermodynamical systems. Pressure and volume are not discussed in traditional treatments of the first law of black hole thermodynamics. However following works of (Kastor et al. 2009, Dolan 2011b, Kubizňák and Mann 2012) cosmological constant is interpreted as thermodynamic pressure and viewed as a thermodynamic variable in an extended phase space. The mass of the black hole is associated with enthalpy in this method rather than being considered internal energy. As a result, a comprehensive dictionary of black hole thermodynamic quantities emerges, including a definition of thermodynamic volume for a given black hole spacetime.

In the first part of this chapter, we briefly explained the laws of black hole thermo-

dynamics. We derived the Smarr relation for asymptotically flat black holes using the geometrical method based on Komar integrals. The following sections have demonstrated the failure of these approaches in asymptotically AdS black holes. Due to the failure of the Smarr relation for AdS black holes, an extended form of thermodynamics was developed, with the cosmological constant interpreted as the thermodynamic pressure P. The modified Komar integrals yield the Smarr relation involving the PV term in the extended space. AdS black holes in this extended phase space exhibits d a van der Waals fluid-like phase diagram (Kubizňák and Mann 2012).

Chapter 3

Thermodynamics of Regular Bardeen Black Hole

This chapter explains the details of the calculation of thermodynamics and phase transition of regular Bardeen AdS black holes in the extended phase space without and with quintessence. This analysis reveals a first-order phase transition similar to the van der Waal system, which is confirmed by the specific heat divergence at the critical points.

3.1 Introduction

The effort to incorporate quantum mechanical nature into a black hole, which had a purely classical origin in general relativity, led to the development of black hole thermodynamics. Hawking and Bekenstein took the initial step by introducing temperature and entropy for a black hole related to surface gravity and black hole area, respectively (Hawking 1975, Bekenstein 1972b). The four laws of black hole thermodynamics, which are analogous to classical thermodynamics, were soon proposed (Bardeen et al. 1973). The importance of AdS black holes in black hole thermodynamics was realized in the early stages of these developments because thermodynamically stable black holes can only exist in AdS space. The AdS space boundary behaves as the walls of

a thermal cavity. The common *PdV* term is missing from the first law of black hole thermodynamics in the elementary approach. The role of the cosmological constant in Einstein's equations, where it gives the pressure term, provides a hint for solving this problem. The dynamical cosmological constant introduces the pressure term to black hole thermodynamics, which has other significant implications, such as the consistency of the Smarr relation with the first law (Kastor et al. 2009). The thermodynamic volume is taken to be the conjugate quantity in this approach.

The general theory of relativity allows for black hole spacetimes with singularities, where the classical theory is no longer predictive and no concept of classical space-time appears to be viable. On the other hand, singularities are an artifact of general relativity because their presence indicates a failure or incompleteness of the theory. Quantum gravity is thought to play a role at short distances in preventing the limit-less expansion of spacetime curvature scalars and other physical quantities. Initially, Sakharov (Sakharov 1966a) proposed that to avoid such singular nature at close distances to the singularity, one must offer a de-Sitter core with $p = -\rho$ as the superdense matter equation of state. Later, Gliner (Gliner 1966) viewed $p = -\rho$ as a non-zero density vacuum that may provide a good explanation of gravitational collapse in its final stages. Quantum fluctuations dominate during gravitational collapse, putting an upper bound on the value of the spacetime curvature and forming a de-Sitter core around the center, which inhibits matter from moving towards the center, preventing a singularity from forming in the spacetime. Bardeen (Bardeen 1968) developed the first model of regular black holes based on Sakharov and Gliner's ideas. Ayon-Beato and Garcia (Ayón-Beato and Garcıa 2000) later proposed some regular black holes that may be interpreted as exact solutions coupled to nonlinear electrodynamics with a magnetic monopole charge. Regular black hole models are significant because they provide a valuable test-bed for investigating minimal, localized departures from classical black hole geometry (Carballo-Rubio et al. 2018). Other regular black hole models have also been obtained using both magnetic and electric sources (Ayon-Beato and Garcia 1998, Ayon-Beato and Garcıa 1999, Ayón-Beato and Garcıa 2000, Ayón-Beato and Garcia 2005, Hayward 2006, Dymnikova 1992, 2004, Ahluwalia-Khalilova and Dymnikova

2003, Dymnikova and Galaktionov 2005, Bronnikov 2001a,b, Bronnikov et al. 2003b, Bronnikov and Fabris 2006, Bronnikov et al. 2003a, Bronnikov and Dymnikova 2007, Bronnikov and Fabris 2006) . The rotating regular black holes (Bambi and Modesto 2013, Toshmatov et al. 2014, Ghosh 2015, Tinchev 2019) were created to investigate their horizon structure, particle acceleration, particle collision, and energy extraction using the Penrose process (Ghosh and Amir 2015, Amir et al. 2016, Ghosh et al. 2014, 2020).

In order to study the thermal and stability features of dS/AdS spaces, regular black hole solutions have been extended. The horizon and extended phase space thermodynamics of regular dS/AdS black holes have been investigated (Ahluwalia-Khalilova and Dymnikova 2003, Dymnikova 2002, Fan 2017). Similarly, the phase transitions and heat engine efficiency for regular Bardeen AdS black holes. Another regular black hole solution coupled to nonlinear electrodynamics in an asymptotically dS space was derived (Matyjasek and Tryniecki 2009). Motivated by the recent progress, here we study the thermodynamics of the Bardeen black hole surrounded by quintessence. In the first part of this chapter, we discuss Bardeen black hole and its internal structure. Then calculate the thermodynamics and phase transition of regular Bardeen AdS black holes in the extended phase space; then, we investigate the effect of quintessence parameters on it in the next section.

3.2   The Bardeen Solution

Several motivations exist for attempting to develop consistent solutions to Einstein's equations that explain regular spacetimes. The existence of various singularity theorems (Penrose 1965, Hawking 1965, Geroch 1966, Hawking and Penrose 1970, Clarke 1975, Borde 1994, De Sitter 1918), which apply both to cosmology and gravitational collapse, limits the possibilities. The essential question is whether or not it is possible to violate some of the singularity theorems' hypotheses without obtaining unphysical models. The literature has progressed significantly in this direction, particularly in cosmology and gravitational collapse. Of course, solutions without horizons provide a natural framework in which singularity theorems cannot be used, and regular solutions can be found. On the other hand, it appears natural that horizons arise in various phys-

45

ically reasonable situations. As a result, it is important to know whether singularities may be avoided in the presence of horizons. Regular black holes are solutions in which this is true. A wide range of these solutions has been studied (Elizalde and Hildebrandt 2002, Bronnikov and Dymnikova 2007). Bardeen's solution (Bardeen 1968, Borde
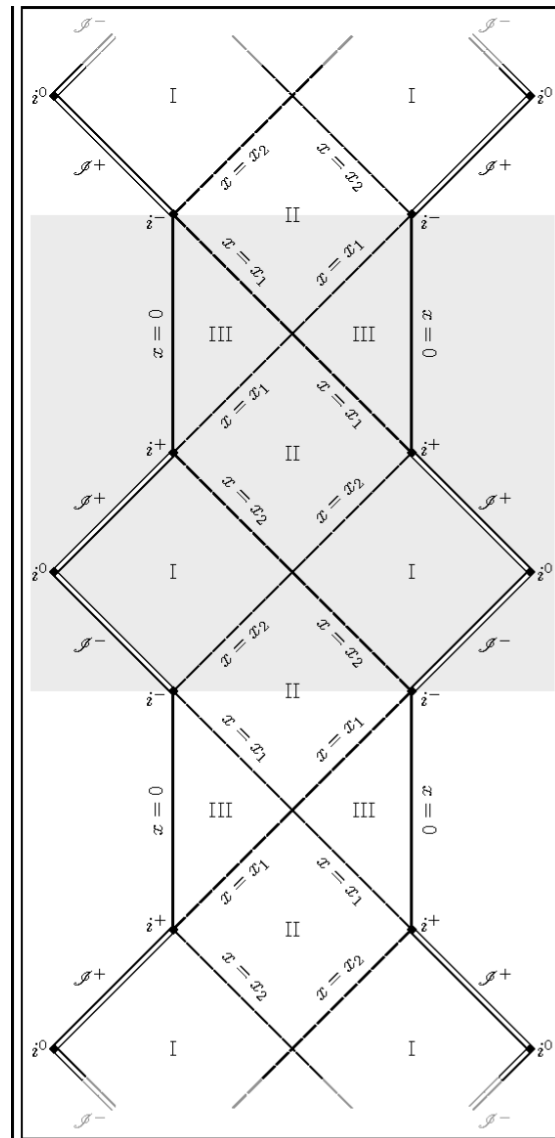
Figure 3.1: Penrose diagram of regular black hole

1994) is a solution of Einstein equations in the presence of an electromagnetic field that is parametrized by mass m and charge β, similar to the well-known Reissner-Nordström solution (Reissner 1916, Nordström 1918). The line element can also be expressed in the same way, in the static and spherically symmetric form , with the metric function

$f(r)$ equal to

$$f(r) = 1 - \frac{2mr^2}{(r^2 + \beta^2)^{3/2}} = 1 - \left(\frac{m}{\beta}\right) \frac{2\left(\frac{r}{\beta}\right)^2}{\left(\left(\frac{r}{\beta}\right)^2 + 1\right)^{3/2}}, \tag{3.1}$$

and $r \geq 0$. It is easy to observe that i) there are m/β ratio values for which $f(r)$ has no zeroes (and is therefore always positive), ii) values for which it has two zeroes, and a situation in between, where iii) the function is always non-negative but disappears at only one point along with its first derivative. This function, like the curvature tensors and scalar of the solution it represents, is well defined everywhere; for small r, it behaves like the de Sitter metric, whereas for large r, it asymptotically acts like the Schwarzschild metric (Ansoldi 2008). In scenario ii), the black hole interior does not terminate in a singularity but instead crosses an interior Cauchy horizon and evolves into a region that resembles de Sitter, eventually ending with a regular origin at $r = 0$. However it acts as a counterexample, this solution imposes a strong constraint on possible generalizations of current singularity theorems. Even though this was discovered many years ago, it has interesting properties, and its causal and geometrical structures have been investigated in depth (Borde 1994, 1997). The research revealed that a reasonably generic method for singularity avoidance in classical general relativity might involve a topological change. Let us look at the values of the parameters for which the Bardeen solution has both an event and a Cauchy horizon. We can see that its global structure resembles the maximum extension (Graves and Brill 1960, Carter 1966) of Reissner-Nordström (Schwarzschild 1916, Nordström 1918) spacetime but with a regular origin (See figure (3.1) [5] (Ansoldi 2008)). According to Borde (Borde 1994, 1997), the singularity avoidance may be explained by the fact that in regions where spacelike slices in the Reissner-Nordström solution would have the topology $\mathbb{R} \times \mathbb{S}^1$, the same spacelike slices in the Bardeen solution have the topology $\mathbb{S}^3$. There are corresponding regions of the extended manifold where spacelike slices of both the Reissner-Nordström and the Bardeen solutions have the topology $\mathbb{R} \times \mathbb{S}^1$, the avoidance of singularity has

---

[5] Spherical black holes with regular center: a review of existing models including a recent realization with Gaussian sources

been linked in (Borde 1994, 1997) to the topology change that appears in the structure of the spacelike slices, which change from open to closed; this allows singularity avoidance because in the closed case (Ansoldi 2008).

3.2.1 Black Hole Interiors

The Bardeen solution is the first concrete scenario that implements the early physical idea of Sakharov (Sakharov 1966a) and Gliner (Gliner 1966), replacing the singularity with a regular de Sitter core. Given the early appearance of the Schwarzschild (Schwarzschild 1916) and de Sitter (De Sitter 1918) solutions and the global nature of these spacetimes, it is natural that the idea to replace the black hole interior of Schwarzschild spacetime with the interior (i.e., before the cosmological horizon) region of de Sitter spacetime (Gonzalez-Diaz 1981) together with charged generalizations (Wenda and Shitong 1985, Shen and Zhu 1985). This intuitive idea can be supported, in fact, by the valuable formalism of Israel junction conditions (Israel 1966, Barrabes and Israel 1991). Even though the simpler idea of performing the junction at a null surface (Wenda and Zhu 1988) fails due to stability issues (Grøn and Soleng 1989) and the appearance of a pressure discontinuity at the null junction (Grøn 1985, Poisson and Israel 1988). It is possible to replace part of the black hole interior with de Sitter spacetime by interposing a layer of non-inflationary material (Grøn 1985). The scenario in which this layer is spacelike (Frolov et al. 1989, 1990), resulting in the so-called Schwarzschild–de Sitter model, is exciting. The curvature becomes unbounded as one approaches a singularity is a natural motivation for these investigations. On the other hand, a consistent framework for singularity avoidance should prevent this divergence, so it is natural to assume an upper bound for the curvature (Markov 1982, 1984, Markov and Mukhanov 1984), which was naturally taken at the Planck size in these early studies. It can be demonstrated that the Schwarzschild metric's black hole area may be linked to de Sitter space through a spacelike junction, with the transition being on the order of Planck time (Frolov et al. 1989, 1990). The procedure can be carried out not only between eternal, static spacetimes but also when considering the black hole as a result of gravitational collapse. Furthermore, the de Sitter space can decay into a Friedman universe, giving rise to the exciting notion that gravitational col-

lapse could result in the creation of a new universe. Focusing a little further on the technical elements of this early suggestion, (Ansoldi 2008) points out that, due to the spacelike character of the junction, the resultant spacetime has Cauchy horizons and is therefore not universally hyperbolic. Also note that the spacelike hypersurface where the Kasner-like contraction of the Schwarzschild collapse is transformed into deflation of de Sitter spacetime is followed by another hypersurface where the transition to an inflationary space occurs. The new universe generated within the black hole is truly closed since this last surface is topologically a three-sphere $\mathbb{S}^3$. It is also worth noting that this model may be proven (Balbinot and Poisson 1990) to be stable in the following sense: The T_t^t component of the stress-energy tensor can be interpreted as tension along the axis of a three-cylinder of constant time $r = $ constant inside the black hole region. This is especially true along the surface where the junction is made, as it can be seen that there are values of the parameters for which fluctuations of the Schwarzschild mass M and/or the de Sitter cosmological constant Λ and/or other internal parameters, such as surface pressures, do not cause the three-cylinder to collapse to zero radii, but instead cause spatial oscillations of its radius with a longitudinal dependence (Ansoldi 2008). In a current context, it is also worth recalling a subsequent expansion of this early concept (Barrabes and Frolov 1996), which discussed the idea of creating many de Sitter universes with null boundaries inside the black hole region, a picture that's very similar to that of an eternally inflating universe.

Other types of matching may be accomplished without the presence of a surface layer: in (Markov and Mukhanov 1984), the mass function is presented in two explicit instances, where the junctions are performed at the horizon of Schwarzschild spacetime, which represents the solutions' exterior asymptotically flat area. Complete manifold extensions are also explored, and they cannot be produced using analytical continuation, which is impossible across the horizon (Mars and Senovilla 1993). It is also possible to execute the junction away from the horizon without changing the general features of the result, as detailed in (Markov and Mukhanov 1984). However, the spacetime manifold that may be extended to completeness is not analytical; therefore, its extension is not unique. It is also possible to obtain more complex models with comparable features

(Ansoldi 2008).

3.3 Thermodynamics of Regular Bardeen AdS Black Hole

The action for regular black hole solution coupled with nonlinear electrodynamics in AdS space read as (Fan and Wang 2016),

$$S = \int d^4x \sqrt{-g} \left(\frac{1}{16\pi} R + \frac{3}{8\pi l^2} - \frac{1}{4\pi} \mathcal{L}(\mathcal{F}) \right), \tag{3.2}$$

where R is the Einstein scalar, l the AdS radius and $\mathcal{L}(\mathcal{F})$ is from nonlinear electrodynamics source.

$$\mathcal{L}(\mathcal{F}) = \frac{3M}{\beta^3} \left(\frac{\sqrt{4\beta^2 \mathcal{F}}}{1 + \sqrt{4\beta^2 \mathcal{F}}} \right)^{\frac{5}{2}}, \tag{3.3}$$

where $\mathcal{F} = F_{\mu\nu} F^{\mu\nu}$, $\mathcal{F}_{\mu\nu}$ is the strength of the electromagnetic field and β is the magnetic monopole charge associated with it.

The solution of the action will give regular Bardeen AdS black hole metric has the form (Fan 2017, Fan and Wang 2016),

$$ds^2 = -f(r)dt^2 + \frac{dr^2}{f(r)} + r^2 d\theta^2 + r^2 \sin^2\theta d\phi^2, \tag{3.4}$$

where $f(r) = 1 - \frac{2\mathcal{M}(r)}{r} - \frac{\Lambda r^2}{3}$ and $\mathcal{M}(r) = \frac{Mr^3}{(r^2+\beta^2)^{3/2}}$. Here M is the black hole mass, Λ is the cosmological constant given by $-\frac{3}{\ell^2}$. The cosmological constant is treated as thermodynamic pressure in extended phase space (1.7).

The event horizon of the Black hole is articulated by $f(r_h) = 0$, which gives the black hole mass,

$$M = \frac{\left(\beta^2 + r_h^2\right)^{3/2} \left(8\pi P r_h^2 + 3\right)}{6 r_h^2}. \tag{3.5}$$

Now the first law of thermodynamics equation (1.5) can be rewritten as (Tzikas 2019),

$$dM = TdS + VdP + \Psi d\beta, \tag{3.6}$$

where Ψ is the potential conjugate to the magnetic charge β. Temperature T can be obtained from surface gravity κ as,

$$T = \frac{\kappa}{2\pi} = \frac{1}{4\pi} f'(r)|_{r=r_h} = \frac{-2\beta^2 + 8\pi P r_h^4 + r_h^2}{4\pi r_h \left(\beta^2 + r_h^2\right)}. \tag{3.7}$$

When $\Lambda = 0$, then (3.5) and (3.7) reduces to the mass and temperature of the Bardeen regular black hole (Akbar et al. 2012). The thermodynamic volume V and the entropy S can be derived from the first law (3.6) as,

$$V = \left.\frac{\partial M}{\partial P}\right|_{V,\beta} = \frac{4}{3}\pi r_h^3 \left(\frac{\beta^2}{r_h^2} + 1\right)^{3/2}, \tag{3.8}$$

$$S = \int \frac{dM}{T} = \pi r_h^2 \left(\left(1 - \frac{2\beta^2}{r_h^2}\right)\sqrt{\frac{\beta^2}{r_h^2} + 1} + \frac{3\beta^2 \log\left(\sqrt{\beta^2 + r_h^2} + r_h\right)}{r_h^2} \right). \tag{3.9}$$

The thermodynamic quantities depends on charge β explicitly. In the large r limit the entropy of Bardeen-AdS black hole is πr_h^2. Rearranging the equation (3.7) we get

$$P = \frac{4\pi r_h T \left(\beta^2 + r_h^2\right) + 2\beta^2 - r_h^2}{8\pi r_h^4}. \tag{3.10}$$

Consider $v = 2r_h$ as specific volume, we obtain the equation of state $P(T, v, \beta)$,

$$P = \frac{2\pi T v \left(4\beta^2 + v^2\right) + 8\beta^2 - v^2}{2\pi v^4}. \tag{3.11}$$

The $P - v$ isotherm and $T - S$ curves using the equations (3.7) and (3.11) as shown in figure (3.2). The behavior of the $P - v$ diagram resembles that of van der Waals gas. The isotherm corresponding to $T = T_C$ called critical isotherm has an inflection point below which a critical behavior is displayed. The corresponding pressure and volume at that point are called critical pressure (P_C) and critical volume (v_C), respectively. The isotherms above critical isotherm (for $T > T_C$) gradually approach equilateral hyperbolas, which corresponds to the ideal gas case. On the other hand, the lower set of isotherms (for $T < T_C$) have a positive slope region ($\partial P/\partial v > 0$), which is thermodynamically unstable. The critical behavior is also apparent in the $T - S$ plot.
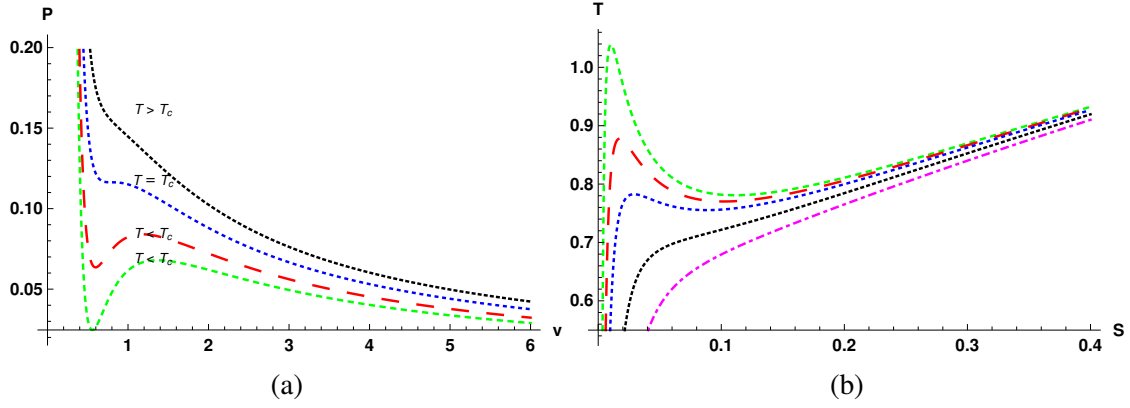
Figure 3.2: $P - v$ diagram for regular AdS black hole for different values of temperature with $\beta = 0.1$ (figure (3.2a)). In figure (3.2b) $T - S$ plot for different values of β is shown.

The critical point is characterized by the conditions,

$$\frac{\partial P}{\partial v} = 0 \quad , \qquad \frac{\partial^2 P}{\partial v^2} = 0. \tag{3.12}$$

The critical parameters hence obtained are,

$$v_c = \sqrt{2\left(\sqrt{273}+15\right)}\beta \quad , \quad T_c = -\frac{\left(\sqrt{273}-17\right)\sqrt{\frac{1}{2}\left(\sqrt{273}+15\right)}}{24\pi\beta} \quad , \tag{3.13}$$

$$P_c = \frac{\sqrt{273}+27}{12\left(\sqrt{273}+15\right)^2\pi\beta^2}. \tag{3.14}$$

We can compute $\frac{P_c v_c}{T_c}$ ratio ,

$$\frac{P_c v_c}{T_c} = 0.367, \tag{3.15}$$

which almost matches with that of the van der Waals gas, which is $3/8$ (Kubizňák and Mann 2012).

One of the important physical quantities in thermodynamics is heat capacity. It is customary to define heat capacity in two different ways for a given system, i.e., at constant volume and at constant pressure. It is straight forward to show the following result,

$$C_V = T\left(\frac{\partial S}{\partial T}\right)_V = 0. \tag{3.16}$$

In the large r limit, the heat capacity at constant pressure is calculated as

$$C_P \quad = T \left(\frac{\partial S}{\partial T} \right)_P = \frac{2S\left(\pi\beta^2+S\right)\left(-2\pi\beta^2+8PS^2+S\right)}{2\pi^2\beta^4+\pi\beta^2S(24PS+7)+S^2(8PS-1)}. \tag{3.17}$$
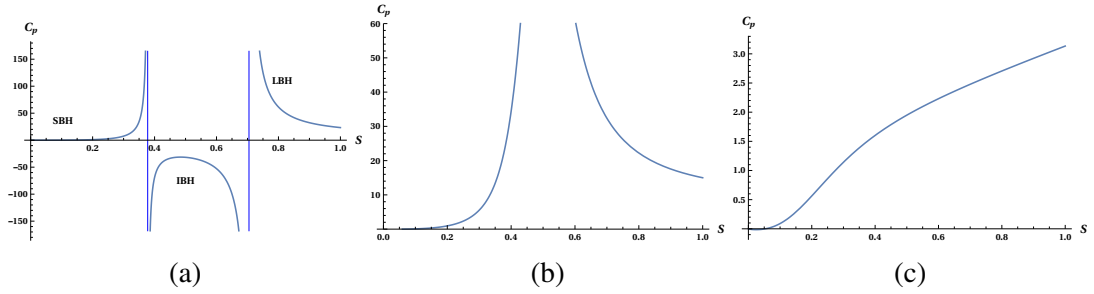
Figure 3.3: Specific heat versus entropy diagram for regular AdS black hole with $\beta = 0.1$, for $P < P_c$ in figure (3.3a), for $P = P_c$ in figure (3.3b) and for $P > P_c$ in figure (3.3c).

The first-order phase transition for the black hole is confirmed from the $C_P - S$ plot (figure (3.3)). The critical behavior is seen only below certain pressure (P_c). There exist three distinct regions, and hence two divergence points for $P < P_C$. The positive specific heat for the small black hole region (SBH) and large black hole region (LBH) means that those black holes are thermodynamically stable. Having negative specific heat, the intermediate black hole region (IBH) represents an unstable system. Therefore the actual phase transition takes place between SBH and LBH. The unstable region disappears at pressure $P = P_C$ resulting in a single divergence point.

3.4 Thermodynamics of Regular Bardeen AdS Black Hole with Quintessence

Presence of quintessence throughout the universe makes it important to probe its effects on the black holes. Quintessence is one of the dark energy candidates, which leads to the accelerated expansion of our universe (Kiselev 2003, Tsujikawa 2013). Kiselev was the first to study the effects of quintessence on a black hole (Kiselev 2003). Since then, there were many studies in black holes surrounded by quintessence, to mention a few, in the contexts of gauge gravity duality (Chen et al. 2013a) and quasi-normal modes (Chen and Jing 2005). Phase transitions in Reissner-Nordström and regular black holes with this exotic field were also studied (Wei and Chu 2011, Thomas et al.

2012, Li 2014, Fan 2017, Saleh et al. 2018, Rodrigue et al. 2018). By using Kislev's phenomenological model, one can construct a regular Bardeen black hole surrounded by quintessence. According to this model, the quintessence comes from a fluid with the energy-momentum tensor,

$$T_r^r = T_t^t = \rho_q,$$
$$T_\theta^\theta = T_\phi^\phi = -\frac{1}{2}\rho_q\left(3\omega_q + 1\right),$$
$$\text{and} \quad \rho_q = -\frac{a}{2}\frac{3\omega_q}{r^{3(\omega_q + 1)}},$$

ω_q and a are the state parameter and the normalization constant related to quintessence energy density ρ_q. Solving the Einstein equations, one can obtain the metric for a regular Bardeen AdS black hole with quintessence (Saleh et al. 2018, Fan 2017, Li 2014, Kiselev 2003) (for details see Appendix A),

$$ds^2 = -f(r)dt^2 + \frac{dr^2}{f(r)} + r^2 d\theta^2 + r^2\sin^2\theta d\phi^2, \tag{3.18}$$

where

$$f(r) = \left(1 - \frac{2\mathcal{M}(r)}{r} + \frac{r^2}{l^2} - \frac{a}{r^{3\omega_q + 1}}\right). \tag{3.19}$$

AG Tzikas (Tzikas 2019) studied the phase transition in Bardeen AdS black hole. In this section, we investigate the thermodynamic phase transition of regular Bardeen AdS black hole with quintessence.

The mass M corresponding to the above metric (3.18),

$$M = \frac{1}{6}r_h^{-3(1+\omega_q)}(\beta^2 + r_h^2)^{3/2}[-3a + r_h^{1+3\omega_q}(3 + 8P\pi r_h^2)]. \tag{3.20}$$

First law of black hole thermodynamics must be modified to include quintessence as follows (Rodrigue et al. 2018),

$$dM = TdS + \Psi d\beta + VdP + \mathcal{A}da. \tag{3.21}$$

54

Where Ψ is the potential conjugate to the magnetic charge β and $\mathcal{A}$ is a quantity conjugate to quintessence parameter a.

$$\mathcal{A} = \left(\frac{\partial M}{\partial a}\right)_{S,\beta,P} = -\frac{1}{2r_h^{3\omega_q}}. \tag{3.22}$$

The quintessence parameters $\mathcal{A}$ and a are introduced similar to the pressure-volume term to make the first law consistent with the Smarr relation,

$$M = 2TS + \Psi\beta - 2PV + (3\omega_q + 1)\mathcal{A}a. \tag{3.23}$$

The quintessence parameter a being a thermodynamic variable contributes to the internal energy of black holes and hence to the thermodynamics. The appearance of a and its conjugate variable $\mathcal{A}$ in first law and Smarr relation justifies our motivation to study its effect in phase transition. It is also worth recalling that these modifications due to quintessence is parallel to the extension by identifying cosmological constant as thermodynamic pressure. These two identifications play a crucial role in the critical phenomena of AdS black holes.

From Hawking temperature (3.24), we can derive the equation of state (equation (3.26)).

$$T = \frac{r_h^{-3\omega_q-2}\left(3a\left(\beta^2(\omega_q+1)+r_h^2\omega_q\right)+r_h^{3\omega_q+1}\left(-2\beta^2+8\pi Pr_h^4+r^2\right)\right)}{4\pi\left(\beta^2+r_h^2\right)}. \tag{3.24}$$

$$P = \frac{r_h^{-3\omega_q-5}\left(r_h^{3\omega_q+1}\left(\beta^2(4\pi r_h T+2)+r_h^2(4\pi r_h T-1)\right)-3a\left(\beta^2(\omega_q+1)+r_h^2\omega_q\right)\right)}{8\pi} \tag{3.25}$$

$$= \frac{v^{-3\omega_q-5}\left(v^{3\omega_q+1}\left(8\beta^2(\pi Tv+1)+v^2(2\pi Tv-1)\right)-3a2^{3\omega_q+1}\left(4\beta^2(\omega_q+1)+v^2\omega_q\right)\right)}{2\pi}. \tag{3.26}$$

where $v = 2r_h$ is specific volume. When $\omega_q = 0$ and $a = 0$, then (3.24) and (3.25) reduces to (3.7) and (3.10). Using the above equations the $P-v$ and $T-S$ curves are plotted in figure (3.4a) and (3.4b). Below a critical temperature T_C, $P-v$ isotherm
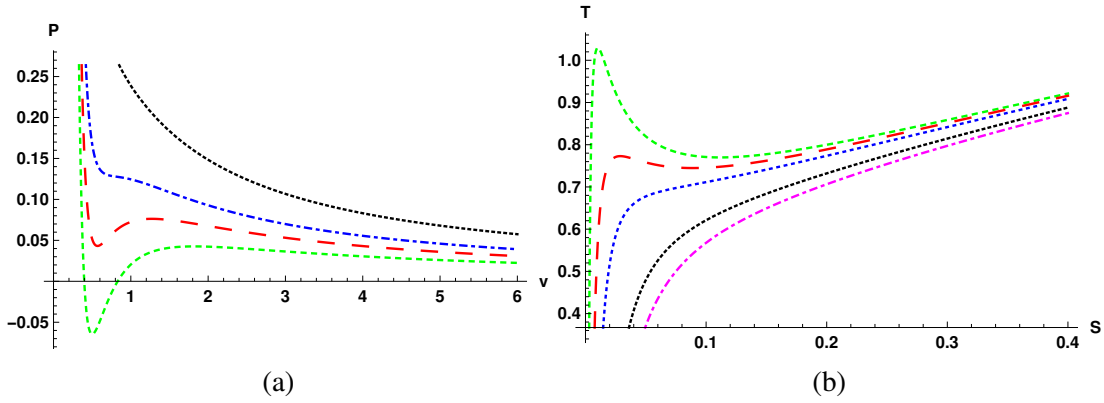
Figure 3.4: To the left we have $P - v$ diagram for regular AdS black hole surrounded by quintessence ($a = 0.07$, $\beta = 0.1$, $\omega_q = -2/3$) for different values of temperature. In the right side $T - S$ plot for different values of β is shown.

has three branches corresponding to small, intermediate, and large black holes. This behavior is quite similar to liquid/gas transition van der Waals fluids. Around the critical points, two plots clearly display critical phenomena. The conditions are used to determine the critical points are ,

$$\frac{\partial P}{\partial v} = 0 \quad , \quad \frac{\partial^2 P}{\partial v^2} = 0. \tag{3.27}$$

The quintessence parameter's inclusion increases the ratio, which implies a change in the microscopic interaction and phase structure.
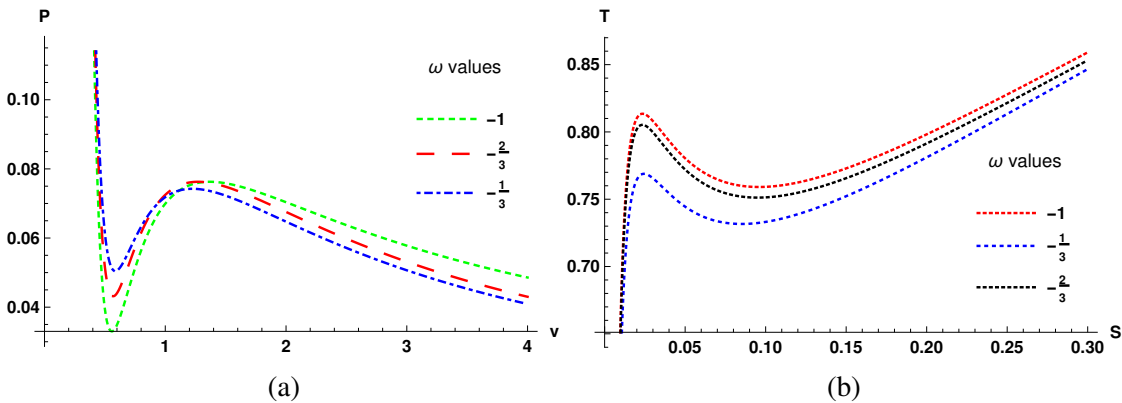
Figure 3.5: Effect of quintessence parameter ω_q on $P - v$ isotherms (figure 3.5a) and $T - S$ diagram (figure 3.5b).

We can see how the existence of quintessence influences the phase transition by looking at the critical values of temperature, pressure, and volume. Since the analytic

expression is difficult to obtain, the critical quantities are obtained numerically for the state parameter $\omega_q = -1, -2/3, -1/3$ (table 3.1). Effect of quintessence in the $P - v$ isotherms and $T - S$ plots are shown in figure (3.5). Increase in the value of ω_q from -1 to 0, leads to decrease in the $\frac{P_c V_c}{T_c}$ ratio, which approaches to 3/8.

Table 3.1: Critical points are found using equation (3.27) with quintessence state parameter $\omega_q = -1, -2/3, -1/3$ for $a = 0.07$ and $\beta = 0.1$. The ratio $\frac{P_c v_c}{T_c}$ is calulated for each case.

ω_q	P_c	v_c	T_c	$\frac{P_c v_c}{T_c}$
-1	0.124537	0.794011	0.251314	0.3973468
$-2/3$	0.118448	0.788029	0.242862	0.384335
$-1/3$	0.108049	0.794011	0.233722	0.367069

A phase transition is described in statistical mechanics by divergences in second moments such as specific heat, compressibility, and susceptibility. As a result, we concentrate on the heat capacity of the system to know more about phase transition. The thermodynamic stability of black holes is indicated by the sign of heat capacity, which is positive for stable and negative for unstable. The heat capacity at constant pressure is given by,

$$
C_P = T \left(\frac{\partial S}{\partial T} \right)_P
$$
$$
= \frac{2S\left(\pi\beta^2 + S\right)\left(3a\pi^{\frac{3\omega_q}{2}+\frac{1}{2}}\left(\pi\beta^2(\omega_q+1)+S\omega_q\right)+S^{\frac{3\omega_q}{2}+\frac{1}{2}}\left(-2\pi\beta^2+8PS^2+S\right)\right)}{S^{\frac{3\omega_q}{2}+\frac{1}{2}}\left(2\pi^2\beta^4+\pi\beta^2 S(24PS+7)+S^2(8PS-1)\right)-3a\pi^{\frac{3\omega_q}{2}+\frac{1}{2}}\left(\pi^2\beta^4\left(3\omega_q^2+5\omega_q+2\right)+C+D\right)}.
$$

where $C = \pi\beta^2 S\left(6\omega_q^2 + 7\omega_q + 4\right)$ and $D = S^2\omega_q(3\omega_q + 2)$

$C_P - S$ plot is obtained from this equation, which shows critical behavior (figure 3.6) below certain pressure (P_c). These plots show that below the critical pressure $P < P_c$, there are two singular points, which reduce to one when $P = P_c$, and above $P > P_c$, these divergence disappears. In figure (3.6a), there are three distinct regions separated by two singular points. The SBH and LBH regions with positive specific heat, and the IBH with negative specific heat. As the positive specific heat regions are thermodynamically stable, a phase transition occurs between the small black hole and large black hole. This
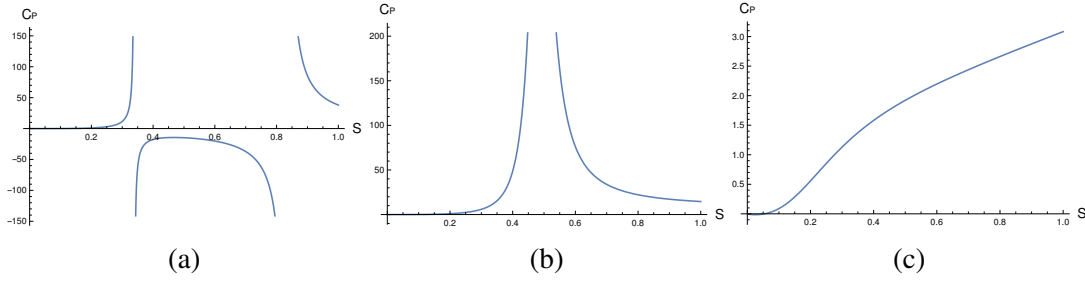
Figure 3.6: Specific heat versus entropy diagram for regular AdS black hole surrounded by quintessence ($a = 0.07$, $\beta = 0.1$, $\omega_q = -\frac{2}{3}$). (3.6a) for $P = Pc$, (3.6b) for $P < Pc$, (3.6c) for $P > Pc$.

result is analogous to Reissner-Nordström AdS black holes surrounded by quintessence (Thomas et al. 2012).

3.5 Conclusions and Discussions

The Thermodynamics of a regular Bardeen AdS black hole with and without the effect of quintessence have been investigated in this chapter. When $\Lambda = 0$ case, the thermodynamic quantities match with regular Bardeen blackhole (Akbar et al. 2012). We observed a critical behavior from the P–v and T–S plots in the thermodynamic analysis, similar to van der Waals gas (Kubizňák and Mann 2012). For $\omega_q = -1, -2/3$, and $-1/3$, we obtain critical values for pressure, volume, and temperature. The $\frac{P_c v_c}{T_c}$ ratio decreases significantly as ω_q increases from -1 to $-1/3$. The critical point is found to be dependent on the quintessence parameters a and ω_q. A discontinuity in the specific heat illustrates a phase transition in the system.

Chapter 4

Regular Bardeen AdS Black Hole as Heat Engine

In this chapter, a traditional heat engine is designed with the black hole as the working substance. The efficiency is achieved through a thermodynamic cycle in the P - V plane that receives and expels heat. The efficiency of the heat engine is increased by the addition of a quintessence field. In terms of the quintessence dark energy parameter, an analytical expression for heat engine efficiency is derived.

4.1 Introduction

In human history, the discovery of the heat engine was a turning point. Even though primitive models existed as early as the first century, Nicolas Sadi Carnot was the first to idealize them in 1824. A heat engine transfers heat from a heat source (hot reservoir) to mechanical work, and the remaining heat is rejected to a lower-temperature heat sink (cold reservoir). A working substance in the engine is moved from a higher to a lower temperature state. A working substance can be any substance with a non-zero heat capacity, commonly a gas or liquid. It generates work while transferring heat to the colder sink. During the process, the working substance undergoes a cycle, such as

the Stirling, Otto, or Diesel cycles. These heat engines can be found in autos, thermal power plants, and even natural heat engines.

(a)   (b)
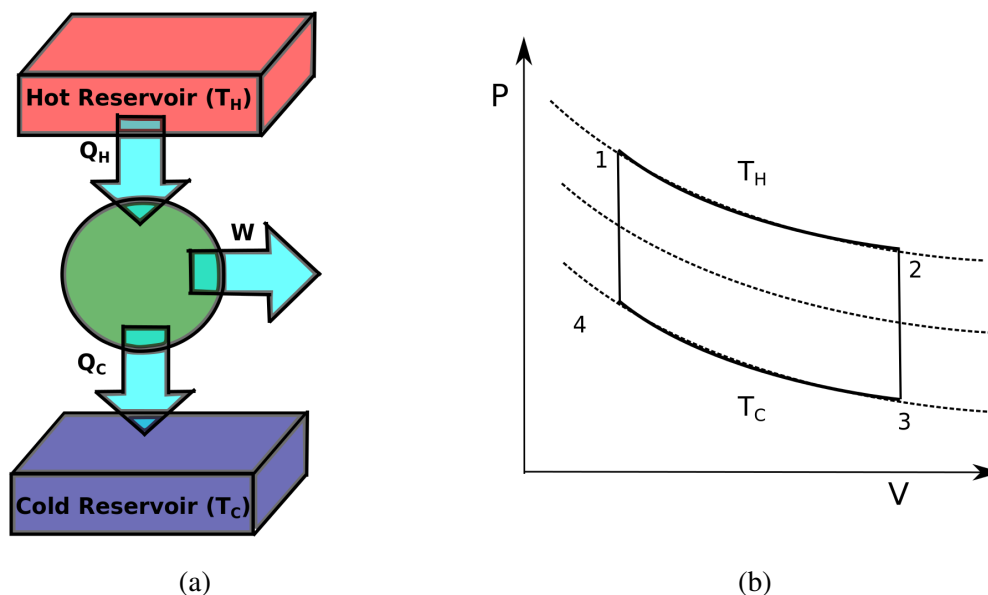
Figure 4.1: The left figure is the schematic diagram of heat engine and right is Carnot engine cycle

A heat engine is constructed as a closed path in the $P-V$ plane, that absorbs Q_H amount of heat, and exhaust Q_C amount of heat (figure 4.1a). From the first law, the total mechanical work is $W = Q_H - Q_C$. The efficiency of heat engine is given by (Zemansky 1968)

$$\eta = \frac{W}{Q_H}. \tag{4.1}$$

The maximum possible efficiency for a heat engine is estimated from a Carnot engine, which is a theoretical thermodynamic cycle. The efficiency of Carnot engine is (Zemansky 1968)

$$\eta_c = 1 - \frac{Q_C}{Q_H} = 1 - \frac{T_C}{T_H}, \tag{4.2}$$

where T_C and T_H are the lower and higher temperatures of the reservoir. This upper limit on efficiency is due to second law.

Now construct a heat engine in the context of static black hole which has a simple heat cycle (figure 4.1b) with a pair of isotherms at high temperature T_H and low temperature T_C. During isothermal expansion, Q_H amount of heat is being absorbed, and it

will exhaust Q_C amount of heat during isothermal compression. We can connect these two temperatures by either isochoric paths as in Stirling cycle or adiabatic paths as in Carnot cycle, which is reversible. Entropy and volume for a static black hole are dependent on each other. So adiabats and isochores are alike, implies Carnot engine and Stirling engine are identical.

In figure (4.1b) along the isotherm $1 \rightarrow 2$, the amount of heat absorbed

$$Q_H = T_H \Delta S_{1 \rightarrow 2} = T_H \left(\frac{3}{4\pi} \right)^{\frac{2}{3}} \pi \left(V_2^{\frac{2}{3}} - V_1^{\frac{2}{3}} \right). \tag{4.3}$$

Along the isotherm $3 \rightarrow 4$, the amount of heat rejected

$$Q_C = T_C \Delta S_{3 \rightarrow 4} = T_C \left(\frac{3}{4\pi} \right)^{\frac{2}{3}} \pi \left(V_3^{\frac{2}{3}} - V_4^{\frac{2}{3}} \right). \tag{4.4}$$

Choose isochores to connect those isotherms, i.e., $V_2 = V_3$ and $V_1 = V_4$. Then equations (4.3) and (4.4) leads to

$$\eta = 1 - \frac{Q_C}{Q_H} = 1 - \frac{T_C}{T_H}. \tag{4.5}$$

which is same as the efficiency of the Carnot engine (Liu and Meng 2017).

It is natural to construct a heat engine out of black holes because they are a thermal system that exhibits van der Waals fluid analogies. Clifford V. Johnson has just designed a remarkable engine called the holographic heat engine (Johnson 2014). The importance of the heat engine in the holographic picture of spacetime has given rise to the name "holographic". In the dual field theory, a renormalization flow is triggered by heat cycles in bulk. The holographic heat engine hence bridges the gap between extended thermodynamics and holography. These events can only occur in systems with large degrees of freedom when thermal effects take priority over quantum effects. This concept gained much attention, and the idea of holographic heat engines was subsequently extended to several black holes (Johnson 2014, 2016a,b,c, Jafarzade and Sadeghi 2017, Setare and Adami 2015, Chakraborty and Johnson 2018, Zhang and Liu 2016, Wei and Liu 2019, Mo et al. 2017, Hendi et al. 2018, Xu et al. 2017, Hennigar et al. 2017, Zhang et al. 2018). Motivated by these studies in this chapter, we construct

a heat engine by taking regular Bardeen AdS black hole as a working substance and showing the quintessence's effect on efficiency.

The first part of this chapter discusses the heat engine model in the regular Bardeen AdS black hole with no singularity at the origin. The quintessence field's effect on efficiency also investigate in the next section.

4.2   Regular Black Hole as a Heat Engine
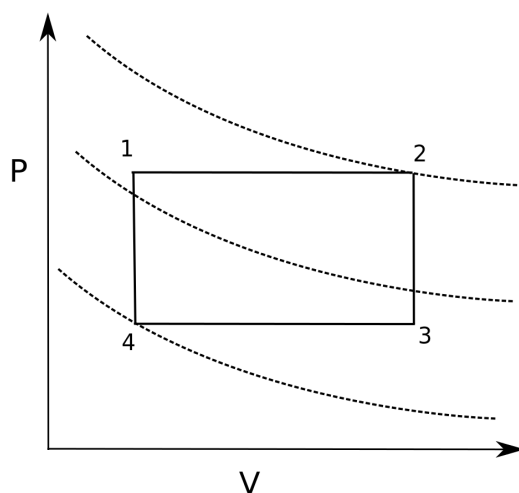
Figure 4.2: Heat engine cycle

Following the idea of Clifford V. Johnson (Johnson 2014), for calculating the efficiency of the heat engine constructed by taking regular Bardeen AdS black hole as working substance, consider figure (4.2), the new engine consists two isobars and two isochores/adiabats. For simplicity, consider a rectangular cycle ($1 \rightarrow 2 \rightarrow 3 \rightarrow 4 \rightarrow 1$) in the $P - V$ plane. The area of the rectangle gives the work done, which reads

$$W = \oint P dV. \tag{4.6}$$

The total workdone during one complete cycle,

$$W_{tot} = W_{1\to2} + W_{3\to4} = P_1(V_2 - V_1) + P_4(V_4 - V_3) \tag{4.7}$$

$$= \frac{4(P_1 - P_4)\left(\left(\pi\beta^2 + S_2\right)^{3/2} - \left(\pi\beta^2 + S_1\right)^{3/2}\right)}{3\sqrt{\pi}}. \tag{4.8}$$

Since the heat capacity at constant volume is $C_V = 0$, no heat exchange occurs in the isochoric phase. Therefore calculate only heat absorbed Q_H during the process $1 \to 2$. C_p is given by (2.79) (Dolan 2011c). The heat absorbed (Johnson 2014),

$$Q_H = \int_{T_1}^{T_2} C_P(P_1, T)dT = \int_{S_1}^{S_2} C_P\left(\frac{\partial T}{\partial S}\right)dS = \int_{S_1}^{S_2} TdS = M_2 - M_1, \tag{4.9}$$

$$= \frac{\left(\pi\beta^2 + S_2\right)^{3/2}(8P_1 S_2 + 3)}{6\sqrt{\pi}S_2} - \frac{\left(\pi\beta^2 + S_1\right)^{3/2}(8P_1 S_1 + 3)}{6\sqrt{\pi}S_1}. \tag{4.10}$$

Therefore efficiency of the engine,

$$\eta = \frac{W}{Q_H} = \frac{8(P_1 - P_4)\left(\left(\pi\beta^2 + S_2\right)^{3/2} - \left(\pi\beta^2 + S_1\right)^{3/2}\right)}{\frac{\left(\pi\beta^2 + S_2\right)^{3/2}(8P_1 S_2 + 3)}{S_2} - \frac{\left(\pi\beta^2 + S_1\right)^{3/2}(8P_1 S_1 + 3)}{S_1}}. \tag{4.11}$$

The efficiency η can be compared with that of Carnot engine, η_C, which is the maximum possible efficiency. Take the higher temperature T_H as T_2 and lower temperature T_C as T_4 in equation (4.2). Then efficiency of Carnot engine is

$$\eta_C = 1 - \frac{\sqrt{S_2}\left(\pi\beta^2 + S_2\right)\left(-2\pi\beta^2 + 8P_4 S_1^2 + S_1\right)}{\sqrt{S_1}\left(\pi\beta^2 + S_1\right)\left(-2\pi\beta^2 + 8P_1 S_2^2 + S_2\right)}. \tag{4.12}$$
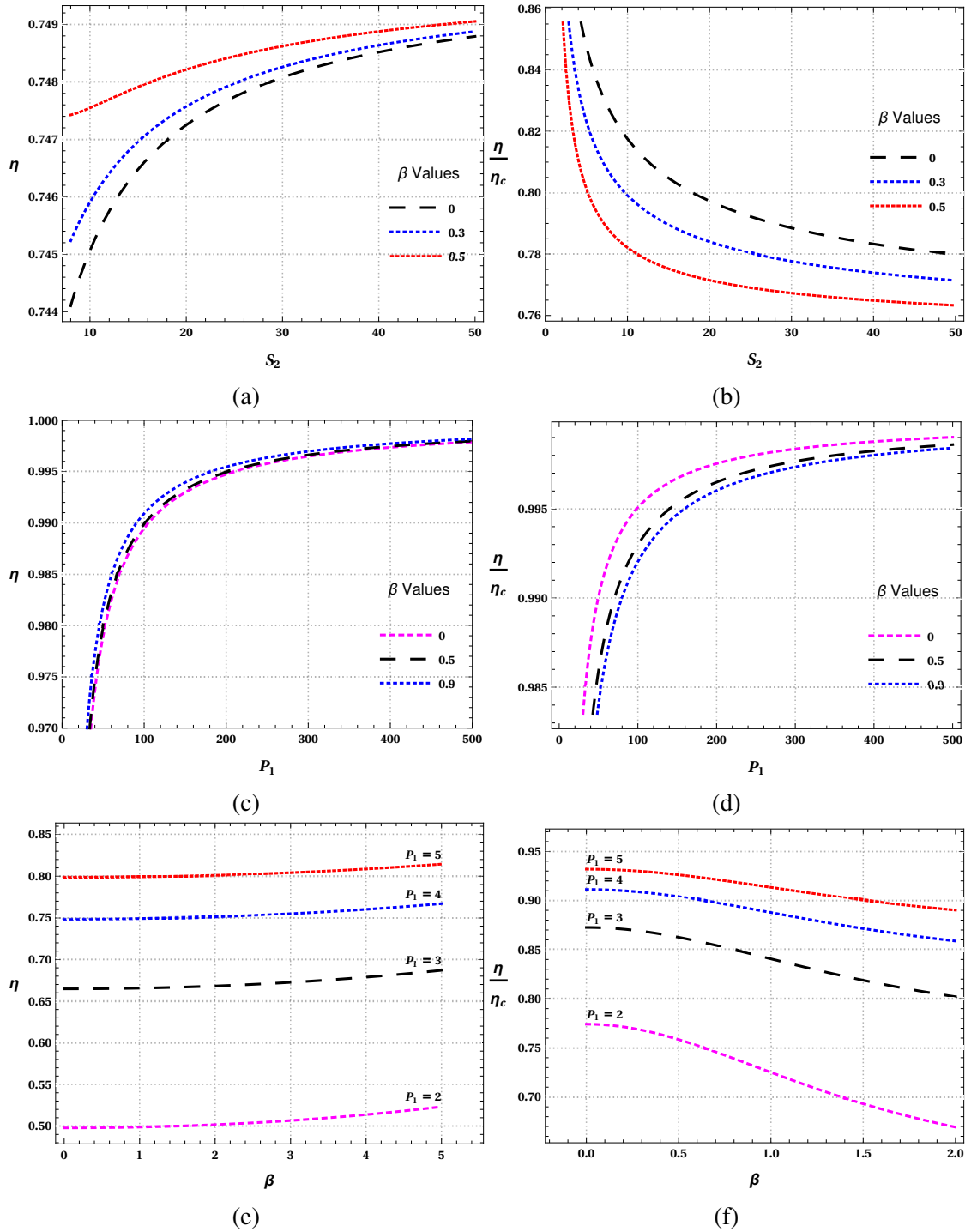
Figure 4.3: *The variation of efficiency* η *of the engine with regular Bardeen black hole as the working substance and the ratio* η/η_c *with different variables.* In figure (4.3a) and (4.3b) the entropy dependence is shown with different values of β. Here we take $P_1 = 4, P_4 = 1$ and $S_1 = 1$. In the second set of figures (4.3c) and (4.3d) the variation with pressure is studied with different values of β. In this case we take $P_4 = 1, S_2 = 4$ and $S_1 = 1$. In the last set figure (4.3e) and (4.3f) the behavior against charge β with different values of P_1 is displayed. Here we take $S_2 = 20, P_4 = 1$ and $S_1 = 10$. The parameters P_1, P_4, S_1 and S_4 are chosen accordingly for the proper display of the nature of the plots.

The efficiency η and the ratio η/η_C are plotted against entropy S_2 using the equations (4.11) and (4.12). As we can see in figure (4.3a) the heat engine efficiency monotonously increases with S_2 (corresponding volume V_2) for all values of β, which implies that the increase in volume difference between small black hole (V_1) and large blackhole (V_2) increases the efficiency. However this trend does not continue forever as the efficiency reaches saturation values after certain value of S_2. The dependence on charge β also visible from the same figure; the rates of increment are different for different β values. The plot η/η_C versus S_2 in figure (4.3b) is consistent with second law, as it is bounded below 1. With the increase in charge β the ratio decreases. We also investigate the dependence of efficiency η on pressure P_1, the pressure at the source, which is shown in figure (4.3c) and (4.3d). Those two figures clearly show that the efficiency of the engine will approach the maximum possible value as the pressure approaches infinity. Before concluding this section we also mention that the monopole charge β has a positive effect on efficiency, i.e., higher the charge higher is the efficiency (figure (4.3e), (4.3f)).

4.3 Influence of Quintessence on Efficiency of Heat Engine

Following the work of Hang Liu and Meng, we study the effect of dark energy on thermodynamics and heat engine efficiency of regular black holes (Liu and Meng 2017). Quintessence is one of the dark energy candidates (Kiselev 2003, Tsujikawa 2013). The real scalar field acts as a cosmic source having equation of state $p_q = \omega_q \rho_q$ ($-1 < \omega_q < -1/3$). The density of quintessence field is given by,

$$\rho_q = -\frac{a}{2} \frac{3\omega_q}{r^{3(\omega_q+1)}}. \tag{4.13}$$

When we include quintessence term in the metric of regular Bardeen AdS black hole, $f(r)$ is modified to

$$f(r) = 1 - \frac{2Mr^2}{(\beta^2+r^2)^{3/2}} - \frac{a}{r^{3\omega_q+1}} - \frac{\Lambda r^2}{3}. \tag{4.14}$$

Where a is the normalization constant or strength parameter related to quintessence density and ω_q is the state parameter. (Liu and Meng 2017) studied the effect of dark energy on the heat engine efficiency of charged AdS black holes. It would be interesting to study whether and how quintessence affects the heat engine efficiency of regular Bardeen AdS black holes. Now we proceed as in the earlier sections to obtain an expression for the efficiency of the engine. Using the defining condition of event horizon, $f(r_h) = 0$, one can calculate the black hole mass as,

$$M = -\frac{1}{6}\left(\beta^2 + r_h^2\right)^{3/2} r^{-3(\omega_q+1)}\left(3a + \left(-8\pi Pr_h^2 - 3\right)r_h^{3\omega_q+1}\right). \qquad (4.15)$$

We can write the expression for temperature as,

$$T = \frac{r_h^{-3\omega_q-2}\left(3a\left(\beta^2(\omega_q+1) + r_h^2\omega_q\right) + r_h^{3\omega_q+1}\left(-2\beta^2 + 8\pi Pr_h^4 + r_h^2\right)\right)}{4\pi\left(\beta^2 + r_h^2\right)}. \qquad (4.16)$$

The heat capacity at constant pressure is,

$$C_P = \frac{2S\left(\pi\beta^2 + S\right)\left(3a\pi^{\frac{3\omega_q+1}{2}}\left(\pi\beta^2(\omega_q+1) + S\omega_q\right) + S^{\frac{3\omega_q+1}{2}}\left(-2\pi\beta^2 + 8PS^2 + S\right)\right)}{S^{\frac{3\omega_q+1}{2}}f_1(S) - 3a\pi^{\frac{3\omega_q+1}{2}}f_2(S)}, \qquad (4.17)$$

where,

$$f_1(S) = \left(2\pi^2\beta^4 + \pi\beta^2 S(24PS+7) + S^2(8PS-1)\right), \qquad (4.18)$$

$$f_2(S) = \left(\pi^2\beta^4\left(3\omega_q^2 + 5\omega_q + 2\right) + \pi\beta^2 S\left(6\omega_q^2 + 7\omega_q + 4\right) + S^2\omega_q(3\omega_q+2)\right). \qquad (4.19)$$

Then we compute the heat Q_H along the process $1 \rightarrow 2$ (the earlier arguments on no heat transfer for isochoric processes still holds),

$$Q_H = \int_{T_1}^{T_2} C_P(P_1, T) dT = M_2 - M_1, \tag{4.20}$$

$$= \frac{1}{6\sqrt{\pi}} \left\{ \left(\pi\beta^2 + S_1\right)^{3/2} S_1^{-\frac{3}{2}(\omega_q+1)} \left[3a\pi^{\frac{3\omega_q+1}{2}} - (8P_1S_1+3)S_1^{\frac{3\omega_q+1}{2}} \right] \right.$$
$$\left. + \left(\pi\beta^2 + S_2\right)^{3/2} S_2^{-\frac{3}{2}(\omega_q+1)} \left[(8P_1S_2+3)S_2^{\frac{3\omega_q+1}{2}} - 3a\pi^{\frac{3\omega_q+1}{2}} \right] \right\}. \tag{4.21}$$

Having all the required quantities, the heat engine efficiency is expressed interms of quintessence parameters a and ω_q as,

$$\eta = \frac{8(P_1 - P_4)\left(\left(\pi\beta^2 + S_2\right)^{3/2} - \left(\pi\beta^2 + S_1\right)^{3/2}\right)}{f(S_1) + f(S_2)}. \tag{4.22}$$

where

$$f(S) = \left(\pi\beta^2 + S\right)^{\frac{3}{2}} S^{-\frac{3}{2}(\omega_q+1)} \left[3a\pi^{\frac{3\omega_q}{2}+\frac{1}{2}} - (8P_1S+3)S^{\frac{3\omega_q}{2}+\frac{1}{2}} \right].$$

The efficiency of the Carnot engine is also obtained as earlier,

$$\eta_C = 1 - \frac{\left(\pi\beta^2 + S_2\right) S_1^{-\frac{3\omega_q}{2}-1} S_2^{\frac{3\omega_q}{2}+1} g(S_1, P_4)}{\left(\pi\beta^2 + S_1\right) g(S_2, P_1)}, \tag{4.23}$$

where,

$$g(S, P) = \left(3a\pi^{\frac{3\omega_q}{2}+\frac{1}{2}} \left(\pi\beta^2(\omega_q+1) + S\omega_q\right) + S^{\frac{3\omega_q}{2}+\frac{1}{2}} \left(-2\pi\beta^2 + 8PS^2 + S\right) \right).$$

The heat engine efficiency depends on pressure P, entropy S, monopole charge β and quintessence parameters a and ω_q. The above expressions reduce to the previous case when quintessence parameters $a = 0$ and $\omega_q = 0$. There is a significant increment in the efficiency against S_2 when we increase the quintessence strength a with other parameters being fixed (figure 4.4a). This change is visible in the ratio plot also (figure 4.4b). The plot for efficiency versus S_2 for different values of ω_q show similar functional

67

behavior in figure (4.4c) and (4.4d). But there is a difference in the physical effect, higher values of ω_q lead to smaller efficiency. With $\omega_q = -1$, black hole shows higher efficiency than $\omega_q = -1/3$ case, where efficiency takes a constant value of 0.75. This is not surprising result because the quintessence density (ρ_q) decreases with increase in ω_q (4.13). Then we study the role of pressure P_1 on η and η/η_C with different values of quintessence strength a shown in figure (4.4e) and (4.4f), where the functional appearance remains same. The efficiency and its ratio improves with higher pressures and with quintessence. But it is noticed that there is a faster convergence to limiting value 1 in the quintessence case.

For all three values of ω_q efficiency increases exponentially, when it is plotted against quintessence constant a (figure 4.5a). The scenario remains same for the ratio plot, with an exception at $\omega_q = -1/3$, which has a slight decaying nature initially (figure 4.5b). We note that in these two plots the efficiency shoots over unity which is a clear violation of second law of thermodynamics. To avoid this unphysical situation we must be careful enough to choose quintessence parameters. In figure (4.5c) and (4.5d), we present the effect of ω_q on η and η/η_C for different values of a. In the light of earlier point, quintessence density (ρ_q) decreases with increasing ω_q, the efficiency is higher for smaller values of ω_q. This inference is drawn by considering the physically meaningful range $-1 < \omega_q < -1/3$.

The effect of quintessence on the efficiency of regular black hole heat engine is summarised in the table 4.1.

a	ω_q	η	a	ω_q	η
1	-1/3	0.800	3	-1/3	0.804
1	-2/3	0.809	3	-2/3	0.833
1	-1	0.817	3	-1	0.859

Table 4.1: Deviation in heat engine efficiency η, with variation of quintessence equation of state parameter ω_q and strength parameter a.
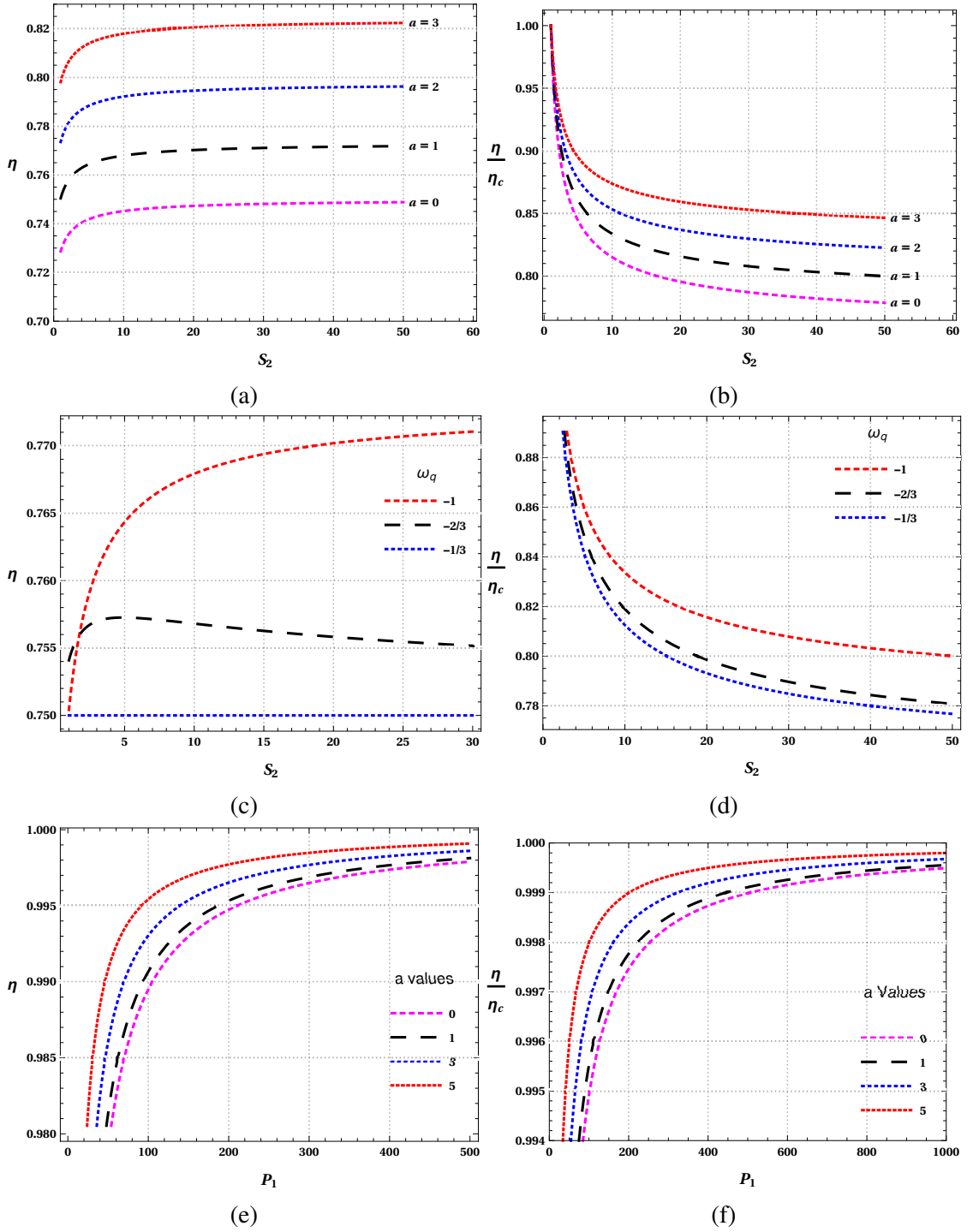
Figure 4.4: *The effect of quintessence on the efficiency* η *of the engine and on the ratio* η/η_c *with different variables.* In the first set of figures (4.4a) and (4.4b) the variation with entropy is displayed with different values of a. Here we take $P_1 = 4, P_4 = 1$ $S_1 = 1$, $\omega_q = -1$ and $\beta = 0.1$. In the second set of figures (4.4c) and (4.4d) the variation with entropy for different values of ω_q is shown. In this case we take $P_1 = 4, P_4 = 1$ $S_1 = 1$, $a = 1$ and $\beta = 0.1$. In the last set (4.4e) and (4.4f) dependence on pressure for different values of a is observed with $P_4 = 1$ $S_1 = 1$, $S_2 = 4$, $\omega_q = -1$ and $\beta = 0.1$. Here also the fixed parameters are chosen appropriately for the proper observation of the effect.
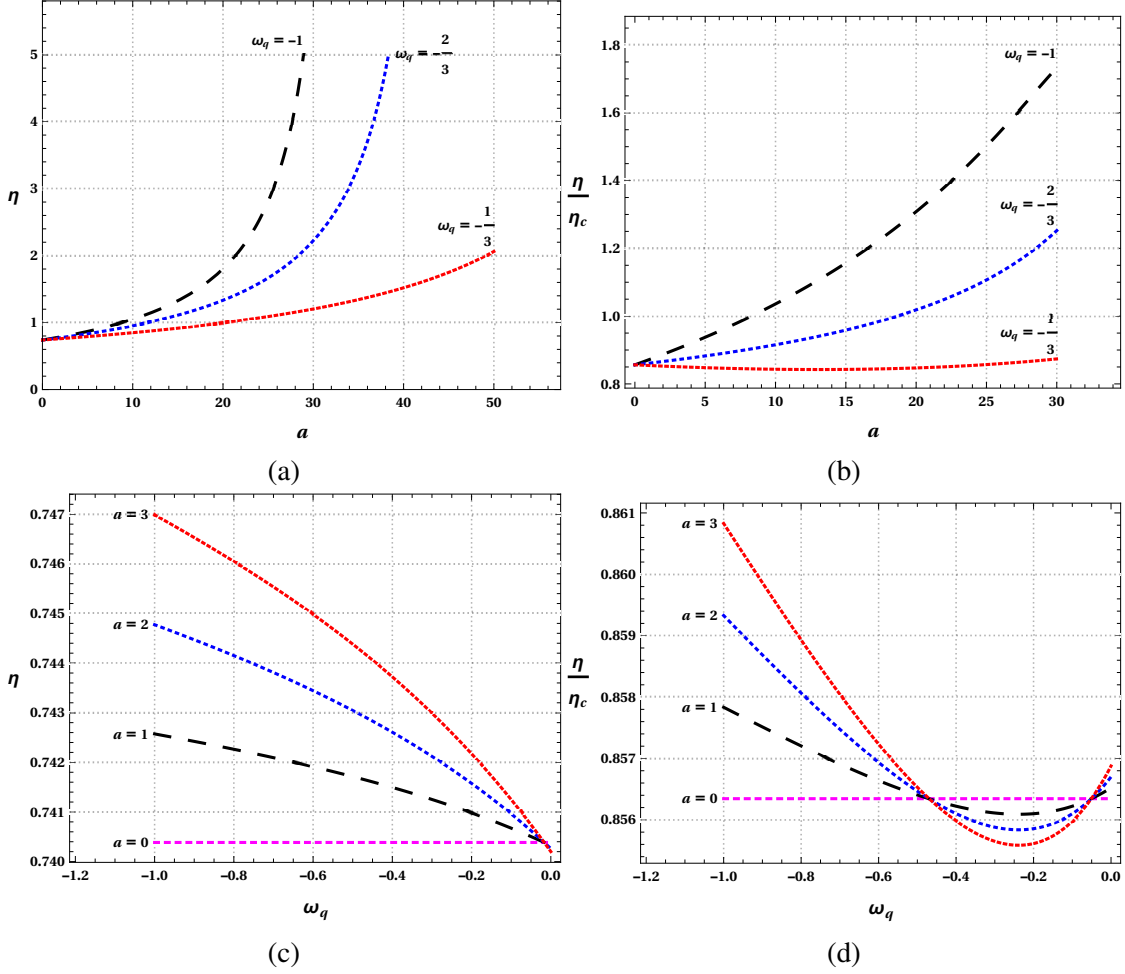
Figure 4.5: *The effect of quintessence on the efficiency* η *of the engine and on the ratio* η/η_c *with different variables.* In the figures (4.5a) and (4.5b) the dependence on a is studied with different values of ω_q. Here we take $P_1 = 4, P_4 = 1$ $S_1 = 1$, $S_2 = 4$ and $\beta = 0.1$. In the second set of figures (4.5c) and (4.5d) behavior against state parameter ω_q with different values of a is shown. In this case we take $P_1 = 4, P_4 = 1$ $S_1 = 1$, $S_2 = 4$ and $\beta = 0.1$.

4.4 Conclusions and Discussions

Regular black holes are of great interest in physics as they do not possess singularity. In this work, we demonstrated that the regular Bardeen AdS black hole can be used as an engine to extract enegy. The efficiency of the engine is improved by immersing the black hole system in a quintessential field, which has the motivations from cosmology where quintessence can be interpreted as a candidate for dark energy.

We constructed a heat engine by taking the regular Bardeen black hole as working substance. A cycle in $P - V$ plane is assigned for the black hole with two isotherms and

isochores. The efficiency of the engine is calculated by using the work done and heat absorbed during the cycle. As it is customary to compare the efficiency of any engine with Carnot engine, we have compared our results with the corresponding Carnot efficiency. Detailed analysis of the dependence of efficiency η on S_2 (entropy of LBH phase), P_1 (pressure in SBH phase) and β (monopole charge) are done. Among the several observations, we emphasize that the increase in entropy difference between SBH phase (S_1) and LBH phase (S_2) increases the efficiency of the engine. We have made a successful attempt to improve the efficiency of engine by adding a quintessence field. The heat engine efficiency depends on the quintessence parameters ω_q and a. We have presented detailed discussion on the improvement of engine efficiency with quintessence parameters. The quintessence parameter a increases the efficiency and ω_q decreases the efficiency η. We observed a drop in the efficiency η in the quintessence range $-1 < \omega_q < -1/3$. This happens because quintessence matter density (ρ_q) decreases with increase in ω_q value. It is worth mentioning that accelerated expansion of universe takes place in this quintessence range of ω_q. And in this range, the presence of quintessence matter around the black hole improves the efficiency of heat engine. The effect of intensity of quintessential matter field on the heat engine efficiency of regular black hole underlines the importance of quintessence in black hole thermodynamics.

Chapter 5

Joule-Thomson Expansion of Regular Bardeen AdS Black Hole Surrounded by Quintessence Field

In this chapter, investigate the JT expansion in regular Bardeen AdS black holes in the quintessence background through the analysis of inversion temperature and isenthalpic curves and plot the inversion and isenthalpic curves with it. The impact of the quintessence parameters a and ω_q on the JT coefficient and inversion temperature is discussed.

5.1 Introduction

Joule Thomson expansion in thermodynamics is an irreversible process that explains gas temperature change when passing through a porous plug from the high-pressure region to low pressure region. Enthalpy of the system remains constant during this expansion. The set of values (T, P) throughout the process with constant enthalpy constraint defines the isenthalpic curve. The expression for Joule Thomson coefficient

(slope of the isenthalpic curve) is given by,

$$\mu_j = \left(\frac{\partial T}{\partial P} \right)_H. \tag{5.1}$$

The sign of this coefficient tells about the cooling and heating phases. During the expansion, pressure always decreases. The coefficient of Joule Thomson expansion can also be written as (for details see Appendix C),

$$\mu_j = \left(\frac{\partial T}{\partial P} \right)_M = \frac{1}{C_P} \left[T \left(\frac{\partial V}{\partial T} \right)_P - V \right]. \tag{5.2}$$

From this, one can get the inversion temperature by setting q$\mu_j = 0$,

$$T_i = V \left(\frac{\partial T}{\partial V} \right)_P. \tag{5.3}$$

This is at the maxima of the isenthalpic curve, with the corresponding inversion pressure. The point defined by inversion temperature and inversion pressure is called the inversion point (Zemansky 1968).

In an extended phase space with a *PdV* term in the first law of black hole thermodynamics, treating the cosmological constant as pressure *P* and its corresponding thermodynamic volume *V* completes the resemblance between AdS black holes and the Van der Waals fluid. Many studies are going on in this field about various thermodynamic phenomena. The Joule - Thomson expansion of black holes is one of the thermodynamic phenomena that has gotten much attention recently. Okcu and Aydmer (Ökcü and Aydıner 2017) were the first to investigate the Joule- Thomson expansion of black holes in AdS space-time. Following this a number of investigations for various classes of black holes in various theories of gravity (Ökcü and Aydıner 2018, Chabab et al. 2018, Ahmed Rizwan et al. 2018, Rostami et al. 2019, Hoang Nam 2019, Li et al. 2020, Mo and Li 2020, Sadeghi and Toorandaz 2020, Lan 2019, Haldar and Biswas 2018, Cisterna et al. 2019, Lan 2018, Mo et al. 2018, Ghaffarnejad et al. 2018) have been performed. Motivated by these results, in this chapter, we study the Joule Thomson expansion of regular Bardeen AdS black hole surrounded by quintessence.

5.2 Joule Thomson expansion of the Black Hole

(a) $a = 1/4$, $\omega_q = -1$ (b) $a = 1/4$, $\omega_q = -2/3$ (c) $a = 1/4$, $\omega_q = -1/3$

(d) $a = 1$, $\omega_q = -1$ (e) $a = 1$, $\omega_q = -2/3$ (f) $a = 1$, $\omega_q = -1/3$
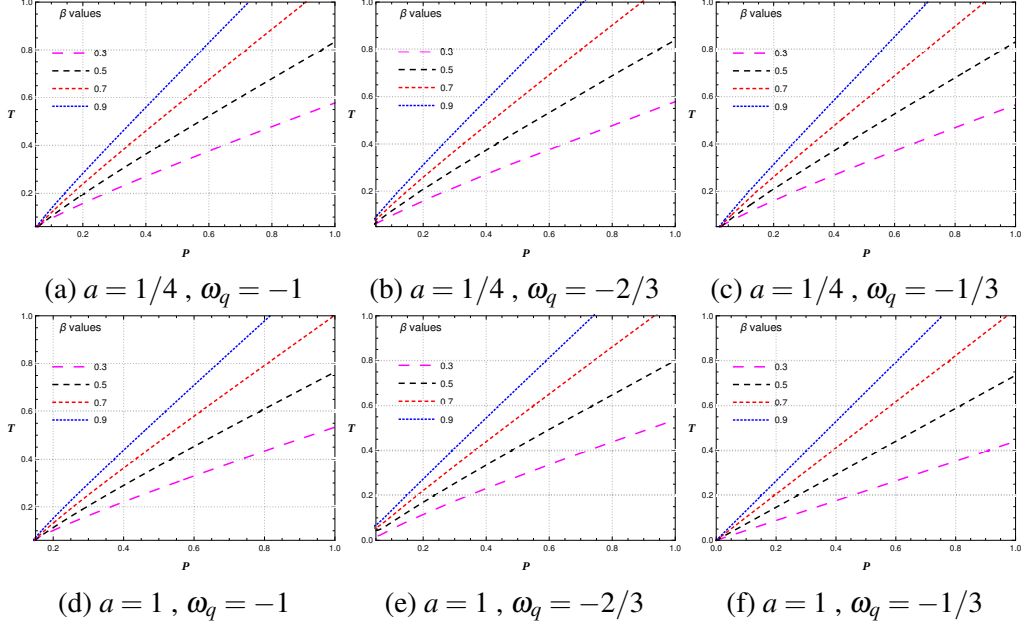
Figure 5.1: Inversion curve for different values of β.

Similar to the case of a van der Waals system, the JT expansion is also studied in AdS black hole with the same definitions of the isenthalpic curve and inversion temperature (Ökcü and Aydıner 2017). This connection is evident from the similarity between the van der Waals system and the black hole in extended phase space. The pressure P and temperature T of the regular Bardeen AdS black hole with quintessence in terms of M and r_h are,

$$P(M, r_h) = \frac{3\left(a r_h^{-3w_q - 1} + \frac{2M r_h^2}{\left(\beta^2 + r_h^2\right)^{3/2}} - 1\right)}{8\pi r_h^2}, \tag{5.4}$$

and

$$T(M, r_h) = \frac{3a(w_q + 1) r_h^{-3w_q} + \frac{6M r_h^5}{\left(\beta^2 + r_h^2\right)^{5/2}} - 2r_h}{4\pi r_h^2}. \tag{5.5}$$

Using the above equations (5.4) and (5.5), we plot the isenthalpic curves for the regular Bardeen black hole.

To obtain the JT coefficient for the black hole under consideration, we rewrite Eq.
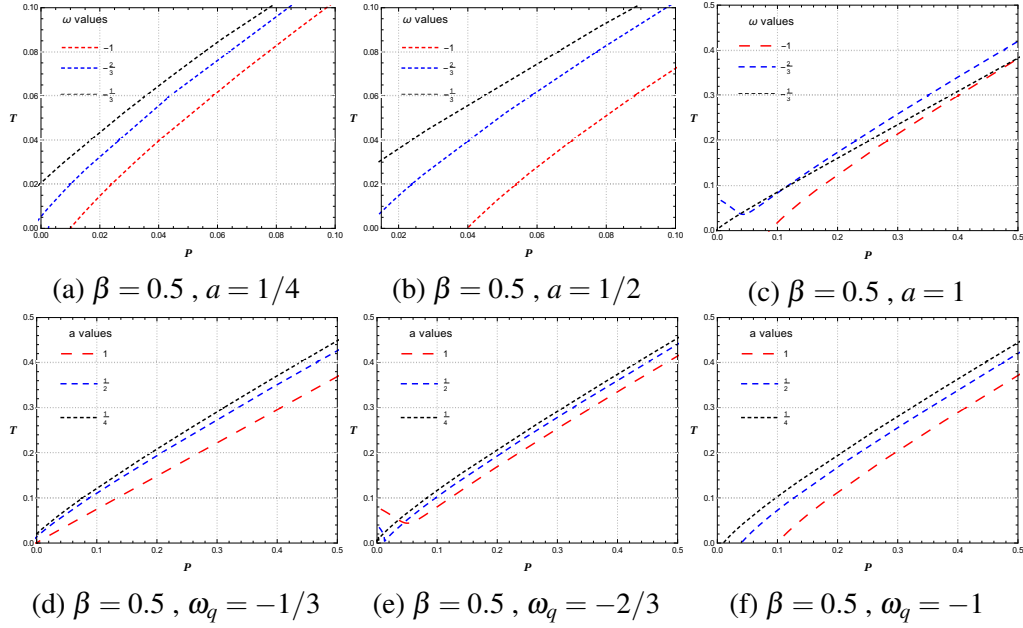
Figure 5.2: Inversion curve for different values of quintessence parameters ω_q and a.

(5.1) as follows,

$$\mu_j = \left(\frac{\partial T}{\partial P}\right)_M = \left(\frac{\partial T}{\partial r_h}\right)_M \Big/ \left(\frac{\partial P}{\partial r_h}\right)_M. \tag{5.6}$$

Using Eqs. (5.4) and (5.5) we get,

$$\mu_j = \frac{2r_h\left[3aA + r_h^{3w_q+1}B\right]}{3\left(\beta^2 + r_h^2\right)C}, \tag{5.7}$$

where,

$$A = \left[\beta^4\left(3w_q^2 + 5w_q + 2\right) + r_h^4 w_q(3w_q + 5) + \beta^2 r_h^2\left(6w_q^2 + 10w_q + 7\right)\right],$$

$$B = \left[-2\beta^4 + 16\pi P r_h^6 + r_h^4\left(4 - 24\pi\beta^2 P\right) - 13\beta^2 r_h^2\right],$$

$$C = \left[3a\left(\beta^2(w_q + 1) + r_h^2 w_q\right) + r_h^{3w_q+1}\left(-2\beta^2 + 8\pi P r_h^4 + r_h^2\right)\right].$$

And by setting $\mu_j = 0$, the inversion temperature is,

$$T_i = \frac{r_h^{-3w_q-4}\left[r_h^{3w_q+1}X - 3aY\right]}{12\pi\left(\beta^2 + r_h^2\right)}, \tag{5.8}$$

where,

$$X = \left[2\beta^4 + \beta^2 r_h^2 \left(24\pi P r_h^2 + 7 \right) + r_h^4 \left(8\pi P r_h^2 - 1 \right) \right],$$

$$Y = \left[\beta^4 \left(3w_q^2 + 5w_q + 2 \right) + \beta^2 r_h^2 \left(6w_q^2 + 7w_q + 4 \right) + r_h^4 w_q (3w_q + 2) \right].$$

Setting $\mu_j = 0$ in equation (5.7) we solve for r_h. From that choosing an appropriate root and substituting in equation (3.24) we plot the inversion curve in the $T - P$ plane, which is shown in the figure (5.1) and (5.2).

(a) $\beta = 0.5$, $a = 1/4$, $\omega_q = -1$ (b) $\beta = 0.7$, $a = 1/4$, $\omega_q = -1$ (c) $\beta = 0.9$, $a = 1/4$, $\omega_q = -1$

(d) $\beta = 0.5$, $a = 1/4$, $\omega_q = -2/3$ (e) $\beta = 0.7$, $a = 1/4$, $\omega_q = -2/3$ (f) $\beta = 0.9$, $a = 1/4$, $\omega_q = -2/3$

(g) $\beta = 0.5$, $a = 1/4$, $\omega_q = -1/3$ (h) $\beta = 0.7$, $a = 1/4$, $\omega_q = -1/3$ (i) $\beta = 0.9$, $a = 1/4$, $\omega_q = -1/3$
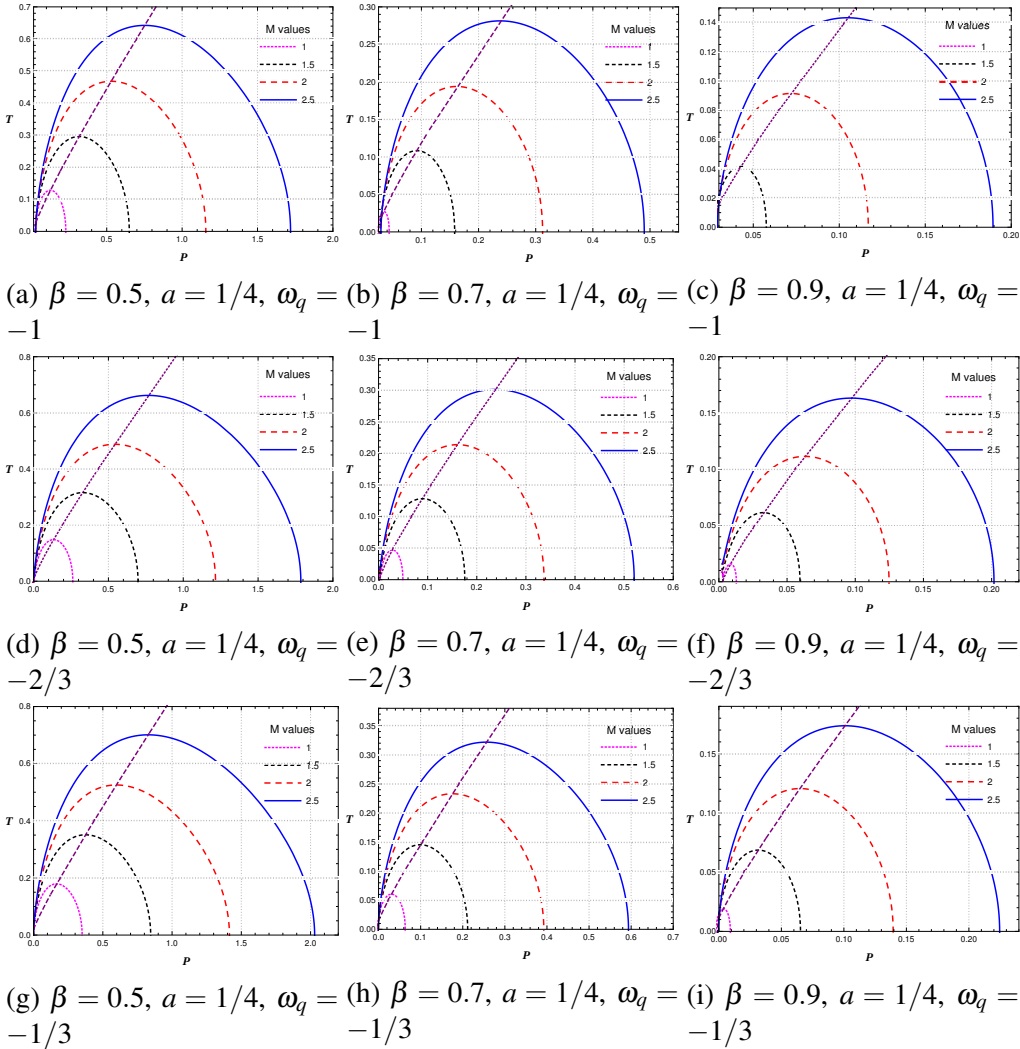
Figure 5.3: Isenthalpic curves for different values of mass. The varition with respect to ω_q for a fixed $a = 1/4$.

We have studied the inversion curves for different values of monopole charge β in

(a) $\beta = 0.5$, $a = 1$, $\omega_q = -1$ (b) $\beta = 0.7$, $a = 1$, $\omega_q = -1$ (c) $\beta = 0.9$, $a = 1$, $\omega_q = -1$

(d) $\beta = 0.5$, $a = 1$, $\omega_q = -2/3$ (e) $\beta = 0.7$, $a = 1$, $\omega_q = -2/3$ (f) $\beta = 0.9$, $a = 1$, $\omega_q = -2/3$

(g) $\beta = 0.5$, $a = 1$, $\omega_q = -1/3$ (h) $\beta = 0.7$, $a = 1$, $\omega_q = -1/3$ (i) $\beta = 0.9$, $a = 1$, $\omega_q = -1/3$
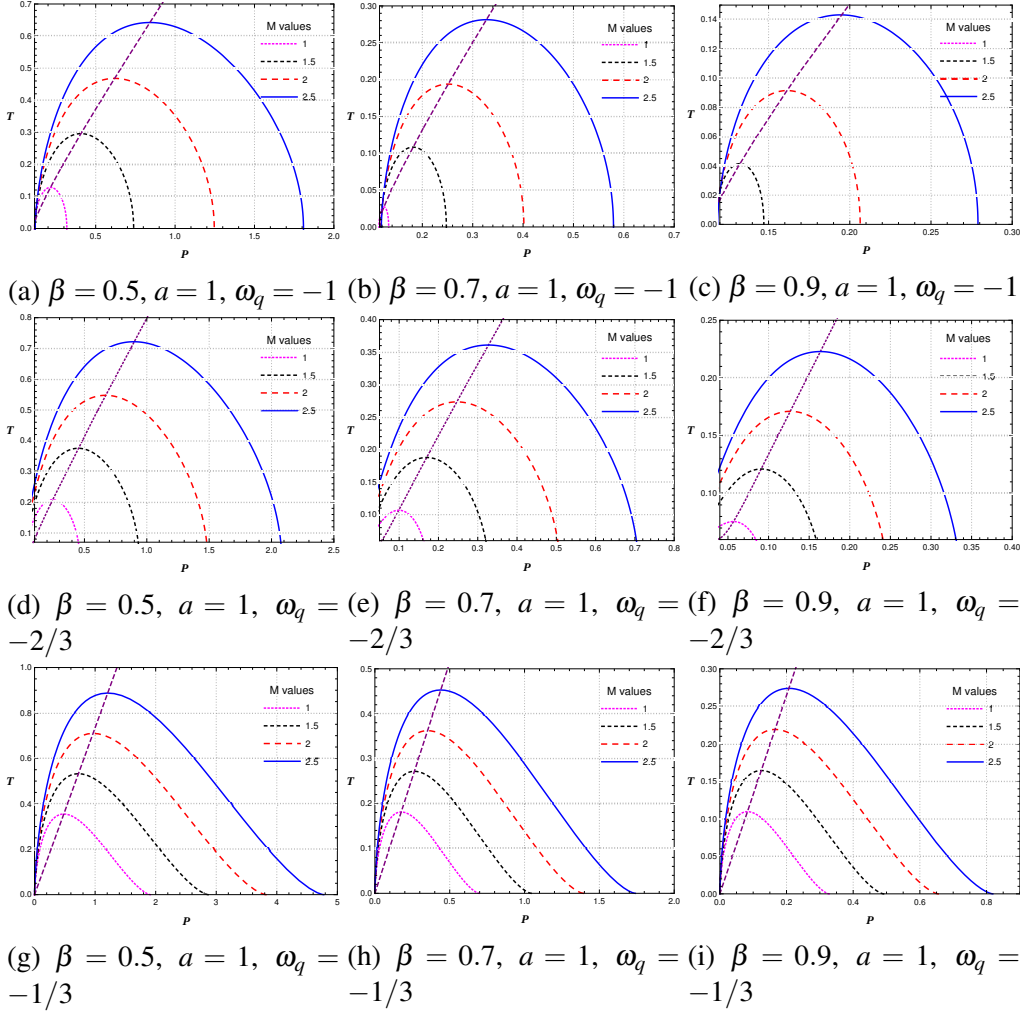
Figure 5.4: Isenthalpic curves for different values of mass. The varition with respect to ω_q for a fixed $a = 1$.

figure (5.1). In all the six plots, the position of inversion point (T_i, P_i) shifts to higher values with an increase in charge β. The effect of quintessence parameters ω_q and a are explicitly depicted in figure (5.2). In the figures (5.2a), (5.2b) and (5.2c), we plotted inversion curves with different quintessence state parameters, which show that increase of w_q from -1 to $-1/3$ increases the inversion temperature. They also show that the separation between the inversion curves for different values of ω_q depends on a. In the second set in figure (5.2) (the curves (5.2d), and (5.2f)), we have plotted the inversion curves by varying the quintessence normalization constant a. These plots show a minor decrease in the inversion points with increase in a. In summary, the slope of the inversion curve increases sharply for an increase in charge β. But the same is not

observed for the change in quintessence parameters w_q and a. The slope of the inversion curve remains the same in this case.

The isenthalpic (constant mass) curves are also studied for the JT expansion. We plot the isenthalpic curves on the $T - P$ plane for fixed values of enthalpy (mass). The intersection point of the inversion curve and isenthalpic curve ($\mu = 0$) separates the cooling and heating phases. Moreover, that happens at maxima of isenthalpic. The figure (5.3) and (5.4) show that the inversion point and isenthalpic curve depend significantly on the mass (enthalpy) of the black hole. With the increase of mass, the inversion temperature T_i and pressure P_i increases.

We show the effect of quintessence parameters (ω_q and a) and charge β in six-set of figures (set 1: figure (5.3a) - (5.3c), set 2: figure (5.3d) - (5.3f), set 3: figure (5.3g) - (5.3i), set 4: figure (5.4a) - (5.4c), set 5: figure (5.4d) - (5.4f), set 6: figure (5.4g) - (5.4i)). In all four sets, we observe that the height of the isenthalpic curve and the value of inversion temperature reduces with an increase in charge β. Comparing set 1 with 2 and 3 also 4 with 5 and 6, we see that, for an increase in quintessence state parameter w_q from -1 to $-1/3$, there is a slight increase in the constant enthalpy curves and the inversion temperature. The effect of quintessence normalization factor a can be seen by comparing figure (5.3) with (5.4). An increase in the value a also increases the height of isenthalpic curves and the inversion temperature. A notable point here is that the isenthalpic curve for $a = 1$, $\omega_q = -1/3$ case shows a deviation in shape from a usual semicircle to a more concave form. This results in the shift of inversion pressure to lower values. These results are consistent with the earlier findings that the thermodynamics of a black hole is affected by the quintessence field. The JT expansion is an inherent feature of van der Waals fluid. Furthermore, therefore the changes in thermodynamic properties and JT expansion are correlated.

5.3 Conclusions and Discussions

In this work, we have studied the JT expansion of regular Bardeen AdS black holes surrounded by quintessence field. The key feature that leads to JT expansion in the black hole is the identification of cosmological constant as pressure which enables us to redefine the black hole mass as enthalpy. We have calculated an exact expression

for the JT coefficient (μ), which depends on the quintessence parameters ω_q and a. We investigated the JT expansion intuitively by using the inversion and isenthalpic curves in the $T - P$ plane. The inversion curve divides the isenthalpic curves in the $T - P$ plane into two regions. The upper region leads to cooling, and the lower region results in heating in the JT expansion's final state. Nevertheless, the slope of the inversion curve always remains positive.

We have studied the isenthalpic curves and the inversion curves for different values of enthalpy (mass), charge β, and quintessence parameters (a, w_q), separately. The constant enthalpy curves show that the inversion temperature T_i increases for the larger enthalpy and reduces with an increase in the charge β. It is observed that the slope of inversion curves increases with the charge β. However, the quintessence dark energy affects the inversion and isenthalpic curves significantly, which is an exciting result from our study. Both the quintessence parameters influence the JT expansion in the same manner. An increase in the value of both ω_q and a increases the height of isenthalpic curves and the inversion temperature.

This result is interesting because the thermodynamics of black holes with quintessence depends on their quintessence parameters. The dependence of JT expansion on these parameters is intriguing as the quintessence plays the role of dark energy in many cosmological models.

Chapter 6

Regular Bardeen AdS Black Hole in Higher Dimension

In this chapter we computed the thermodynamics of regular Bardeen black hole in higher dimensions and also investigate the thermodynamic geomtry.

6.1 Introduction

The Bardeen model is the most relevant regular black hole model, generating a significant increase in the study of regular black holes (Ayón-Beato and Garcıa 2000, Ayon-Beato and Garcıa 1999, Ayón-Beato and Garcia 2005). The Bardeen solution is extended to noncommutative inspired geometry (Sharif and Javed 2011) and the Bardeen de Sitter black holes (Fernando 2017). Moreno and Sarbach (Moreno and Sarbach 2003) studied the stability of the Bardeen black hole, which has gotten much interest recently. The Keplerian disk orbiting around the Bardeen black holes was addressed in (Schee and Stuchlík 2016). Several writers (Fernando and Correa 2012, Flachi and Lemos 2013, Ulhoa 2014) have investigated the quasinormal modes of the Bardeen black holes. (Singh and Singh 2017) looked at the anti-evaporation effect of Bardeen de Sitter black holes. Man and Cheng (Man and Cheng 2014) looked at the thermodynamic quantities of Bardeen black holes. Zhou et al. (Zhou et al. 2012) in-

vestigated the velocity of a test particle in the spacetime of Bardeen black holes. There was also a study about revolving Bardeen black holes (Ghosh and Amir 2015, Bambi and Modesto 2013).

Ideas such as cosmology in brane-world scenarios, string theory, and the AdS/CFT correspondence (Maldacena 1999, Klein 1926) have motivated the research of black hole solutions and their various features in dimensions higher than four. The most successful quantum gravity theory is string theory, which requires more than four dimensions to describe gravity. String phenomenology (Arkani-Hamed et al. 2001), which describes how the study of string theory may explain and, as a result, anticipate real-world scenarios, may motivate the research for black hole solutions in higher dimensions. As a result, understanding string theory in general, and the gauge/gravity duality relationship in particular, will need extensive research into black holes in extra dimensions. These observations lead us to conclude that, while the research of higher-dimensional black holes is unlikely to be avoided in a real-world setting, its impact on other fields of physics may be significant. For a higher dimensional black hole, the first successful statistical counting of black hole entropy was done (Strominger and Vafa 1996). In situations with large extra dimensions and TeV-scale gravity, the formation of higher-dimensional black holes at the LHC becomes a possibility (Aharony et al. 2000, Cavaglia 2003). The AdS/CFT describes the connection between the dynamics of d dimensional black holes and quantum field theories in $(d-1)$ dimensional spacetimes. These considerations might conclude that gravity in higher dimensions is more challenging than gravity in four dimensions. Higher-dimensional black holes, particularly five-dimensional black holes, have recently gained much attention and investigation (Emparan and Reall 2002, Myers and Perry 1986, Randall and Sundrum 1999, Reall 2003). The uniqueness theorem fails because there are more degrees of freedom in more than four dimensions (Hollands and Yazadjiev 2008). Non-trivial topologies are permissible in five dimensions, as shown by black ring solutions (Emparan and Reall 2002). Black holes in higher dimensions have several rotating planes independent of one another. Black holes have more complicated horizon structures in higher dimensions, and gravity is richer than in four dimensions. There is growing ev-

idence that the physics of higher-dimensional black holes vary significantly from those of four-dimensional black holes. As a result, as seen by the growing number of recent works, there is tremendous interest in understanding black holes in higher dimensions. Meyers-Perry (Myers and Perry 1986) discovered Schwarzschild, Reissner-Nordström, and Kerr solutions in asymptotically flat higher dimensional spacetimes, which were later extended by Dianyan (Dianyan 1988) to find charged-dS black holes, and later by Liu and Sabra (Liu and Sabra 2004) to find d dimensional charged black holes in (A)dS spaces. The Baados-Teitelboim-Zanelli black holes (Ghosh 2012, Hendi 2011), as well as the radiating black holes (Ghosh and Dawood 2008, Ali and Ghosh 2018), have been expanded to higher dimensions. The gravitational collapse of various fluids (Ghosh and Deshkar 2003, Ghosh and Banerjee 2003, Dadhich et al. 2005, DeBenedictis and Das 2003) is another example from higher-dimensional spacetime. Finding the Bardeen solution in higher-dimensional spacetimes is also interesting. It is crucial to think about the d dimensional analog of Bardeen-de Sitter black holes and their thermodynamic properties. (Ali and Ghosh 2018) studied the thermodynamics of Bardeen de Sitter black hole in higher dimensions, and (Kumar et al. 2019) investigated the d dimensional Bardeen AdS black holes in Einstein Gauss Bonet theory. Motivated by these studies, in the first section, we calculate the thermodynamics of the d dimensional regular Bardeen AdS black hole, and in the next section, we study its thermodynamic geometry.

6.2 Thermodynamics of Regular Bardeen Black Hole in Higher Dimensions

The metric of the regular Bardeen black hole in higher dimension is given by (Ali and Ghosh 2018),

$$ds^2 = -f(r)dt^2 + \frac{1}{f(r)}dr^2 + r^2 d\Omega_{d-2}^2,$$ (6.1)

with

$$f(r) = 1 - \frac{mr^2}{(r^{d-2} + \beta^{d-2})^{\frac{d-1}{d-2}} \Omega_{d-2}} - \frac{2\Lambda r^2}{(d-1)(d-2)},$$ (6.2)

and (Myers and Perry 1986)

$$m = \frac{16\pi M}{(d-2)\Omega_{d-2}}, \qquad \Omega_{d-2} = \frac{2\pi^{\frac{d-1}{2}}}{\Gamma(\frac{d-1}{2})}. \tag{6.3}$$

In the above expressions, M represents the black hole mass. The black hole mass is

$$M = \frac{\Omega_{d-2}\left(\beta^{d-2} + r_h^{\,d-2}\right)^{\frac{d-1}{d-2}}\left(d^2 - 3d - 2\Lambda r_h^2 + 2\right)}{16\pi(d-1)r_h^2}. \tag{6.4}$$

When $\beta \to 0$, (6.2) reduces to the d dimensional Schwarzschild-Tangherlini black hole (Tangherlini 1963). The relation between pressure and cosmological constant in higher dimension is given by (Kastor et al. 2009),

$$P = -\frac{\Lambda}{8\pi} = \frac{(d-1)(d-2)}{16\pi\ell^2}. \tag{6.5}$$

The temperature of a black hole can be calculated as follows:

$$T = \frac{\beta^2 r_h^{\,d}\left(d^2 - 5d + 16\pi P r_h^2 + 6\right) - 2(d-2)r_h^2\beta^d}{4\pi(d-2)r_h\left(r_h^2\beta^d + \beta^2 r_h^{\,d}\right)}. \tag{6.6}$$

Rearranging the above expression, we obtain the equation of state,

$$P = \frac{(d-2)r_h^{-d-2}\left(2r_h^2\beta^d(2\pi r_h T + 1) - \beta^2 r_h^{\,d}(d - 4\pi r_h T - 3)\right)}{16\pi\beta^2}. \tag{6.7}$$

Entropy in the large r_h limit is

$$S = \frac{\Omega_{d-2}r_h^{\,d-2}}{4}. \tag{6.8}$$

When $d = 4$ and $\Lambda = 0$, (6.6) reduces to the temperature of the Bardeen black hole (Akbar et al. 2012)

$$T = \frac{1}{4\pi r_h}\left(\frac{r_h^2 - 2\beta^2}{r_h^2 + \beta^2}\right). \tag{6.9}$$

Now we focus on another important thermodynamic variable, the heat capacity. The heat capacity at constant pressure is calculated as,

$$C_P = \frac{8(d-2)S^2\left(\Omega_{d-2}\beta^d+4\beta^2 S\right)\left(\frac{1}{4}\beta^2\left(d^2+2^{\frac{4(d-1)}{d-2}}P\pi\left(\frac{S}{\Omega_{d-2}}\right)^{\frac{2}{d-2}}-5d+6\right)-\frac{(d-2)\Omega_{d-2}\beta^d}{8S}\right)}{\beta^4 S^2\left(-8d^2+2^{\frac{7d-10}{d-2}}P\pi\left(\frac{S}{\Omega_{d-2}}\right)^{\frac{2}{d-2}}+40d-48\right)+8(d-2)S\Omega_{d-2}\beta^{d+2}+d(d-2)\Omega_{d-2}^2\beta^{2d}}.$$ (6.10)

The behavior of this heat capacity in different spacetime dimensions is shown in figure (6.1). The divergence of C_P is seen in all cases that correspond to phase transitions.
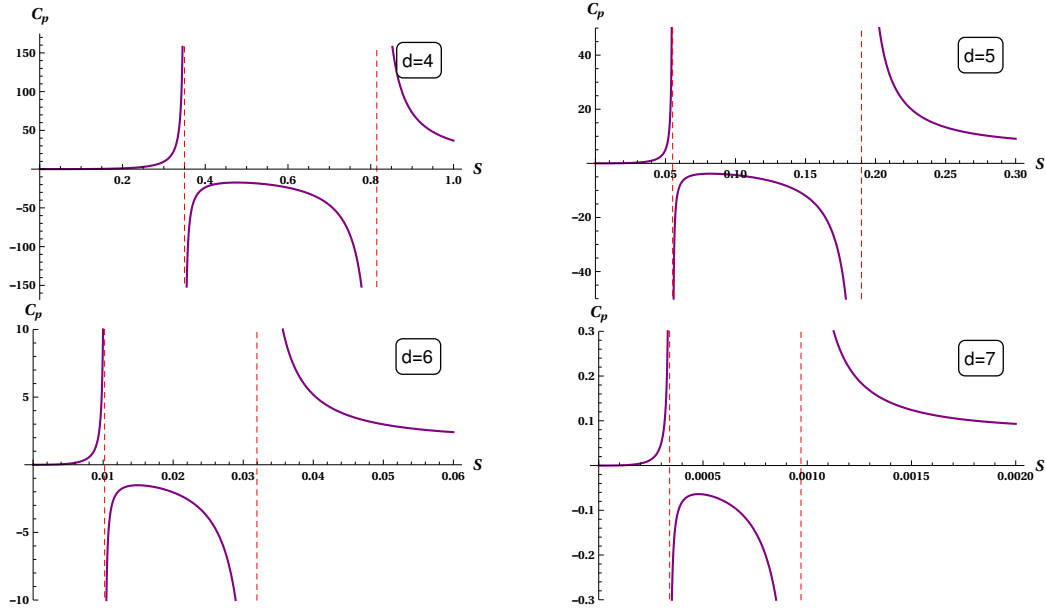
Figure 6.1: Specific heat versus Entropy diagram for regular AdS black hole in different dimensions with $\beta = 0.1$.

6.3 Thermodynamics Geometry of Regular Bardeen Black Hole in Higher Dimensions

G. Ruppeiner (Ruppeiner 1979, 1983, 1995, 2007, 2008) proposed an alternative technique, popularly known as thermodynamic state space geometry, to explain conventional thermodynamic systems as well as black holes, inspired by the beauty of Riemannian geometry. In this section, encouraged by the success of this concept in explaining the thermodynamic phases of various black hole systems (Ferrara et al. 1997, Cai and Cho 1999, Åman and Pidokrajt 2006, Sarkar et al. 2006, Åman et al. 2007, Myung et al.

2008a, Niu et al. 2012, Weinhold 1975, Åman et al. 2003, Sahay et al. 2010), we aim to use it to examine the phase transition phenomena in regular Bardeen AdS black holes in higher dimensions.

The method of thermodynamic geometry is an interesting technique to approach black hole phase transition. Ruppeiner geometry is a geometric formalism in which the Hessian of the entropy function is considered as a metric tensor on the state space. The corresponding thermodynamic scalar curvature gives the knowledge of underlying microscopic interactions of the system. Near the critical points, the curvature scalar shows a divergence behavior. The Ruppeiner geometry is conformally related to another thermodynamic geometry, namely the Weinhold geometry. In Ruppeiner geometry, the equilibrium thermodynamic state space is defined by a metric which is a function of entropy instead of the mass as in the Weinhold case. The Ruppeiner metric is given by (for more details see Appendix E) (Ruppeiner 1979, 1995),

$$g_{ij}^R = -\frac{\partial^2 S(x^i)}{\partial x^i \partial x^j},$$

(6.11)

where $x^i = x^i(M,\beta)$ are the extensive variables. Similarly the Weinhold metric components are defined as (Weinhold 1975),

$$g_{ij}^W = \frac{\partial^2 M(x^i)}{\partial x^i \partial x^j},$$

(6.12)

with $x^i = x^i(S,\beta)$. However the Weinhold geometry and Ruppeiner geometry are related to each other as follows due to their conformal relation (Janyszek and Mrugała 1989, Ferrara et al. 1997),

$$dS_R^2 = \frac{dS_W^2}{T}.$$

(6.13)

For calculating metric components we express the blackhole mass and temperature in terms of entropy,

$$M = \frac{4^{-\frac{2}{d-2}-2}\Omega_{d-2}\left(\frac{S}{\Omega_{d-2}}\right)^{-\frac{2}{d-2}}\left(e^{d-2}+\left(4^{\frac{1}{d-2}}\left(\frac{S}{\Omega_{d-2}}\right)^{\frac{1}{d-2}}\right)^{d-2}\right)^{\frac{d-1}{d-2}}\left(d^2+\pi 2^{\frac{4(d-1)}{d-2}}P\left(\frac{S}{\Omega_{d-2}}\right)^{\frac{2}{d-2}}-3d+2\right)}{\pi(d-1)},$$

(6.14)
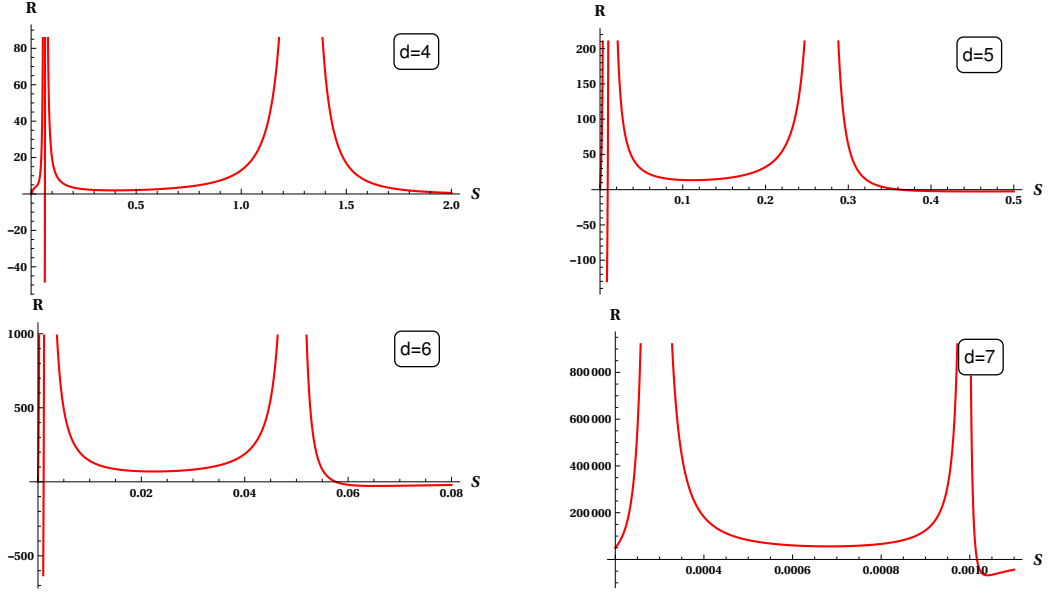
Figure 6.2: Curvature divergence plots for Ruppeiner metric for regular AdS black hole in different dimensions with $\beta = 0.1$.

$$T = \frac{4^{\frac{1}{2-d}-1}\left(\frac{S}{\Omega_{d-2}}\right)^{\frac{1}{2-d}}\left(e^2\left(4^{\frac{1}{d-2}}\left(\frac{S}{\Omega_{d-2}}\right)^{\frac{1}{d-2}}\right)^d\left(d^2+\pi 4^{\frac{2}{d-2}+2}P\left(\frac{S}{\Omega_{d-2}}\right)^{\frac{2}{d-2}}-5d+6\right)-2^{\frac{d+2}{d-2}}(d-2)e^d\left(\frac{S}{\Omega_{d-2}}\right)^{\frac{2}{d-2}}\right)}{\pi(d-2)\left(4^{\frac{2}{d-2}}e^d\left(\frac{S}{\Omega_{d-2}}\right)^{\frac{2}{d-2}}+e^2\left(4^{\frac{1}{d-2}}\left(\frac{S}{\Omega_{d-2}}\right)^{\frac{1}{d-2}}\right)^d\right)}.$$

(6.15)

Plugging this expression into equation (6.12) and then using equation (6.13) we obtain the metric components, and we compute the curvature scalar R_R using the metric components g_{ij}^R. The result is used to plot curvature scalar versus entropy diagram to study phase transition (figure 6.2). For all spacetime dimensions, the curvature scalar shows the same functional behavior.

6.4   Results and Discussions

In this chapter, we investigated the thermodynamic phase transition in regular Bardeen AdS black holes in higher dimensions and also studied its thermodynamic geometry. It is observed that there exist phase transitions in any arbitrary dimensions in the case of regular Bardeen AdS black hole. The divergence in specific heat and curvature scalar confirms critical behavior. However, the result, in this case, is physically more relevant since the scalar curvature is related to the microscopic structure of the black hole.

Chapter 7

Summary and Future Work

"No one undertakes research in physics with the intention of winning a prize. It is the joy of discovering something no one knew before."- **Stephen Hawking**

7.1   Summary

This Chapter summarises all of the topics and results discussed throughout the thesis. We investigated the thermodynamic phase transition and its applications, such as heat engine, Joule Thomson expansion, and thermodynamic geometry of regular Bardeen AdS black holes in the extended phase space. Black hole thermodynamics is surprisingly normal in the sense that they resemble the thermodynamics of ordinary matter systems. Because it connects gravity in curved spacetime with quantum physics, it is believed that black hole thermodynamics will give a possible route to quantum gravity. In the perspective of AdS/CFT correspondence, the thermodynamics of black holes in AdS spacetime have played a vital role. The study of black hole thermodynamics and its applications has become a vibrant field in theoretical physics. Physicists use black hole thermodynamics to uncover the deep relation between gravitation, quantum theory, and statistical physics. When the cosmological constant is treated as the pressure in the extended phase space, the thermodynamics of black holes in AdS spacetime become consistent with the Smarr relation. In general relativity, the existence of singularities

is a fascinating issue. Regular black holes are singularity-free. Bardeen proposed one of the first regular black hole models. The thermodynamics and applications of regular Bardeen AdS black holes in extended phase space with and without quintessence have been investigated in this thesis. In **Chapter 1**, we reviewed a brief history of black holes, their observational evidence, and their thermodynamic properties.

Chapter 2 briefly explained the laws of black hole thermodynamics and thermodynamic phase transition in extended phase space. **Chapter 3** studied the thermodynamic phase transition of regular Bardeen AdS black holes in the extended phase space with and without quintessence. It shows that the critical behavior is similar to the $P - v$ and $T - S$ plots of a van der Waals gas. The quintessence parameters a and ω_q depend on the thermodynamics of the black hole.

Chapter 4 investigated the efficiency of the heat engine, which is constructed by taking a regular Bardeen black hole as a working substance. The engine's efficiency is determined by using the work done and heat absorbed during the cycle. A comprehensive investigation of the dependence of efficiency (η) was performed on entropy (S_2), pressure (P_1) and charge (β) . Among many observations, we emphasize that the increase in entropy difference between a small black hole (S_1) and a large black hole (S_2) increases the efficiency. Also, the greater difference in pressure increases the efficiency of the engine. In all these studies, the efficiency remains bounded below unity, consistent with the second law. We have made a successful attempt to improve the efficiency of the engine by adding a quintessence field. This finding may deepen our understanding of the thermodynamics of asymptotic AdS black holes.

Chapter 5 investigated the Joule-Thomson expansion of regular Bardeen AdS black hole surrounded by a quintessence field and shows that an exact expression for the JT coefficient (μ) depends on the quintessence parameters ω_q and a. In the $T - P$ plane, the inversion curve divides the isenthalpic curves into two regions. The upper region of the JT expansion causes cooling, while the lower region causes heating in its final state. However, the slope of the inversion curve always remains positive. The study of isenthalpic curves and the inversion curves for various values of enthalpy (mass), charge β, and quintessence parameters (a, ω_q), independently show that the inversion temper-

ature T_i increases for the greater enthalpy and reduces with increase in the charge β. The slope of inversion curves appears to increase as the charge β increases. However, the quintessence dark energy greatly influences the inversion and isenthalpic curves. Each of the quintessence parameters similarly affects the JT expansion. An increase in the value of both ω_q and a increases the height of isenthalpic curves and the inversion temperature.

In **chapter 6**, we studied the thermodynamic phase transition in higher dimensions which shows that the critical behavior of the regular Bardeen black hole exists in any arbitrary dimensions.

This thesis's outcome is promising when one considers the quintessence as a viable model for dark energy. We expect that our study in such a manner will shed light on the thermodynamics of quintessential AdS black holes.

7.2   Future Prospects

- To study the microstructure of regular Bardeen black hole.

- To study the phase structure and quasi-normal modes of regular Bardeen black hole.

- To investigate the fractional-order phase transition in different black holes.

- To study the thermodynamic phase transition in Rastall gravity and its applications.

Appendices

Appendix A

The Metric for Bardeen Black Hole Surrounded by Quintessence

We start with a static spherically symmetric metric *ansatz* in four dimensions such that

$$ds^2 = -\left(1 - \frac{2m(r)}{r}\right) dt^2 + \frac{dr^2}{\left(1 - \frac{2m(r)}{r}\right)} + r^2 \left(d\theta^2 + \sin^2\theta d\phi^2\right). \tag{A.1}$$

The field equation can be written as,

$$G_{\mu\nu} + \Lambda g_{\mu\nu} = T_{\mu\nu}^{(q)} + T_{\mu\nu}^{(ND)}. \tag{A.2}$$

where $G_{\mu\nu} = R_{\mu\nu} - \frac{1}{2} g_{\mu\nu} R$, and $g_{\mu\nu}$ are the Eintstein field tensor and the metric tensor, respectively. $R_{\mu\nu}$ and R are, respectively, the Ricci tensor and Ricci scalar. And $T_{\mu\nu}^{(q)}$, and $T_{\mu\nu}^{(ND)}$ are, respectively, the energy-momentum tensors for quintessence field and the nonlinear electrodynamics. The independent components of the field equations are written as,

$$\frac{2m'(r)}{r^2} - \Lambda = T_t^{t\,(q)} + T_t^{t\,(ND)}, \tag{A.3}$$

$$\frac{m''(r)}{r} - \Lambda = T_\theta^{\theta\,(q)} + T_\theta^{\theta\,(ND)}, \tag{A.4}$$

where

$$T_t^{t\,(q)} = T_r^{r\,(q)} \quad = \quad \rho_q = \frac{3a\omega_q}{r^{3(\omega_q+1)}}, \tag{A.5}$$

$$T_t^{t\,(ND)} = T_r^{r\,(ND)} \quad = \quad 2\mathcal{L}(r) = \frac{6M\beta^2}{(r^2+\beta^2)^{5/2}}, \tag{A.6}$$

$$T_\theta^{\theta\,(q)} = T_\phi^{\phi\,(q)} \quad = \quad -\frac{1}{2}\rho_q\left(3\omega_q+1\right) = -\frac{a}{2}\frac{3\omega_q\left(3\omega_q+1\right)}{r^{3(\omega_q+1)}}, \tag{A.7}$$

$$T_\theta^{\theta\,(ND)} = T_\phi^{\phi\,(ND)} \quad = \quad 2\left(\mathcal{L}(r) - \frac{\partial\mathcal{L}}{\partial r}\left(\frac{\partial\mathcal{F}}{\partial r}\right)^{-1}F^{\theta\phi}F_{\theta\phi}\right) = \frac{3M\beta^2\left(3r^2-2\beta^2\right)}{(r^2+\beta^2)^{7/2}} \tag{A.8}$$

Substituting for $T_r^{r\,(q)}$ and $T_r^{r\,(ND)}$, we have

$$\frac{2m'(r)}{r^2} - \Lambda \quad = \quad \frac{3a\omega_q}{r^{3(\omega_q+1)}} + \frac{6M\beta^2}{(r^2+\beta^2)^{5/2}}, \tag{A.9}$$

$$\text{i.e,} \quad m'(r) \quad = \quad \frac{\Lambda r^2}{2} + \frac{a}{2}\frac{3\omega_q}{r^{(3\omega_q+1)}} + \frac{3M\beta^2 r^2}{(r^2+\beta^2)^{5/2}}. \tag{A.10}$$

$$\tag{A.11}$$

Integrating the above equation, we get

$$m(r) \quad = \quad \int_0^r dr\frac{\Lambda r^2}{2} + \int_0^r dr\frac{a}{2}\frac{3\omega_q}{r^{(3\omega_q+1)}} + \int_0^r dr\frac{3M\beta^2 r^2}{(r^2+\beta^2)^{5/2}}, \tag{A.12}$$

$$= \quad \frac{\Lambda r^3}{6} + \frac{a}{2}\frac{1}{r^{3\omega_q}} + \frac{Mr^3}{(r^2+\beta^2)^{3/2}}. \tag{A.13}$$

$$\tag{A.14}$$

Therefore, the metric function reads,

$$f(r) \quad = \quad 1 - \frac{2m(r)}{r} = 1 - \frac{2M\,r^2}{(r^2+\beta^2)^{3/2}} - \frac{a}{r^{(3\omega_q+1)}} - \frac{\Lambda r^2}{3}, \tag{A.15}$$

$$\text{or} \quad f(r) \quad = \quad 1 - \frac{2Mr^2}{(r^2+\beta^2)^{3/2}} - \frac{a}{r^{(3\omega_q+1)}} + \frac{r^2}{l^2}, \quad \text{with } \Lambda = -\frac{3}{l^2}. \tag{A.16}$$

$$\tag{A.17}$$

This way, we can get the required solution for regular Bardeen black hole with quintessence.

Appendix B

Singularity

A spacetime singularity is a "place" where the metric's curvature "blows up" due to other "pathological behavior". We may easily argue that a point in spacetime has a singularity if a physical quantity is infinite or otherwise undefined. The manifold and metric structure of spacetime must be solved in GR. The most obvious approach in GR suggests that a spacetime consists of a manifold M and a metric g_{ab} defined everywhere on M.

Let $O \subset M$ be open and M be a manifold. A congruence in O is a set of curves that passes through each $p \in O$ with exactly one curve from this set. As a result, the tangents to a congruence produce a vector field O. If the related vector field is smooth, the congruence is said to be smooth. Consider a smooth congruence of timelike geodesics as an example. Assume geodesics are parameterized by proper time τ and that the tangent vector field, ξ^a, is normalized to unit length, $\xi^a \xi_a = -1$.

The vector field B_{ab}, which is specified by $B_{ab} = \nabla_b \xi_a$, will then be solely spatial, i.e.,

$$B_{ab}\xi^a = B_{ab}\xi^b = 0. \tag{B.1}$$

Let η^a be the orthogonal deviation vector from γ_0 for a smooth one-parameter subgroup $\gamma_s(\tau)$ of geodesics in the congruence. We have,

$$\pounds_\xi \eta^a = 0, \tag{B.2}$$

and thus

$$\xi^b \nabla_b \eta^a = \eta^b \nabla_b \xi^a = B_b^a \eta^b. \tag{B.3}$$

As a result, B_b^a measures the failure of η^a to be transported parallelly. According to an observer on the geodesic γ_0, the linear map B_b^a would extend and rotate the close geodesics surrounding him.

The spatial metric h_{ab} is defined as,

$$h_{ab} = g_{ab} + \xi_a \xi_b. \tag{B.4}$$

As a result, $h_b^a = g^{ac} h_{cb}$ is the projection operator onto the subspace of the tangent space orthogonal to ξ^a. Thus, B_{ab} is decomposed as

$$B_{ab} = \frac{1}{3} \theta h_{ab} + \sigma_{ab} + \omega_{ab}, \tag{B.5}$$

with expansion $\theta = B^{ab} h_{ab}$, shear $\sigma_{ab} = B_{(ab)} - \frac{1}{3} \theta h_{ab}$, and twist $\omega_{ab} = B_{[ab]}$. σ_{ab} and ω_{ab} are solely spatial in nature, with $\sigma_{ab} \xi^b = \omega_{ab} \xi^b = 0$. θ measures the average expansion of the infinitesimally adjacent surrounding geodesics along any geodesic in the congruence; according to equation B.3, ω_{ab}, as the antisymmetric part of the linear map B_{ab}, measures their rotation, while σ_{ab} measures their shear; that is, an initial sphere in the tangent space that is Lie transported along ξ^a will distort toward an ellipsoid with principal axes given by the eigenvector of σ_b^a, and rate given by the eigenvalue of σ_b^a. The geodesic equation clearly produces equations for the rate of change of θ, σ_{ab}, and ω_{ab} along each geodesic in the congruence. However, creating these equations are simple. We have,

$$\xi^c \nabla_c B_{ab} = \quad \xi^c \nabla_c \nabla_b \xi_a = \xi^c \nabla_b \nabla_c \xi_a + R_{cba}^d \xi^c \xi_d \tag{B.6}$$

$$= \nabla_b (\xi^c \nabla_c \xi_a) - (\nabla_b \xi^c)(\nabla_c \xi_a) + R_{cba}^d \xi^c \xi_d \tag{B.7}$$

$$= -B_b^c B_{ac} + R_{cba}^d \xi^c \xi_d \tag{B.8}$$

We get

$$\xi^c \nabla_c \theta = \frac{d\theta}{d\tau} = -\frac{1}{3} \theta^2 - \sigma_{ab} \sigma^{ab} + \omega_{ab} \omega^{ab} - R_{cd} \xi^c \xi^d,$$

(B.9)

by taking the trace of the equation. This is known as Raychaudhuri's equation, and it is the crucial equation in proving the singularity theorem.

Appendix C

Joule Thomson Effect

Joule Thomson expansion in thermodynamics, is an irreversible mechanism that describes how the temperature of a gas changes as it passes through a porous plug from a high-pressure to a low-pressure area. The enthalpy of the system remains constant during this expansion. The isenthalpic curve is defined by the set of values (T, P) that occur throughout the process with a constant enthalpy condition. The Joule Thomson coefficient (slope of the isenthalpic curve) is calculated as follows:

$$\mu_j = \left(\frac{\partial T}{\partial P}\right)_H. \tag{C.1}$$

At the isenthalpic curve's maximum, the Joule–Thomson coefficient is zero. The inversion curve is the location of such points. The region of cooling is the interior of the inversion curve, where the gradient of isenthalps (μ_j) is positive, and the region of heating is the exterior, where (μ_j) is negative. The enthalpy differential is equal to

$$dH = TdS + VdP. \tag{C.2}$$

Using second TdS equation,

$$TdS = C_P dT - T\left(\frac{\partial V}{\partial T}\right)_P dP, \tag{C.3}$$

$$C_P dT = \frac{1}{C_P} TdS + \frac{T}{C_P}(\frac{\partial V}{\partial T}_P dP, \tag{C.4}$$

$$dT = \frac{1}{C_P}[dH - VdP] + \frac{T}{C_P}(\frac{\partial V}{\partial T}_P dP, \tag{C.5}$$

$$dT = \frac{1}{C_P}\left[T\left(\frac{\partial V}{\partial T}\right)_P - V\right]dP + \frac{1}{C_P}dH. \tag{C.6}$$

The coefficient of Joule Thomson expansion can also be written as,

$$\mu_j = \left(\frac{\partial T}{\partial P}\right)_M = \frac{1}{C_P}\left[T\left(\frac{\partial V}{\partial T}\right)_P - V\right]. \tag{C.7}$$

From this, one can get the inversion temperature by setting $q\mu_j = 0$,

$$T_i = V\left(\frac{\partial T}{\partial V}\right)_P. \tag{C.8}$$

This is at the maxima of the isenthalpic curve, with the corresponding inversion pressure. The point defined by inversion temperature and inversion pressure is called the inversion point.

Appendix D

Anti-de Sitter Space

Anti-de Sitter (AdS) is the maximally symmetric constant negative scalar curvature spacetime. $d+1$ dimensional Anti-de Sitter space can be easily defined by an embedding space $R^{d,2}$. Consider an anti-de Sitter space having radius ℓ. The hyperboloid can be given by constraint equation

$$-X_0^2 - X_1^2 + X_2^2 + X_3^2 + \ldots\ldots + X_d^2 = -\ell^2. \qquad (D.1)$$

The metric of the $(d+1)$ dimensional hyperbolic space can be written as,

$$ds^2 = -dX_0^2 - dX_1^2 + dX_2^2 + dX_3^2 + \ldots\ldots + dX_d^2. \qquad (D.2)$$

Consider five dimensional flat manifold embedded in a hyperboloid, then the space is $R^{3,2}$.

$$-X_0^2 - X_1^2 + X_2^2 + X_3^2 + + X_4^2 = -\ell^2. \qquad (D.3)$$

The metric becomes,

$$ds^2 = -dX_0^2 - dX_1^2 + dX_2^2 + dX_3^2 + dX_4^2. \qquad (D.4)$$

Here X_0 and X_1 having timelike dimensions and X_2, X_3 and X_4 having spacelike dimensions.

We can parametrize the AdS space by introducing new coordinates (t, ρ, θ, ϕ), then

$$X_0 = \ell \sin t \cosh\rho, \tag{D.5}$$

$$X_1 = \ell \cos t \cosh\rho, \tag{D.6}$$

$$X_2 = \ell \sinh\rho \cos\theta, \tag{D.7}$$

$$X_3 = \ell \sinh\rho \sin\theta \cos\phi, \tag{D.8}$$

$$X_4 = \ell \sinh\rho \sin\theta \sin\phi. \tag{D.9}$$

These equations will satisfy D.3, then the metric D.4 become,

$$ds^2 = \ell^2 \left(-\cosh^2\rho \, dt^2 + d\rho^2 + \sinh^2\rho \, d\Omega_2^2 \right), \tag{D.10}$$

where $d\Omega_2^2 = d\theta^2 + \sin^2\theta d\phi^2$ is the metric of 2-sphere.

The coordinates (t, ρ, θ, ϕ) are known as global coordinates, because which cover entire space $(\rho \geq 0, 0 \leq t \leq 2\pi)$. The timelike coordinate is periodic. The timelie curve form a circle for constant (ρ, θ, ϕ). Here the hyperbolic space has the topology of R^3 and the timelike curve is of S^1. Hence the AdS space is the product of S^1 and R^3 i.e., $S^1 \times R^3$. This periodic identification of timelike curve can be avoided by considering $R^{3,2}$ space. The range of time coordinate can be taken as $-\infty \leq t \leq \infty$. This has the topology of R^1. Thus the entire AdS spacetime topology be R^4. This space time is called universal covering space of AdS space. This makes the AdS space unique.

The space is conformally compactifying by defining $\cosh\rho := \frac{1}{\cos\chi}$ thus $\tan\chi := \sinh\rho$, then

$$ds^2 = \frac{\ell^2}{\cos^2\chi} \left(-dt^2 + d\chi^2 + \sinh^2\chi d\Omega_2^2 \right). \tag{D.11}$$

The time coordinate ranges from $-\infty \leq t \leq \infty$, and radial coordinates ranges from $\frac{-\pi}{2} \leq \chi \leq \frac{\pi}{2}$. Conformal boundary of d-dimensional AdS space $(R \times S^{d-2})$ is same as that of one lesser dimensional $(R^{1,d-1})$ conformally compactifying Minkowski space. That means AdS space is conformally flat. Consider static coordinates $r = \ell \sinh\rho$, then

$$ds^2 = -\left(1 + \frac{r^2}{\ell^2}\right) dt^2 + \left(1 + \frac{r^2}{\ell^2}\right)^{-1} dr^2 + r^2 d\Omega_2^2. \tag{D.12}$$

Any spacetime which asymptotically approaches this metric is known as asymptotically AdS spacetime.

Appendix E

Thermodynamic Geometry

To study black hole microstructure, in 2008, George Ruppeiner proposed a phenomenological model based on fluctuation theory. Fluctuation theory describes that, in equilibrium, the physical quantities of a microscopic body are nearly equal to their mean values. However, they fluctuate from their mean value in a small amount. For fluctuation, we need to calculate the probability distribution of a physical quantity x to be in between $(x_0, x_1, ..., x_N)$ and $(x_0 + dx_0, x_1 + dx_1, ..., x_N + dx_N)$. The probability is proportional to the number of microstates Ω.

$$P(X_0...x_N)dx_0...dx_N = K\Omega(X_0...x_N), \tag{E.1}$$

where K is proportionality constant.

According to Boltzmann entropy formula

$$S = k_B ln\Omega \implies \Omega = e^{\frac{S(x)}{k_b}}, \tag{E.2}$$

$$P(x)dx = Ke^{\frac{S(x)}{k_b}} dx. \tag{E.3}$$

Using Taylor expansion around equilibrium valu x_0, then

$$S(x) = S(x_0) + (x - x_0)\frac{\partial S}{\partial x}|_{x=x_0} + \frac{1}{2}(x - x_0)^2\frac{\partial^2 S}{\partial x^2}|_{x=x_0} + ..., \tag{E.4}$$

$\frac{\partial S}{\partial x}|_{x=x_0} = 0$, because system will have maximum entropy around x_0. Define : $-x - x_0 =$

Δx and $\left(\dfrac{-k_B}{\left(\frac{\partial^2 S}{\partial x^2} \right)_{x=x_0}} \right) = <(\Delta x)^2> = \sigma^2$, then the equation becomes,

$$P(x)dx = Kexp \left(\frac{-(\Delta x)^2}{2 <(\Delta x)^2>} \right) dx. \tag{E.5}$$

We can express standard deviation of the energy, when it fluctuate in canonical ensembe, which is same as heat capacity

$$\sigma_E^2 = <(\Delta E)^2> = <E^2> - <E>^2 = k_B T^2 C_v. \tag{E.6}$$

Consider two fluctuating variables x^μ and x^ν, then
$\Delta x^\mu = x^\mu - x_0^\mu$ and $\Delta x^\nu = x^\nu - x_0^\nu$,
where x_0^μ and x_0^ν are their equilibrium values.
So

$$P(x)dx = \quad Ke^{S(x)|_{x0} + \frac{1}{2} \frac{\partial^2 S}{\partial x^\mu \partial x^\nu}|_{x0} \Delta x^\mu \Delta x^\nu}, \tag{E.7}$$

$$= \quad \frac{1}{(2\pi)^{\frac{1}{2}}} e^{-\frac{1}{2} g_{\mu\nu} \Delta x^\mu \Delta x^\nu} \sqrt{det(g_{\mu\nu})} dx. \tag{E.8}$$

We have line element $(\Delta \ell)^2 = g_{\mu\nu} \Delta x^\mu \Delta x^\nu$, which is the distance between thermodynamic states, and $g_{\mu\nu} = -\frac{1}{k_B} \frac{\partial^2 S}{\partial x^\mu \partial x^\nu}$ is a second rank tensor. The fluctuation probability is inversely proportional to the distance between fluctuation states. The metric will tell about thermodynamic stability, which is a hessian of entropy function that contains response functions like heat capacity and compressibility. The approach in thermodynamic makes use of differential geometry is called thermodynamic geometry.

Bibliography

Abbott, B., Abbott, R., Abbott, T., Abraham, S., Acernese, F., Ackley, K., Adams, A., Adams, C., Adhikari, R., Adya, V., et al. (2019). "Search for intermediate mass black hole binaries in the first and second observing runs of the advanced LIGO and Virgo network". *Physical Review D*, 100(6):064064.

Aharony, O., Gubser, S. S., Maldacena, J., Ooguri, H., and Oz, Y. (2000). "Large N field theories, string theory and gravity". *Physics Reports*, 323(3-4):183–386.

Ahluwalia-Khalilova, D. and Dymnikova, I. (2003). "A theoretical case for negative mass-square for sub-eV particles". *International Journal of Modern Physics D*, 12(09):1787–1794.

Ahmed Rizwan, C., Naveena Kumara, A., Vaid, D., and Ajith, K. (2018). "Joule-Thomson expansion in AdS black hole with a global monopole ". *International Journal of Modern Physics A*, 33(35):1850210.

Akbar, M., Salem, N., and Hussein, S. (2012). "Thermodynamics of the Bardeen regular black hole ". *Chinese Physics Letters*, 29(7):070401.

Ali, M. S. and Ghosh, S. G. (2018). "Exact d-dimensional Bardeen-de Sitter black holes and thermodynamics". *Physical Review D*, 98(8):084025.

Altamirano, N., Kubizňák, D., and Mann, R. B. (2013). "Reentrant phase transitions in rotating anti–de Sitter black holes". *Physical Review D*, 88(10):101502.

Altamirano, N., Kubizňák, D., Mann, R. B., and Sherkatghanad, Z. (2014). "Thermodynamics of rotating black holes and black rings: phase transitions and thermodynamic volume". *Galaxies*, 2(1):89–159.

Åman, J. E., Bedford, J., Grumiller, D., Pidokrajt, N., and Ward, J. (2007). "Ruppeiner theory of black hole thermodynamics ". In *Journal of Physics: Conference Series*, volume 66, page 012007. IOP Publishing.

Åman, J. E., Bengtsson, I., and Pidokrajt, N. (2003). "Geometry of black hole thermodynamics ". *General Relativity and Gravitation*, 35(10):1733–1743.

Åman, J. E. and Pidokrajt, N. (2006). "Geometry of higher-dimensional black hole thermodynamics ". *Physical Review D*, 73(2):024017.

Amir, M., Ahmed, F., and Ghosh, S. G. (2016). "Collision of two general particles around a rotating regular Hayward's black holes". *The European Physical Journal C*, 76(10):1–10.

Ansoldi, S. (2008). "Spherical black holes with regular center: a review of existing models including a recent realization with Gaussian sources". *arXiv preprint arXiv:0802.0330*.

Arkani-Hamed, N., Porrati, M., and Randall, L. (2001). "Holography and phenomenology". *Journal of High Energy Physics*, 2001(08):017.

Ashtekar, A. and Das, S. (2000). "Asymptotically anti-de Sitter spacetimes: conserved quantities". *Classical and Quantum Gravity*, 17(2):L17.

Ashtekar, A. and Magnon, A. (1984). "Asymptotically anti-de Sitter space-times". *Classical and Quantum Gravity*, 1(4):L39.

Atamurotov, F., Ghosh, S. G., and Ahmedov, B. (2016). "Horizon structure of rotating Einstein–Born–Infeld black holes and shadow". *The European Physical Journal C*, 76(5):1–16.

Ayon-Beato, E. and Garcia, A. (1998). "Regular black hole in general relativity coupled to nonlinear electrodynamics". *Physical review letters*, 80(23):5056.

Ayon-Beato, E. and García, A. (1999). "New regular black hole solution from nonlinear electrodynamics". *Physics Letters B*, 464(1-2):25–29.

Ayón-Beato, E. and García, A. (2000). "The Bardeen model as a nonlinear magnetic monopole". *Physics Letters B*, 493(1-2):149–152.

Ayón-Beato, E. and Garcia, A. (2005). "Four-parametric regular black hole solution". *General Relativity and Gravitation*, 37(4):635–641.

Balbinot, R. and Poisson, E. (1990). "Stability of the Schwarzschild-de Sitter model". *Physical Review D*, 41(2):395.

Bambi, C. and Modesto, L. (2013). "Rotating regular black holes". *Physics Letters B*, 721(4-5):329–334.

Banerjee, R., Ghosh, S., and Roychowdhury, D. (2011a). "New type of phase transition in Reissner Nordström–AdS black hole and its thermodynamic geometry ". *Physics Letters B*, 696(1-2):156–162.

Banerjee, R., Modak, S. K., and Samanta, S. (2011b). "Second order phase transition and thermodynamic geometry in Kerr-AdS black holes ". *Physical Review D*, 84(6):064024.

Bardeen, J. (1968). "Non-singular general-relativistic gravitational collapse, in proceedings of the International conference gr5 ". *Tbilisi, USSR*.

Bardeen, J. M., Carter, B., and Hawking, S. W. (1973). "The four laws of black hole mechanics". *Communications in mathematical physics*, 31(2):161–170.

Barrabes, C. and Frolov, V. P. (1996). "How many new worlds are inside a black hole?". *Physical Review D*, 53(6):3215.

Barrabes, C. and Israel, W. (1991). "Thin shells in general relativity and cosmology: The lightlike limit". *Physical Review D*, 43(4):1129.

Bekenstein, J. (1972a). "Black holes and entropy ". *Physical Review D*, 7(14):2333–2346.

Bekenstein, J. (1972b). "Black holes and the second law". *Lettere Al Nuovo Cimento (1971–1985)*, 4(4):737–740.

Bekenstein, J. D. (2020). "Generalized second law of thermodynamics in black-hole physics". In *JACOB BEKENSTEIN: The Conservative Revolutionary*, pages 321–329. World Scientific.

Belhaj, A., Chabab, M., El Moumni, H., Masmar, K., Sedra, M., and Segui, A. (2015). "On heat properties of AdS black holes in higher dimensions ". *Journal of High Energy Physics*, 2015(5):1–13.

Belhaj, A., Chabab, M., Moumni, H. E., and Sedra, M. B. (2012). "On thermodynamics of AdS black holes in arbitrary dimensions ". *Chinese Physics Letters*, 29(10):100401.

Bhattacharya, K., Majhi, B. R., and Samanta, S. (2017). "Van der Waals criticality in AdS black holes: a phenomenological study". *Physical Review D*, 96(8):084037.

Birmingham, D. (1999). "Topological black holes in anti-de Sitter space ". *Classical and Quantum Gravity*, 16(4):1197.

Borde, A. (1994). "Open and closed universes, initial singularities, and inflation". *Physical Review D*, 50(6):3692.

Borde, A. (1997). "Regular black holes and topology change". *Physical Review D*, 55(12):7615.

Bronnikov, K., Dobosz, A., and Dymnikova, I. (2003a). "Nonsingular vacuum cosmologies with a variable cosmological term". *Classical and Quantum Gravity*, 20(16):3797.

Bronnikov, K. and Dymnikova, I. (2007). "Regular homogeneous T-models with vacuum dark fluid". *Classical and Quantum Gravity*, 24(23):5803.

Bronnikov, K., Melnikov, V., and Dehnen, H. (2003b). "General class of brane-world black holes". *Physical Review D*, 68(2):024025.

Bronnikov, K. A. (2001a). "Regular magnetic black holes and monopoles from nonlinear electrodynamics". *Physical Review D*, 63(4):044005.

Bronnikov, K. A. (2001b). "Spherically symmetric false vacuum: no-go theorems and global structure". *Physical Review D*, 64(6):064013.

Bronnikov, K. A. and Fabris, J. C. (2006). "Regular phantom black holes". *Physical Review Letters*, 96(25):251101.

Brown, J. D. and Teitelboim, C. (1988). "Neutralization of the cosmological constant by membrane creation ". *Nuclear Physics B*, 297(4):787–836.

Cai, R.-G. (2002). "Gauss-Bonnet black holes in AdS spaces ". *Physical Review D*, 65(8):084014.

Cai, R.-G. and Cho, J.-H. (1999). "Thermodynamic curvature of the BTZ black hole ". *Physical Review D*, 60(6):067502.

Caldarelli, M. M., Cognola, G., and Klemm, D. (2000). "Thermodynamics of Kerr-Newman-AdS black holes and conformal field theories ". *Classical and Quantum Gravity*, 17(2):399.

Carathéodory, C. (1909). "Untersuchungen über die Grundlagen der Thermodynamik". *Mathematische Annalen*, 67(3):355–386.

Carballo-Rubio, R., Di Filippo, F., Liberati, S., Pacilio, C., and Visser, M. (2018). "On the viability of regular black holes". *Journal of High Energy Physics*, 2018(7):1–19.

Carlip, S. and Vaidya, S. (2003). "Phase transitions and critical behaviour for charged black holes ". *Classical and Quantum Gravity*, 20(16):3827.

Carroll, S. M. (2019). *"Spacetime and geometry"*. Cambridge University Press.

Carter, B. (1966). "The complete analytic extension of the Reissner-Nordström metric in the special case $e^2 = m^2$". *Physics Letters*, 21(4):423–424.

Cavaglia, M. (2003). "Black hole and brane production in TeV gravity: A review". *International Journal of Modern Physics A*, 18(11):1843–1882.

Chabab, M., Moumni, H. E., Iraoui, S., Masmar, K., and Zhizeh, S. (2018). "Joule-Thomson expansion of RN-AdS black holes in $f(R)$ gravity ". *Letters in High Energy Physics*, 02(5):10042.

Chakraborty, A. and Johnson, C. V. (2018). "Benchmarking black hole heat engines, I ". *International Journal of Modern Physics D*, 27(16):1950012.

Chamblin, A., Emparan, R., Johnson, C. V., and Myers, R. C. (1999a). "Charged AdS black holes and catastrophic holography ". *Physical Review D*, 60(6):064018.

Chamblin, A., Emparan, R., Johnson, C. V., and Myers, R. C. (1999b). "Holography, thermodynamics, and fluctuations of charged AdS black holes". *Physical Review D*, 60(10):104026.

Chen, S. and Jing, J. (2005). "Quasinormal modes of a black hole surrounded by quintessence ". *Classical and Quantum Gravity*, 22(21):4651.

Chen, S., Pan, Q., and Jing, J. (2013a). "Holographic superconductors in quintessence AdS black hole spacetime ". *Classical and Quantum Gravity*, 30(14):145001.

Chen, S.-B., Liu, X.-F., and Liu, C.-Q. (2013b). "P–V criticality of an AdS black hole in f (R) gravity ". *Chinese Physics Letters*, 30(6):060401.

Cisterna, A., Hu, S.-Q., and Kuang, X.-M. (2019). "Joule-Thomson expansion in AdS black holes with momentum relaxation ". *Physics Letters B*, 797(11):134883.

Clarke, C. (1975). "Singularities in globally hyperbolic space-time". *Communications in Mathematical Physics*, 41(1):65–78.

Couch, J., Fischler, W., and Nguyen, P. H. (2017). "Noether charge, black hole volume, and complexity". *Journal of High Energy Physics*, 2017(3):1–30.

Creighton, J. D. and Mann, R. B. (1995). "Quasilocal thermodynamics of dilaton gravity coupled to gauge fields". *Physical Review D*, 52(8):4569.

Cvetič, M., Gibbons, G. W., Kubizňák, D., and Pope, C. N. (2011). "Black hole enthalpy and an entropy inequality for the thermodynamic volume". *Physical Review D*, 84(2):024037.

Cvetič, M., Nojiri, S., and Odintsov, S. D. (2002). "Black hole thermodynamics and negative entropy in de Sitter and anti-de Sitter Einstein–Gauss–Bonnet gravity". *Nuclear Physics B*, 628(1-2):295–330.

Dadhich, N., Ghosh, S., and Deshkar, D. (2005). "The role of the space–time dimensions and the fluid equation of state in spherical gravitational collapse". *International Journal of Modern Physics A*, 20(07):1495–1501.

Davies, P. C. (1977). "The thermodynamic theory of black holes". *Proceedings of the Royal Society of London. A. Mathematical and Physical Sciences*, 353(1675):499–521.

Davoudiasl, H. and Denton, P. B. (2019). "Ultralight Boson dark matter and Event Horizon Telescope observations of M 87". *Physical review letters*, 123(2):021102.

De Sitter, W. (1918). "On the curvature of space". *Koninklijke Nederlandse Akademie van Wetenschappen Proceedings Series B Physical Sciences*, 20:229–243.

DeBenedictis, A. and Das, A. (2003). "Higher dimensional wormhole geometries with compact dimensions". *Nuclear Physics B*, 653(1-2):279–304.

Dey, T. K., Mukherji, S., Mukhopadhyay, S., and Sarkar, S. (2007). "Phase transitions in higher derivative gravity and gauge theory: R-charged black holes". *Journal of High Energy Physics*, 2007(09):026.

Dianyan, X. (1988). "Exact solutions of Einstein and Einstein-Maxwell equations in higher-dimensional spacetime". *Classical and Quantum Gravity*, 5(6):871.

Dolan, B. P. (2011a). "Compressibility of rotating black holes". *Physical Review D*, 84(12):127503.

Dolan, B. P. (2011b). "Pressure and volume in the first law of black hole thermodynamics". *Classical and Quantum Gravity*, 28(23):235017.

Dolan, B. P. (2011c). "The cosmological constant and black-hole thermodynamic potentials". *Classical and Quantum Gravity*, 28(12):125020.

Dolan, B. P. (2012). "Where is the PdV in the first law of black hole thermodynamics?". *Open Questions in Cosmology*.

Dymnikova, I. (1992). "Vacuum nonsingular black hole". *General relativity and gravitation*, 24(3):235–242.

Dymnikova, I. (2002). "The cosmological term as a source of mass". *Classical and Quantum Gravity*, 19(4):725.

Dymnikova, I. (2004). "Regular electrically charged vacuum structures with de Sitter centre in nonlinear electrodynamics coupled to general relativity". *Classical and Quantum Gravity*, 21(18):4417.

Dymnikova, I. and Galaktionov, E. (2005). "Stability of a vacuum non-singular black hole". *Classical and Quantum Gravity*, 22(12):2331.

Ebisawa, K., Życki, P., Kubota, A., Mizuno, T., and Watarai, K.-y. (2003). "Accretion disk spectra of ultraluminous X-ray sources in nearby spiral galaxies and galactic superluminal jet sources". *The Astrophysical Journal*, 597(2):780.

Ebisuzaki, T., Makino, J., Tsuru, T. G., Funato, Y., Zwart, S. P., Hut, P., McMillan, S., Matsushita, S., Matsumoto, H., and Kawabe, R. (2001). "Missing link found? the runaway path to supermassive black holes". *The Astrophysical Journal*, 562(1):L19.

Eddington, A. S. (1920). *"Space, time and gravitation: An outline of the general relativity theory"*. University Press.

Einstein, A. and Rosen, N. (1935). "The particle problem in the general theory of relativity". *Physical Review*, 48(1):73.

Elizalde, E. and Hildebrandt, S. R. (2002). "Family of regular interiors for nonrotating black holes with $t_0^0 = t_1^1$". *Physical Review D*, 65(12):124024.

Emparan, R. and Reall, H. S. (2002). "A rotating black ring solution in five dimensions". *Physical Review Letters*, 88(10):101101.

Estrada, M. and Aros, R. (2019). "Regular black holes and its thermodynamics in Lovelock gravity". *The European Physical Journal C*, 79(3):1–13.

Fan, Z.-Y. (2017). "Critical phenomena of regular black holes in anti-de Sitter space-time ". *The European Physical Journal C*, 77(4):266.

Fan, Z.-Y. and Wang, X. (2016). Construction of regular black holes in general relativity. *Physical Review D*, 94(12):124027.

Farrell, S. A., Webb, N. A., Barret, D., Godet, O., and Rodrigues, J. M. (2009). "An intermediate-mass black hole of over 500 solar masses in the galaxy ESO 243-49". *Nature*, 460(3):73–75.

Fernando, S. (2017). "Bardeen–de Sitter black holes". *International Journal of Modern Physics D*, 26(07):1750071.

Fernando, S. and Correa, J. (2012). "Quasinormal modes of the Bardeen black hole: Scalar perturbations". *Physical Review D*, 86(6):064039.

Ferrara, S., Gibbons, G. W., and Kallosh, R. (1997). "Black holes and critical points in moduli space ". *Nuclear Physics B*, 500(1-3):75–93.

Finkelstein, D. (1958). "Past-future asymmetry of the gravitational field of a point particle". *Physical Review*, 110(4):965.

Flachi, A. and Lemos, J. P. (2013). "Quasinormal modes of regular black holes". *Physical Review D*, 87(2):024034.

Frolov, V. P., Markov, M., and Mukhanov, V. F. (1989). "Through a black hole into a new universe?". *Physics Letters B*, 216(3-4):272–276.

Frolov, V. P., Markov, M., and Mukhanov, V. F. (1990). "Black holes as possible sources of closed and semiclosed worlds". *Physical Review D*, 41(2):383.

Fronsdal, C. (1959). "Completion and embedding of the Schwarzschild solution". *Physical Review*, 116(3):778.

Geroch, R. P. (1966). "Singularities in closed universes". *Physical Review Letters*, 17(8):445.

Ghaffarnejad, H. and Yaraie, E. (2018). "Effects of a cloud of strings on the extended phase space of Einstein Gauss Bonnet AdS black holes ". *Physics Letters B*, 785(18):105–111.

Ghaffarnejad, H., Yaraie, E., and Farsam, M. (2018). "Quintessence Reissner Nordström Anti de Sitter black holes and Joule Thomson effect ". *International Journal of Theoretical Physics*, 57(6):1671–1682.

Ghosh, S. and Banerjee, A. (2003). "Non-marginally bound inhomogeneous dust collapse in higher dimensional space–time". *International Journal of Modern Physics D*, 12(04):639–648.

Ghosh, S. and Dawood, A. (2008). "Radiating black hole solutions in arbitrary dimensions". *General Relativity and Gravitation*, 40(1):9–21.

Ghosh, S. and Deshkar, D. (2003). "Gravitational collapse of perfect fluid in self-similar higher dimensional space–times". *International Journal of Modern Physics D*, 12(05):913–924.

Ghosh, S. G. (2012). "Nonstatic charged BTZ-like black holes in N+1 dimensions". *International Journal of Modern Physics D*, 21(03):1250022.

Ghosh, S. G. (2015). "A nonsingular rotating black hole". *The European Physical Journal C*, 75(11):1–7.

Ghosh, S. G. and Amir, M. (2015). "Horizon structure of rotating Bardeen black hole and particle acceleration". *The European Physical Journal C*, 75(11):1–12.

Ghosh, S. G., Amir, M., and Maharaj, S. D. (2020). "Ergosphere and shadow of a rotating regular black hole". *Nuclear Physics B*, 957(18):115088.

Ghosh, S. G., Sheoran, P., and Amir, M. (2014). "Rotating Ayón-Beato-García black hole as a particle accelerator". *Physical Review D*, 90(10):103006.

Ghosh, S. G., Singh, D. V., and Maharaj, S. D. (2018). "Regular black holes in Einstein-Gauss-Bonnet gravity". *Physical Review D*, 97(10):104050.

Gibbons, G. W. and Hawking, S. W. (1977). "Cosmological event horizons, thermodynamics, and particle creation". volume 15, page 14. APS.

Gibbs, J. (1948). *"The Collected Works. Vol. 1. Thermodynamics"*. Yale University Press.

Gliner, E. B. (1966). "Algebraic properties of the energy-momentum tensor and vacuum-like states o+ matter". *Soviet Journal of Experimental and Theoretical Physics*, 22(5):378.

Gonzalez-Diaz, P. (1981). "The space-time metric inside a black hole". *Nuovo Cimento Lettere*, pages 161–163.

Graves, J. C. and Brill, D. R. (1960). "Oscillatory character of Reissner-Nordström metric for an ideal charged wormhole". *Physical Review*, 120(4):1507.

Grøn, Ø. (1985). "Space-time inside a black hole". *Lettere al Nuovo Cimento (1971-1985)*, 44(3):177–178.

Grøn, Ø. and Soleng, H. H. (1989). "Dynamical instability of the gonzalez-diaz black hole model". *Physics Letters A*, 138(3):89–94.

Gross, D. J. and Witten, E. (1986). "Superstring modifications of Einstein's equations". *Nuclear Physics B*, 277:1–10.

Gubser, S. S. and Mitra, I. (2001). "The evolution of unstable black holes in anti-de Sitter space ". *Journal of High Energy Physics*, 2001(08):018.

Gunasekaran, S., Kubizňák, D., and Mann, R. B. (2012). "Extended phase space thermodynamics for charged and rotating black holes and Born-Infeld vacuum polarization ". *Journal of High Energy Physics*, 2012(11):1–43.

Haldar, A. and Biswas, R. (2018). "Joule-Thomson expansion of five-dimensional Einstein-Maxwell-Gauss-Bonnet-AdS black holes ". *EPL (Europhysics Letters)*, 123(4):40005.

Hawking, S. W. (1965). "Occurrence of singularities in open universes". *Physical Review Letters*, 15(17):689.

Hawking, S. W. (1972). "Black holes in general relativity ". *Communications in Mathematical Physics*, 25(2):152–166.

Hawking, S. W. (1975). "Particle creation by black holes ". *Communications in mathematical physics*, 43(3):199–220.

Hawking, S. W. and Ellis, G. F. R. (1973). *"The Large Scale Structure of Space-Time "*, volume 1. Cambridge university press.

Hawking, S. W. and Page, D. N. (1983). "Thermodynamics of black holes in anti-de Sitter space ". *Communications in Mathematical Physics*, 87(4):577–588.

Hawking, S. W. and Penrose, R. (1970). "The singularities of gravitational collapse and cosmology ". *Proceedings of the Royal Society of London. A. Mathematical and Physical Sciences*, 314(1519):529–548.

Hayward, S. A. (2006). "Formation and evaporation of nonsingular black holes". *Physical review letters*, 96(3):031103.

Hendi, S. (2011). "Charged BTZ-like black holes in higher dimensions". *The European Physical Journal C*, 71(2):1–7.

Hendi, S., Panah, B. E., Panahiyan, S., Liu, H., and Meng, X.-H. (2018). "Black holes in massive gravity as heat engines ". *Physics Letters B*, 781(8):40–47.

Hendi, S. and Vahidinia, M. (2013). "Extended phase space thermodynamics and $P-V$ criticality of black holes with a nonlinear source ". *Physical Review D*, 88(8):084045.

Henneaux, M. and Teitelboim, C. (1985). "Asymptotically anti-de Sitter spaces". *Communications in Mathematical Physics*, 98(3):391–424.

Hennigar, R. A., McCarthy, F., Ballon, A., and Mann, R. B. (2017). "Holographic heat engines: general considerations and rotating black holes ". *Classical and Quantum Gravity*, 34(17):175005.

Hoang Nam, C. (2019). "Heat engine efficiency and Joule-Thomson expansion of nonlinear charged AdS black hole in massive gravity". *arXiv e-prints*, pages arXiv–1906.

Hollands, S., Ishibashi, A., and Marolf, D. (2005). "Comparison between various notions of conserved charges in asymptotically AdS spacetimes". *Classical and Quantum Gravity*, 22(14):2881.

Hollands, S. and Yazadjiev, S. (2008). "Uniqueness theorem for 5-dimensional black holes with two axial killing fields". *Communications in Mathematical Physics*, 283(3):749–768.

Hut, P. (1977). "Charged black holes and phase transitions". *Monthly Notices of the Royal Astronomical Society*, 180(3):379–389.

Israel, W. (1966). "Singular hypersurfaces and thin shells in general relativity". *Il Nuovo Cimento B (1965-1970)*, 44(1):1–14.

Israel, W. (1968). "Event horizons in static electrovac space-times ". *Communications in Mathematical Physics*, 8(3):245–260.

Itin, Y. (2008). "Mp hobson, gp efstathiou and an lasenby (eds): General relativity: an introduction for physicists".

Jafarzade, K. and Sadeghi, J. (2017). "The thermodynamic efficiency in static and dynamic black holes ". *International Journal of Theoretical Physics*, 56(11):3387–3399.

Janyszek, H. and Mrugała, R. (1989). "Geometrical structure of the state space in classical statistical and phenomenological thermodynamics ". *Reports on mathematical physics*, 27(2):145–159.

Johnson, C. (2016a). "An exact efficiency formula for holographic heat engines ". *Entropy*, 18(4):120.

Johnson, C. V. (2014). "Holographic heat engines". *Classical and Quantum Gravity*, 31(20):205002.

Johnson, C. V. (2016b). "Born– Infeld AdS black holes as heat engines. *Classical and Quantum Gravity*, 33(13):135001.

Johnson, C. V. (2016c). "Gauss–Bonnet black holes and holographic heat engines beyond large N. *Classical and Quantum Gravity*, 33(21):215009.

Kastor, D. (2008). "Komar integrals in higher (and lower) derivative gravity". *Classical and Quantum Gravity*, 25(17):175007.

Kastor, D., Ray, S., and Traschen, J. (2009). "Enthalpy and the mechanics of AdS black holes". *Classical and Quantum Gravity*, 26(19):195011.

Kiselev, V. (2003). "Quintessence and black holes". *Classical and Quantum Gravity*, 20(6):1187.

Klein, O. (1926). "Quantentheorie und fünfdimensionale relativitätstheorie". *Zeitschrift für Physik*, 37(12):895–906.

Konoplya, R. and Zhidenko, A. (2008). "Stability of higher dimensional Reissner-Nordström-anti-de Sitter black holes". *Physical Review D*, 78(10):104017.

Kormendy, J. and Richstone, D. (1995). "Inward bound - the search for supermassive black holes in galactic nuclei". *Annual Review of Astronomy and Astrophysics*, 33(1):581–624.

Kruskal, M. D. (1960). "Maximal extension of Schwarzschild metric". *Physical review*, 119(5):1743.

Kuang, X.-M., Liu, B., and Övgün, A. (2018). "Nonlinear electrodynamics AdS black hole and related phenomena in the extended thermodynamics". *The European Physical Journal C*, 78(10):1–10.

Kubizňák, D. and Mann, R. B. (2012). "P- V criticality of charged AdS black holes". *Journal of High Energy Physics*, 2012(7):33.

Kubizňák, D., Mann, R. B., and Teo, M. (2017). "Black hole chemistry: thermodynamics with Lambda". *Classical and Quantum Gravity*, 34(6):063001.

Kumar, A., Singh, D. V., and Ghosh, S. G. (2019). "*D*-dimensional Bardeen-AdS black holes in Einstein-Gauss-Bonnet theory. *The European Physical Journal C*, 79(3):1–16.

Lan, S.-Q. (2018). "Joule-Thomson expansion of charged Gauss-Bonnet black holes in AdS space ". *Physical Review D*, 98(8):084014.

Lan, S.-Q. (2019). "Joule-Thomson expansion of neutral AdS black holes in massive gravity ". *Nuclear Physics B*, 948:114787.

Landau, L. D. and Lifshitz, E. M. (2013). *"Statistical Physics: Volume 5"*, volume 5. Elsevier.

Li, C., He, P., Li, P., and Deng, J.-B. (2020). "Joule–Thomson expansion of the Bardeen-AdS black holes". *General Relativity and Gravitation*, 52(10):1–10.

Li, G.-Q. (2014). "Effects of dark energy on P–V criticality of charged AdS black holes ". *Physics Letters B*, 735(5):256–260.

Li, H.-F., Zhao, H.-H., Zhang, L.-C., and Zhao, R. (2017). "Clapeyron equation and phase equilibrium properties in higher dimensional charged topological dilaton AdS black holes with a nonlinear source ". *The European Physical Journal C*, 77(5):1–11.

Liu, H. and Meng, X.-H. (2017). "Effects of dark energy on the efficiency of charged AdS black holes as heat engines ". *The European Physical Journal C*, 77(8):556.

Liu, J. T. and Sabra, W. (2004). "Charged configurations in (A) dS spaces". *Nuclear Physics B*, 679(1-2):329–344.

Lukács, B. and Martinás, K. (1984). "Thermodynamics of negative absolute pressures ". Technical report, Hungarian Academy of Sciences.

Majhi, B. R. and Samanta, S. (2017). "PV criticality of AdS black holes in a general framework". *Physics Letters B*, 773(5):203–207.

Maldacena, J. (1999). "The large-N limit of superconformal field theories and supergravity". *International journal of theoretical physics*, 38(4):1113–1133.

Man, J. and Cheng, H. (2013). "The description of phase transition of Bardeen black hole in the Ehrenfest scheme". *arXiv preprint arXiv:1312.6566*.

Man, J. and Cheng, H. (2014). "The calculation of the thermodynamic quantities of the Bardeen black hole". *General Relativity and Gravitation*, 46(2):1–11.

Mann, R. B. (2015). "Black holes: thermodynamics, information, and firewalls". In *Black Holes: Thermodynamics, Information, and Firewalls*, pages 1–95. Springer.

Markov, M. (1982). "Limiting density of matter as a universal law of nature". *JETP Lett.(Engl. Transl.);(United States)*, 36(6).

Markov, M. (1984). "Problems of a perpetually oscillating universe". *Annals of Physics*, 155(2):333–357.

Markov, M. and Mukhanov, V. (1984). "De-Sitter initial state of the universe as a result of the asymptotic disappearance of gravitational interactions of matter". *JETP LETTERS*, 40(6):1043–1047.

Mars, M. and Senovilla, J. M. (1993). "Geometry of general hypersurfaces in spacetime: junction conditions". *Classical and Quantum Gravity*, 10(9):1865.

Matyjasek, J. and Tryniecki, D. (2009). "AdS$_2 \times$ S^2 geometries and the extreme quantum-corrected black holes". *Modern Physics Letters A*, 24(31):2517–2530.

Mezcua, M. (2017). "Observational evidence for intermediate-mass black holes". *International Journal of Modern Physics D*, 26(11):1730021.

Miller, B. P., Gallo, E., Greene, J. E., Kelly, B. C., Treu, T., Woo, J.-H., and Baldassare, V. (2015). "X-ray constraints on the local supermassive black hole occupation fraction". *The Astrophysical Journal*, 799(1):98.

Mo, J.-X. and Li, G.-Q. (2018). "Holographic heat engine within the framework of massive gravity". *Journal of High Energy Physics*, 2018(5):1–14.

Mo, J.-X. and Li, G.-Q. (2020). "Effects of Lovelock gravity on the Joule–Thomson expansion". *Classical and Quantum Gravity*, 37(4):045009.

Mo, J.-X., Li, G.-Q., Lan, S.-Q., and Xu, X.-B. (2018). "Joule-Thomson expansion of *d*-dimensional charged AdS black holes ". *Physical Review D*, 98(12):124032.

Mo, J.-X., Liang, F., and Li, G.-Q. (2017). "Heat engine in the three-dimensional spacetime ". *Journal of High Energy Physics*, 2017(3):1–11.

Modesto, L. and Nicolini, P. (2010). "Charged rotating noncommutative black holes". *Physical Review D*, 82(10):104035.

Moreno, C. and Sarbach, O. (2003). "Stability properties of black holes in self-gravitating nonlinear electrodynamics". *Physical Review D*, 67(2):024028.

Myers, R. C. and Perry, M. J. (1986). "Black holes in higher dimensional space-times". *Annals of Physics*, 172(2):304–347.

Myung, Y. S. (2008). "Phase transition between non-extremal and extremal Reissner–Nordström black holes ". *Modern Physics Letters A*, 23(09):667–676.

Myung, Y. S., Kim, Y.-W., and Park, Y.-J. (2008a). "Ruppeiner geometry and 2D dilaton gravity in the thermodynamics of black holes ". *Physics Letters B*, 663(4):342–350.

Myung, Y. S., Kim, Y.-W., and Park, Y.-J. (2008b). "Thermodynamics and phase transitions in the Born-Infeld-anti-de Sitter black holes ". *Physical Review D*, 78(8):084002.

Nam, C. H. (2018). "Non-linear charged AdS black hole in massive gravity ". *The European Physical Journal C*, 78(12):1–13.

Niu, C., Tian, Y., and Wu, X.-N. (2012). "Critical phenomena and thermodynamic geometry of Reissner-Nordström-anti-de Sitter black holes ". *Physical Review D*, 85(2):024017.

Nordström, G. (1918). "On the energy of the gravitation field in Einstein's theory". *Koninklijke Nederlandse Akademie van Wetenschappen Proceedings Series B Physical Sciences*, 20:1238–1245.

Oka, T., Hasegawa, T., Sato, F., Tsuboi, M., and Miyazaki, A. (1999a). "A large-scale CO imaging of the Galactic Center II. Dynamical properties of molecular clouds". *Advances in Space Research*, 23(5-6):981–984.

Oka, T., White, G. J., Hasegawa, T., Sato, F., Tsuboi, M., and Miyazaki, A. (1999b). "A high-velocity molecular cloud near the center of the Galaxy". *The Astrophysical Journal*, 515(1):249.

Ökcü, Ö. and Aydıner, E. (2017). "Joule–Thomson expansion of the charged AdS black holes ". *The European Physical Journal C*, 77(1):24.

Ökcü, Ö. and Aydıner, E. (2018). "Joule–Thomson expansion of Kerr–AdS black holes". *The European Physical Journal C*, 78(2):1–6.

Padmanabhan, T. (2002). "Classical and quantum thermodynamics of horizons in spherically symmetric spacetimes ". *Classical and Quantum Gravity*, 19(21):5387.

Page, D. N. (2005). "Hawking radiation and black hole thermodynamics". *New Journal of Physics*, 7(1):203.

Parker, L. (1969). "Quantized fields and particle creation in expanding universes. ". *Physical Review*, 183(5):1057.

Peca, C. S. and Lemos, J. P. (1999). "Thermodynamics of Reissner–Nordström–Anti-de Sitter black holes in the grand canonical ensemble ". *Physical Review D*, 59(12):124007.

Penrose, R. (1965). "Gravitational collapse and space-time singularities". *Physical Review Letters*, 14(3):57.

Penrose, R. (1969). "Gravitational collapse: The role of general relativity". *Nuovo Cimento Rivista Serie*, 1:252.

Perlmutter, S., Aldering, G., Goldhaber, G., Knop, R., Nugent, P., Castro, P. G., Deustua, S., Fabbro, S., Goobar, A., Groom, D. E., et al. (1999). "Measurements of ω and λ from 42 high-redshift supernovae". *The Astrophysical Journal*, 517(2):565.

Poisson, E. (2004). *"A relativist's toolkit: the mathematics of black-hole mechanics"*. Cambridge university press.

Poisson, E. and Israel, W. (1988). "Structure of the black hole nucleus". *Classical and Quantum Gravity*, 5(12):L201.

Randall, L. and Sundrum, R. (1999). "Large mass hierarchy from a small extra dimension". *Physical review letters*, 83(17):3370.

Ranjbari, H., Sadeghi, Mehdi andnaatian, M., and Forozani, G. (2020). "Critical behavior of AdS Gauss–Bonnet massive black holes in the presence of external string cloud". *The European Physical Journal C*, 80(1):1–16.

Reall, H. S. (2003). "Higher dimensional black holes and supersymmetry". *Physical Review D*, 68(2):024024.

Rees, M. J. (1984). "Black hole models for active galactic nuclei". *Annual review of astronomy and astrophysics*, 22(1):471–506.

Reines, A. E., Greene, J. E., and Geha, M. (2013). "Dwarf galaxies with optical signatures of active massive black holes". *The Astrophysical Journal*, 775(2):116.

Reissner, H. (1916). Über die Eigengravitation des elektrischen Feldes nach der Einsteinschen Theorie". *Annalen der Physik*, 355(9):106–120.

Riess, A. G., Filippenko, A. V., Challis, P., Clocchiatti, A., Diercks, A., Garnavich, P. M., Gilliland, R. L., Hogan, C. J., Jha, S., Kirshner, R. P., et al. (1998). "Observational evidence from supernovae for an accelerating universe and a cosmological constant". *The Astronomical Journal*, 116(3):1009.

Rodrigue, K. K. J., Saleh, M., Bouetou Thomas, B., and Crepin Kofane, T. (2018). "Thermodynamics phase transition of regular Hayward black hole surrounded by quintessence". *arXiv*, pages arXiv–1808.

Rostami, M., Sadeghi, J., Miraboutalebi, S., Masoudi, A., and Pourhassan, B. (2019). "Charged accelerating AdS black hole of $f(R)$ gravity and the Joule-Thomson expansion". *arXiv preprint arXiv:1908.08410.*

Ruppeiner, G. (1979). "Thermodynamics: A Riemannian geometric model ". *Physical Review A*, 20(4):1608.

Ruppeiner, G. (1983). "Thermodynamic critical fluctuation theory ". *Physical Review Letters*, 50(5):287.

Ruppeiner, G. (1995). "Riemannian geometry in thermodynamic fluctuation theory ". *Reviews of Modern Physics*, 67(3):605.

Ruppeiner, G. (2007). "Stability and fluctuations in black hole thermodynamics ". *Physical Review D*, 75(2):024037.

Ruppeiner, G. (2008). "Thermodynamic curvature and phase transitions in Kerr-Newman black holes ". *Physical Review D*, 78(2):024016.

Ruppeiner, G. (2014). "Thermodynamic curvature and black holes ". In *Breaking of Supersymmetry and Ultraviolet Divergences in Extended Supergravity*, pages 179–203. Springer.

Ruppeiner, G., Sahay, A., Sarkar, T., and Sengupta, G. (2012). "Thermodynamic geometry, phase transitions, and the widom line ". *Physical Review E*, 86(5):052103.

Sadeghi, J. and Toorandaz, R. (2020). "Joule-Thomson expansion of hyperscaling violating black holes with spherical and hyperbolic horizons ". *Nuclear Physics B*, 951(14):114902.

Sahay, A., Sarkar, T., and Sengupta, G. (2010). "On the thermodynamic geometry and critical phenomena of AdS black holes ". *Journal of High Energy Physics*, 2010(7):82.

Sakharov, A. D. (1966a). "The initial stage of an expanding Universe and the appearance of a nonuniform distribution of matter. *Sov. Phys. JETP*, 22:241.

Sakharov, A. D. (1966b). "The initial stage of an expanding Universe and the appearance of a nonuniform distribution of matter ". *Sov. Phys. JETP*, 22:241.

Saleh, M., Thomas, B. B., and Kofane, T. C. (2018). "Thermodynamics and phase transition from regular Bardeen black hole surrounded by quintessence ". *International Journal of Theoretical Physics*, 57(9):2640–2647.

Sarkar, T., Sengupta, G., and Tiwari, B. N. (2006). "On the thermodynamic geometry of BTZ black holes ". *Journal of High Energy Physics*, 2006(11):015.

Schee, J. and Stuchlík, Z. (2016). "Profiled spectral lines generated by Keplerian discs orbiting in the Bardeen and Ayòn-Beato–Garcìa spacetimes". *Classical and Quantum Gravity*, 33(8):085004.

Schmidt, M. (1963). "3c 273: a star-like object with large red-shift". *Nature*, 197(4872):1040–1040.

Schwarzschild, K. (1916). Über das gravitationsfeld eines massenpunktes nach der einsteinschen theorie. *Sitzungsberichte der Königlich Preußischen Akademie der Wissenschaften (Berlin*, pages 189–196.

Setare, M. and Adami, H. (2015). "Polytropic black hole ". *Physical Review D*, 91(8):084014.

Sharif, M. and Javed, W. (2011). "Thermodynamics of a Bardeen black hole in non-commutative space". *Canadian Journal of Physics*, 89(10):1027–1033.

Shen, J., Cai, R.-G., Wang, B., and Su, R.-K. (2007). "Thermodynamic geometry and critical behavior of black holes ". *International Journal of Modern Physics A*, 22(01):11–27.

Shen, W. and Zhu, S. (1985). "Globally regular solutions of a schwarzschild black hole and a reissner-nordström black hole.". *General relativity and gravitation*, 17:739–746.

Singh, D. V. and Singh, N. K. (2017). "Anti-evaporation of Bardeen de-Sitter black holes". *Annals of Physics*, 383:600–609.

Smarr, L. (1973). "Mass formula for Kerr black holes". *Physical Review Letters*, 30(2):71.

Spallucci, E. and Smailagic, A. (2013). "Maxwells equal-area law for charged Anti-de Sitter black holes ". *Physics Letters B*, 723(4-5):436–441.

Strader, J., Chomiuk, L., Maccarone, T. J., Miller-Jones, J. C., Seth, A. C., Heinke, C. O., and Sivakoff, G. R. (2012). "No evidence for intermediate-mass black holes in globular clusters: strong constraints from the JVLA". *The Astrophysical Journal Letters*, 750(2):L27.

Strominger, A. and Vafa, C. (1996). "Microscopic origin of the Bekenstein-Hawking entropy". *Physics Letters B*, 379(1-4):99–104.

Synge, J. L. (1950). "The gravitational field of a particle". In *Proceedings of the Royal Irish Academy. Section A: Mathematical and Physical Sciences*, volume 53, pages 83–114. JSTOR.

Tangherlini, F. R. (1963). "Schwarzschild field in n dimensions and the dimensionality of space problem". *Il Nuovo Cimento (1955-1965)*, 27(3):636–651.

Teitelboim, C. (1985). "The cosmological constant as a thermodynamic black hole parameter ". *Physics Letters B*, 158(4):293–297.

Tharanath, R. and Kuriakose, V. (2013). "Thermodynamics and Spectroscopy of Schwarzschild black hole surrounded by quintessence. *Modern Physics Letters A*, 28(04):1350003.

Thomas, B. B., Saleh, M., and Kofane, T. C. (2012). "Thermodynamics and phase transition of the Reissner–Nordström black hole surrounded by quintessence ". *General Relativity and Gravitation*, 44(9):2181–2189.

Tian, Y. and Wu, X.-N. (2011). "Dynamics of gravity as thermodynamics on the spherical holographic screen". *Physical Review D*, 83(2):021501.

Tinchev, V. K. (2019). "Measuring of the compact objects' parameters by analysis of their shadow". *arXiv preprint arXiv:1911.13262*.

Toshmatov, B., Ahmedov, B., Abdujabbarov, A., and Stuchlík, Z. (2014). "Rotating regular black hole solution". *Physical Review D*, 89(10):104017.

Tsujikawa, S. (2013). "Quintessence: a review ". *Classical and Quantum Gravity*, 30(21):214003.

Tzikas, A. G. (2019). "Bardeen black hole chemistry. *Physics Letters B*, 788:219–224.

Ulhoa, S. (2014). "On the quasinormal modes for gravitational perturbations of the Bardeen black hole". *Brazilian Journal of Physics*, 44(4):380–384.

Wald, R. M. (1993). "Black hole entropy is the Noether charge ". *Physical Review D*, 48(8):R3427.

Webster, B. L. and Murdin, P. (1972). "Cygnus X-1?a spectroscopic binary with a heavy companion?". *Nature*, 235(5332):37–38.

Wei, S.-W. and Liu, Y.-X. (2019). "Charged AdS black hole heat engines ". *Nuclear Physics B*, 946:114700.

Wei, Y.-H. and Chu, Z.-H. (2011). "Thermodynamic properties of a Reissner–Nordström quintessence black hole ". *Chinese Physics Letters*, 28(10):100403.

Weinhold, F. (1975). "Metric geometry of equilibrium thermodynamics ". *The Journal of Chemical Physics*, 63(6):2479–2483.

Wenda, S. and Shitong, Z. (1985). "The space-time metric inside a charged black hole". *Il Nuovo Cimento B (1971-1996)*, 85(2):142–148.

Wenda, S. and Zhu, S. (1988). "Junction conditions on null hypersurface". *Physics Letters A*, 126(4):229–232.

Weyl, H. (1917). "The theory of gravitation". *Annalen Phys*, 54:117.

Witten, E. (1998). "Anti-de Sitter space, thermal phase transition, and confinement in gauge theories". *Advances in Theoretical and Mathematical Physics*, 2(13):505–532.

Xu, H., Sun, Y., and Zhao, L. (2017). "Black hole thermodynamics and heat engines in conformal gravity ". *International Journal of Modern Physics D*, 26(13):1750151.

Zemansky, M. W. (1968). "Heat and thermodynamics: an intermediate textbook ".

Zhang, J., Li, Y., and Yu, H. (2018). "Accelerating AdS black holes as the holographic heat engines in a benchmarking scheme ". *The European Physical Journal C*, 78(8):1–6.

Zhang, L.-C., Zhao, H.-H., Zhao, R., and Ma, M.-S. (2014). "Equal area laws and latent heat for - dimensional RN-AdS black hole ". *Advances in High Energy Physics*, 2014.

Zhang, M. and Liu, W.-B. (2016). "f(R) black holes as heat engines". *International Journal of Theoretical Physics*, 55(12):5136–5145.

Zhao, H.-H., Zhang, L.-C., Ma, M.-S., and Zhao, R. (2015). "Phase transition and Clapeyron equation of black holes in higher dimensional AdS spacetime ". *Classical and Quantum Gravity*, 32(14):145007.

Zhao, R., Zhao, H.-H., Ma, M.-S., and Zhang, L.-C. (2013). "On the critical phenomena and thermodynamics of charged topological dilaton AdS black holes ". *The European Physical Journal C*, 73(12):1–10.

Zhao, Z.-W., Xiu, Y.-H., and Li, N. (2018). "Throttling process of the Kerr Newman anti-de Sitter black holes in the extended phase space ". *Physical Review D*, 98(12):124003.

Zhou, S., Chen, J., and Wang, Y. (2012). "Geodesic structure of test particle in Bardeen spacetime". *International Journal of Modern Physics D*, 21(09):1250077.

LIST OF PUBLICATIONS

1. Peer Reviewed International Journals:

1. C L Ahmed Rizwan, A Naveena Kumara, **K V Rajani** , Deepak Vaid, K M Ajith. (2019)."Effect of dark energy in geometrothermodynamics and phase transitions of regular Bardeen AdS black hole ". *Gen Relativ Gravit 51, 161 (2019).* https://doi.org/10.1007/s10714-019-2649-4

2. **K V Rajani** , C L Ahmed Rizwan, A Naveena Kumara, Deepak Vaid, K M Ajith. (2020). "Regular Bardeen AdS Black Hole as a Heat Engine ". *Nuclear Physics B 960, 115166 (2020).* https://doi.org/10.1016/j.nuclphysb.2020.115166

3. **K V Rajani** , C L Ahmed Rizwan, A Naveena Kumara, Deepak Vaid, Md.Sabir Ali. (2020). "Joule - Thomson expansion of regular Bardeen AdS black hole surrounded by static anisotropic matter field.". *Phys.Dark Univ. 32, 100825 (2021).* https://doi.org/10.1016/j.dark.2021.100825

2. Peer Reviewed International Journal proceedings:

1. **K V Rajani** , C L Ahmed Rizwan, A Naveena Kumara. (2020). "Phase transition and thermodynamic geometry of regular Bardeen black hole in higher dimensions". *AIP Conf. Proc.* 220, 030003.

3. International and National Conferences Presentations:

1. **K V Rajani** , C L Ahmed Rizwan, A Naveena Kumara. "Phase transition and thermodynamic geometry of regular Bardeen black hole in higher dimensions. ". *International Conference on Condensed Matter and Applied Physics* at Govt. Engineering College, Bikaner, Rajasthan, India during October 14-15, 2019.

2. **K V Rajani** , Deepak Vaid. "Comparative study of bulk and boundary bahavior of phase transition in Reissner Nordstrøm AdS black hole.". *30th meeting of the Indian Association for General Relativity and Gravitation(IAGRG)* at BITS Pilani Hydrabad, India during Jauary 3-5, 2019.

3. **K V Rajani** , Deepak Vaid. "Comparative Study of Bulk and Surface Pressure of Charged AdS Black Hole". *XXIII DAE-BRNS HIGH ENERGY PHYSICS SYMPOSIUM* at Indian Institute of Technology, Madrass, India during December 10-14, 2018.

4. **K V Rajani** , Deepak Vaid. "Similarities of Quantum Hall Effect and Black Hole Physics". *National level conference on*'*Cosmology and Particle Physics* at Women's Christian College, Chennai, India during October 1-2, 2018.

CURRICULUM VITAE

RAJANI K V

Permanent Address :

Kochuveettil House, Mayathi,   Mobile:(+91)-9497666654

PO: Panathady, Kasaragod Dist,   E-mail: rajanikv.ph14f07@nitk.ac.in,

Kerala, India - 671532   rajanikv10@gmail.com.

Academic Qualifications :

Master of Science   Score : 80.4%

Kannur University,

Kerala, India

Bachelor of Science   Score : 83%

Kannur University,

Kerala, India

Research Publications :

Articles in International Journals : 3

Articles in International Proceedings : 1

Papers presented in International Conferences : 4

Workshops and Schools attended : 10+